Overview of the Development of the Human Brain and Spinal Cord

Hans J. ten Donkelaar, Tetsuya Takakuwa, Lana Vasung, Shigehito Yamada, Kohei Shiota, and Ton van der Vliet

Corner's ten-somite embryo

Contents

1.1 Introduction – 3

1.2 Major Stages in the Development of the Human Brain and Spinal Cord – 3

1.3 The First Three Weeks of Development – 12

1.3.1 Implantation – 12

1.3.2 Gastrulation – 13

1.3.3 Folding of the Embryo – 16

1.4 Neurulation – 16

1.5 Development of the Spinal Cord – 19

© The Author(s), under exclusive license to Springer Nature Switzerland AG 2023
H. J. ten Donkelaar et al., *Clinical Neuroembryology*, https://doi.org/10.1007/978-3-031-26098-8_1

1.6 Pattern Formation of the Brain – 20

1.7 Early Development of the Brain – 21
1.7.1 Imaging of the Embryonic Brain – 21
1.7.2 Neuromeres – 22
1.7.3 The Ganglionic Eminences – 28

1.8 Foetal Development of the Brain – 29
1.8.1 The Cerebellum – 30
1.8.2 The Cerebral Cortex – 36
1.8.3 Cerebral Commissures – 43
1.8.4 Imaging of the Foetal Brain – 44

1.9 Development of the Meninges and Choroid Plexuses – 45

1.10 Development of the Blood Supply of the Brain – 48

1.11 Development of Fibre Tracts and Their Myelination – 55
1.11.1 Development of Fibre Tracts – 55
1.11.2 Development of Myelination – 58
1.11.3 Prenatal Motor Behaviour – 61

1.12 The Foetal Connectome – 63

References – 66

1.1 Introduction

The development of the human brain and spinal cord may be divided into several phases, each of which is characterized by particular developmental disorders (Volpe 1987; van der Knaap and Valk 1988; Aicardi 1992; ◘ Table 1.3). After implantation, formation and separation of the germ layers occur, followed by dorsal and ventral induction phases, and phases of neurogenesis, migration, organization and myelination. With the transvaginal ultrasound technique, a detailed description of the living embryo and foetus has become possible (Pooh and Kurjak 2009; Rama Murthy 2019). With magnetic resonance imaging (MRI), foetal development of the brain can now be studied in detail from about the beginning of the second half of pregnancy (Garel 2004; Prayer 2011). Much progress has been made in elucidating the mechanisms by which the central nervous system (CNS) develops, and also in our understanding of its major developmental disorders, such as neural tube defects, holoprosencephaly, microcephaly and neuronal migration disorders. Molecular genetic data, that explain programming of development aetiologically, can now be incorporated (Flores-Sarnat and Sarnat 2008; Barkovich et al. 2001, 2009, 2012; Desikan and Barkovich 2016; Barkovich and Raybaud 2018). In this chapter, an overview is presented of (1) major stages in the development of the human CNS, (2) the first three weeks of development, (3) neurulation, (4) pattern formation, (5) early development of the brain, (6) foetal development of the brain, (7) the development of the blood supply of the brain, (8) the development of major fibre tracts and (9) the foetal connectome. Mechanisms of development are discussed in ▶ Chap. 2, and an overview of the causes of developmental malformations and their molecular genetic basis is presented in ▶ Chap. 3. In the second, specialized part of this book the development of the CNS and its disorders are discussed in more detail. In this book, the developmental ontology based on the prosomeric model developed by Luis Puelles and John Rubenstein is applied (Puelles and Rubenstein 2003; Puelles 2013, 2019, 2021; Puelles et al. 2012, 2013). It is a reasonable framework to encompass the current state of knowledge of this fluid topic. The model is 'merely an epistemic instrument; it should be retained only as long as it proves capable of dealing straightforwardly with the available data, and which could in due course be modified or be replaced' (Puelles 2013). Throughout the book, the terminology used follows the second edition of the *Terminologia Embryologica* (TE2 2017) and the *Terminologia Neuroanatomica* (TNA 2017; ten Donkelaar et al. 2017, 2018).

1.2 Major Stages in the Development of the Human Brain and Spinal Cord

The human **embryonic period**, i.e. the first 8 weeks of development, can be divided into 23 stages, the **Carnegie stages** (**CS**; O'Rahilly and Müller 1987), originally described as developmental horizons (XI–XXIII) by Streeter (1951), and completed by Heuser and Corner (1957; developmental horizon X) and O'Rahilly (1973; developmental stages 1–9). Some of the reconstructed models and drawings of the extensive Carnegie Collection are now archived in the Human Developmental Anatomy Center in Washington, DC (▶ http://nmhm.washingtondc.museum/collections/hdac/index.htm). Important contributions to the description of human embryos were also made by Nishimura et al. (1977), Jirásek (1983, 2001, 2004) and from the Zagreb Collection of Human Brains by Ivica Kostović and colleagues (see Judaš et al. 2011; Kostović and Vasung 2009; Kostović et al. 2019a, b). Examples of human embryos, taken from the famous Kyoto Collection (see Shiota 2018; Yamaguchi and Yamada 2018), are shown in ◘ Figs. 1.1 and 1.2. In the embryonic period, **postfertilization** or **postconceptional age** is estimated by assigning an embryo to a developmental stage using a table of norms, going back to the first *Normentafeln* by Keibel and Elze (1908). The term **gestational age** is commonly used in clinical practice, beginning with the first day of the last menstrual period. Usually, the number of **menstrual** or **gestational weeks (GWs)** exceeds the number of postfertilization weeks by 2. During week 1 (CS 2–4) the blastocyst is formed, during week 2 (CS 5 and 6) implantation occurs and the primitive streak is formed, followed by the formation of the notochordal process and the beginning of neurulation (CS 7–10). Somites first appear at stage 9. The neural folds begin to fuse at CS 10, and the rostral and caudal neuropores close at CS 11 and 12, respectively. Gradually, the pharyngeal bars, the optic and otic vesicles, and the limb buds appear. The main external and internal features of human embryos are summarized in ◘ Table 1.1. The first four embryonic weeks are also described as the period of **blastogenesis**, and the fifth to eighth weeks as the period of **organogenesis** (Opitz 1993; Opitz et al. 1997). The **foetal period** cannot be divided into a series of morphologically defined stages. It is the period of **phenogenesis** (Opitz 1993; Opitz et al. 1997). In the clinical literature, a subdivision of the prenatal period into 3 trimesters of 13 weeks each is commonly used. At the junction of the trimesters 1 and 2, the foetus of about 90 days has a greatest length of 90 mm, whereas at the junction of the trimesters 2 and 3, the foetus is about 250 mm

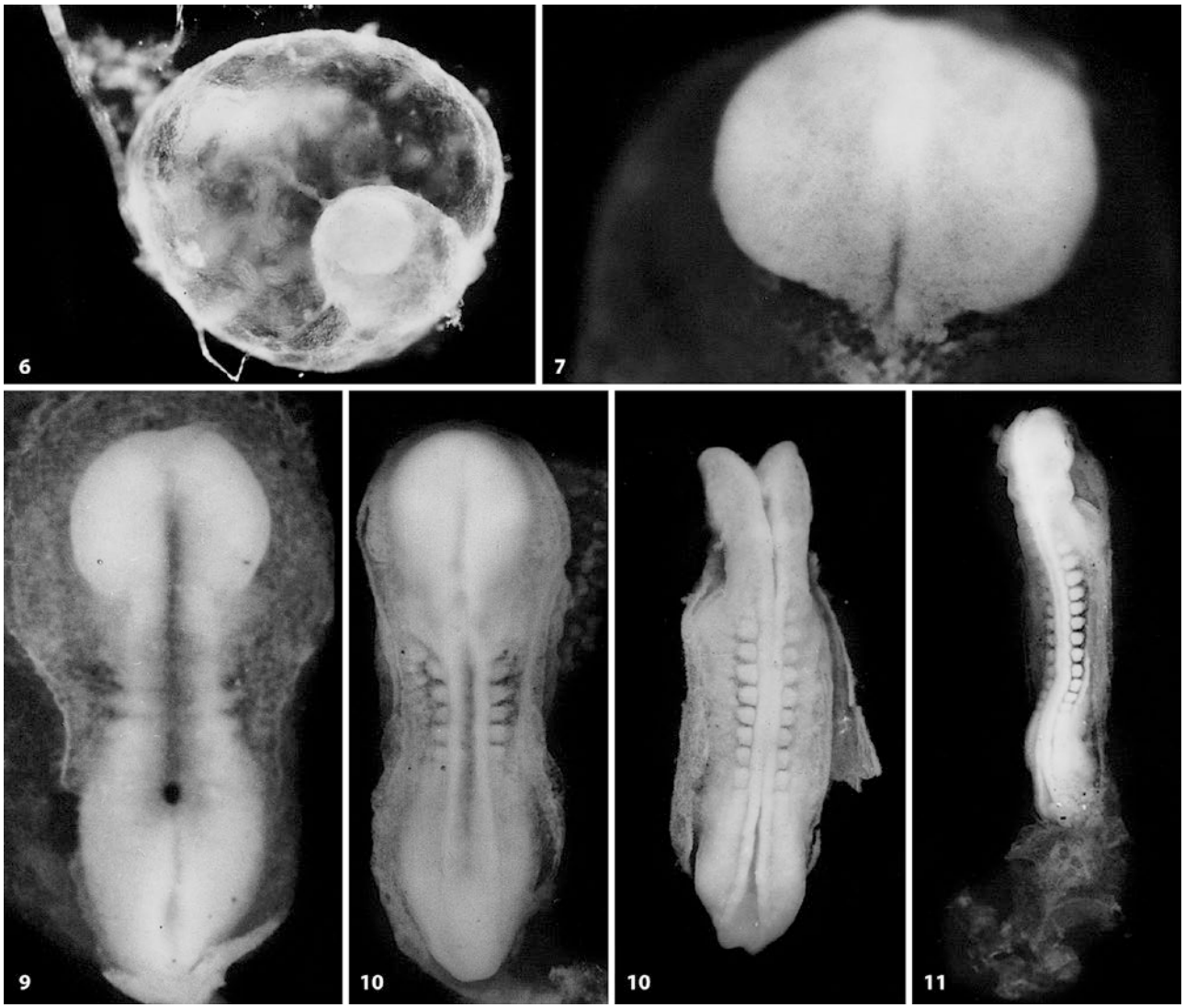

Fig. 1.1 Dorsal views of staged early human embryos (Carnegie stages 6, 7, 9–11). (From the Kyoto Collection of Human Embryos; kindly provided by Kohei Shiota, Kyoto)

in length and weighs approximately 1000 g (O'Rahilly and Müller 2001; Table 1.2). The newborn brain weighs 300–400 g at full term. Male brains weigh slightly more than those of females but, in either case, the brain constitutes 10% of the body weight (Crelin 1973).

The brain and the spinal cord arise from an area of the ectoderm known as the neural plate. The folding of the neural plate, leading to successively the neural groove and the neural tube, is called primary neurulation. The caudal part of the neural tube does not arise by fusion of the neural folds but develops from the so-called caudal eminence. This process is called secondary neurulation (▶ Chap. 4). Before and after the surface ectoderm of the two sides fuses, the fusing neuroectodermal cells of the neural folds give off the neural crest cells. The neural crest is a transient structure and gives rise to the spinal and cranial ganglia. Moreover, the whole viscerocranium and part of the neurocranium are formed from the neural crest (Le Douarin and Kalcheim 1999; Wilkie and Morriss-Kay 2001; Francis-West et al. 2003; Morriss-Kay and Wilkie 2005; Trainor 2014; ▶ Chap. 5).

Remarkable progress has been made in non-destructive imaging technologies, more in particularly MRI. By using a super-parallel magnetic resonance (MR) microscope (Matsuda et al. 2007), over 1400 human embryonic specimens have been imaged in the Kyoto Human Embryo Visualization Project (Yamada et al. 2006, 2010; Shiota et al. 2007; Takakuwa 2018; Fig. 1.3). Selective images from the database can be viewed on the web (▶ http://bird.cac.med.kyoto-u.ac.jp/index_e.html). Episcopic fluorescence image capture is another novel method that can provide registered two-dimensional (2D) image stacks suitable for rapid

three-dimensional (3D) rendering (Weninger and Mohun 2002). This technique has been used in a developmental atlas of the early first-trimester embryo from CS 13 to 23 (Yamada et al. 2010). Another 3D atlas of human embryos is based on the Carnegie Collection of Human Embryos (de Bakker et al. 2012, 2016). Shiraishi et al. (2015) created 3D reconstructions of the human brain from CS 14 till CS 23 with MR imaging data from 101 samples from the Kyoto Collection (◘ Fig. 1.4). The growth rate of the rhombencephalon exceeded that of the prosencephalon until CS 19. With the emergence of the cerebral hemispheres, after CS 20 the growth of the forebrain becomes much greater. The rapid growth of the cerebral hemispheres is largely responsible for the exponential growth of the brain during the foetal period.

The embryonic period includes three in time overlapping phases: formation and separation of the germ layers, and dorsal and ventral induction phases (◘ Table 1.3). During the first phase, the neural plate is formed. In the **dorsal induction phase**, the neural tube is formed and closed, and the three primary divisions or neuromeres of the brain (the prosencephalon, mesencephalon and rhombencephalon) appear. In the **ventral induction phase**, the cerebral hemispheres, the eye vesicles, the olfactory bulbs and tracts, the pituitary gland and part of the face are formed. In the sixth week of development strong proliferation of the ventral walls of the telencephalic vesicles gives rise to the ganglionic or ventricular eminences. These elevations do not only form the basal ganglia but also give rise to many neurons that migrate tangentially to the cerebral cortex. **Neurogenesis** starts in the spinal cord and the brain stem. Neurogenesis in the cerebellum and the cerebral cortex occurs largely in the foetal period. The human **foetal period** extends from the ninth week of development to the time of birth. With regard to the prenatal ontogenesis of the cerebral cortex, Marín-Padilla (1990) suggested to divide this long developmental period into two separate ones: (1) the **foetal period proper** (GW 9–24), characterized by the formation of the cortical plate; and (2) the **perinatal period**, extending from GW 24 to the time of birth. This period is characterized by neuronal maturation. The separation between these two periods at GW 24 is somewhat arbitrary but may be clinically relevant. GW 24 approximates roughly the lower limit for possible survival of the prematurely born infant. Disorders of migration are more likely to occur in the foetal period, whereas abnormalities affecting the architectonic organization of the cerebral cortex are more likely to occur in the perinatal period (▶ Chap. 10). Kostović suggested a further subdivision of the foetal period into four developmental phases and correlated histogenetic events with structural MRI (Kostović and Jovanov-Milošević 2006; Kostović and Vasung 2009; ▶ Chap. 10). More recently, Kostović et al. (2019a) distinguished five developmental phases: (1) an **early foetal phase** (9–13 postconceptional weeks or PCWs) with prominent proliferative zones, a trilaminar cerebral wall and with initial formation of the low MRI signal intensity subplate, known as the presubplate (see ▶ Sect. 1.8); during PCW 13–15, the subplate is formed; (2) a **midfoetal phase** (PCW 15–23) with transient foetal cellular zones fully developed, a synapse-rich subplate dominating on MRI and thalamocortical axons accumulating below the cortical plate; (3) a **late foetal** or **early preterm phase** (PCW 24–28), characterized by the subsequent development of gyri and sulci, thalamocortical fibres penetrating the cortical plate, persistence of the subplate, vulnerable periventricular axonal crossroads and poorly myelinated fibre systems; (4) a **late preterm phase** (PCW 29–36), during which secondary gyri and the volume of the cerebral wall develop rapidly, with a decline in the ventricular and subventricular proliferative zones and the subplate reaching its peak volume and thickness at PCW 30 (Vasung et al. 2016); and (5) a **near-term phase** (PCW 36–41) with gradual disappearance of transient foetal zones.

Each of the developmental phases of the brain is characterized by particular **developmental disorders** (◘ Table 1.3). During the separation of the germ layers, enterogenous cysts and fistulae may occur. In the dorsal induction phase, neural tube defects (▶ Chap. 4) occur. Developmental disorders in the ventral induction phase, in which the prosencephalon is normally divided into the diencephalon and the two cerebral hemispheres, are characterized by a single, incompletely divided forebrain (holoprosencephaly; ▶ Chap. 9). This very heterogeneous disorder may be due to disorders of ventralization of the neural tube (Flores-Sarnat and Sarnat 2008) such as underexpression of the strong ventralizing gene *Sonic hedgehog* (*SHH*). During neurogenesis of the forebrain, malformations due to abnormal neuronal proliferation or apoptosis may occur, leading to microcephaly or megalocephaly. During the migration of the cortical neurons, malformations due to abnormal neuronal migration may appear, varying from classic lissencephaly ('smooth brain'), several types of neuronal heterotopia, and polymicrogyria to minor cortical dysplasias. For many of these malformations, disorders of secretory molecules and genes that mediate migration have been found (▶ Chap. 10). Many of these malformations are characterized by the presence of intellectual disability and epilepsy. Cerebellar disorders are more difficult to fit into this scheme. The Dandy-Walker malformation is thought to arise late in the embryonic period, whereas cerebellar hypoplasia presumably occurs in the foetal period (see ▶ Chap. 8).

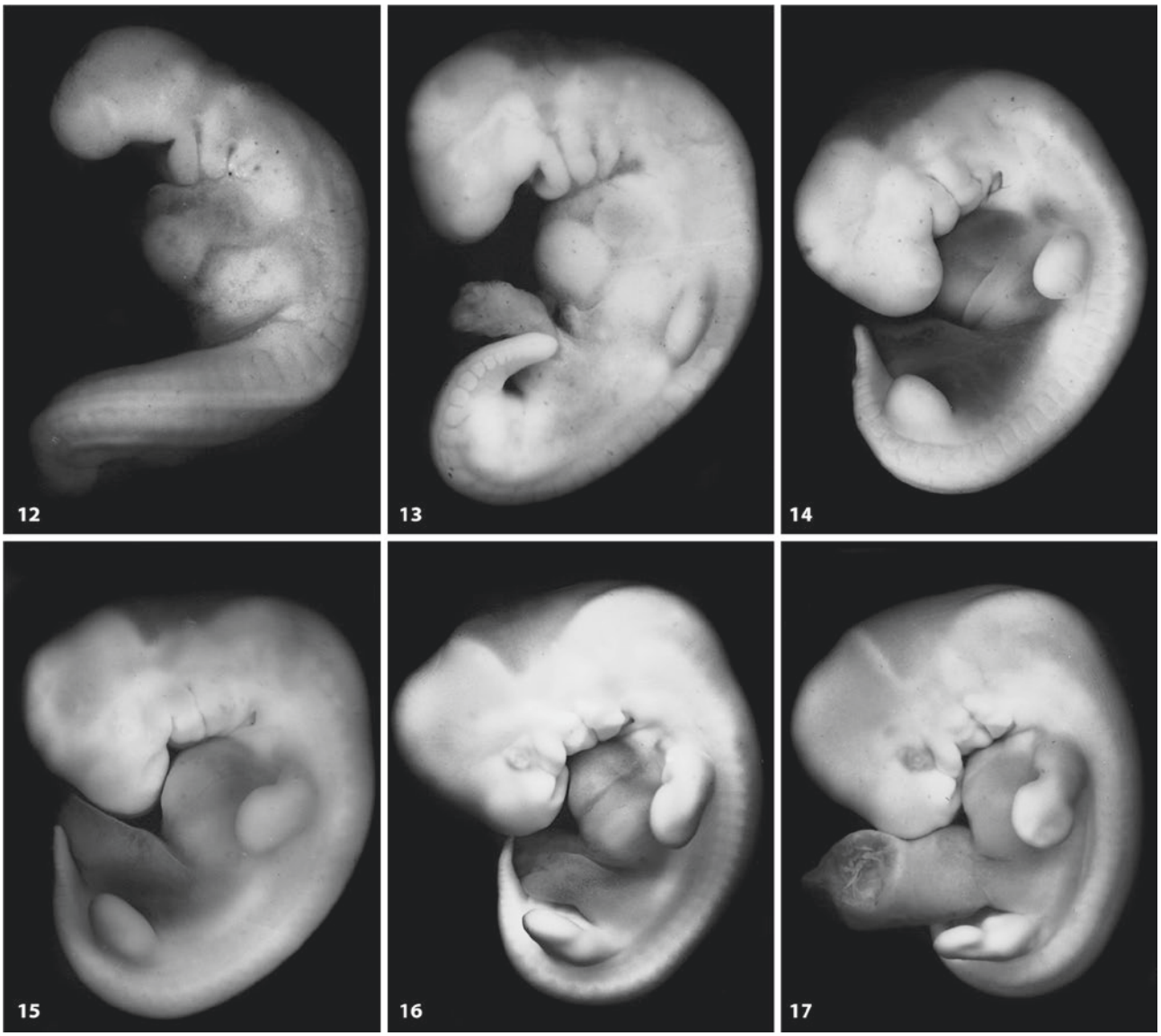

Fig. 1.2 Lateral views of staged human embryos (Carnegie stages 12–23). (From the Kyoto Collection of Human Embryos; kindly provided by Kohei Shiota, Kyoto)

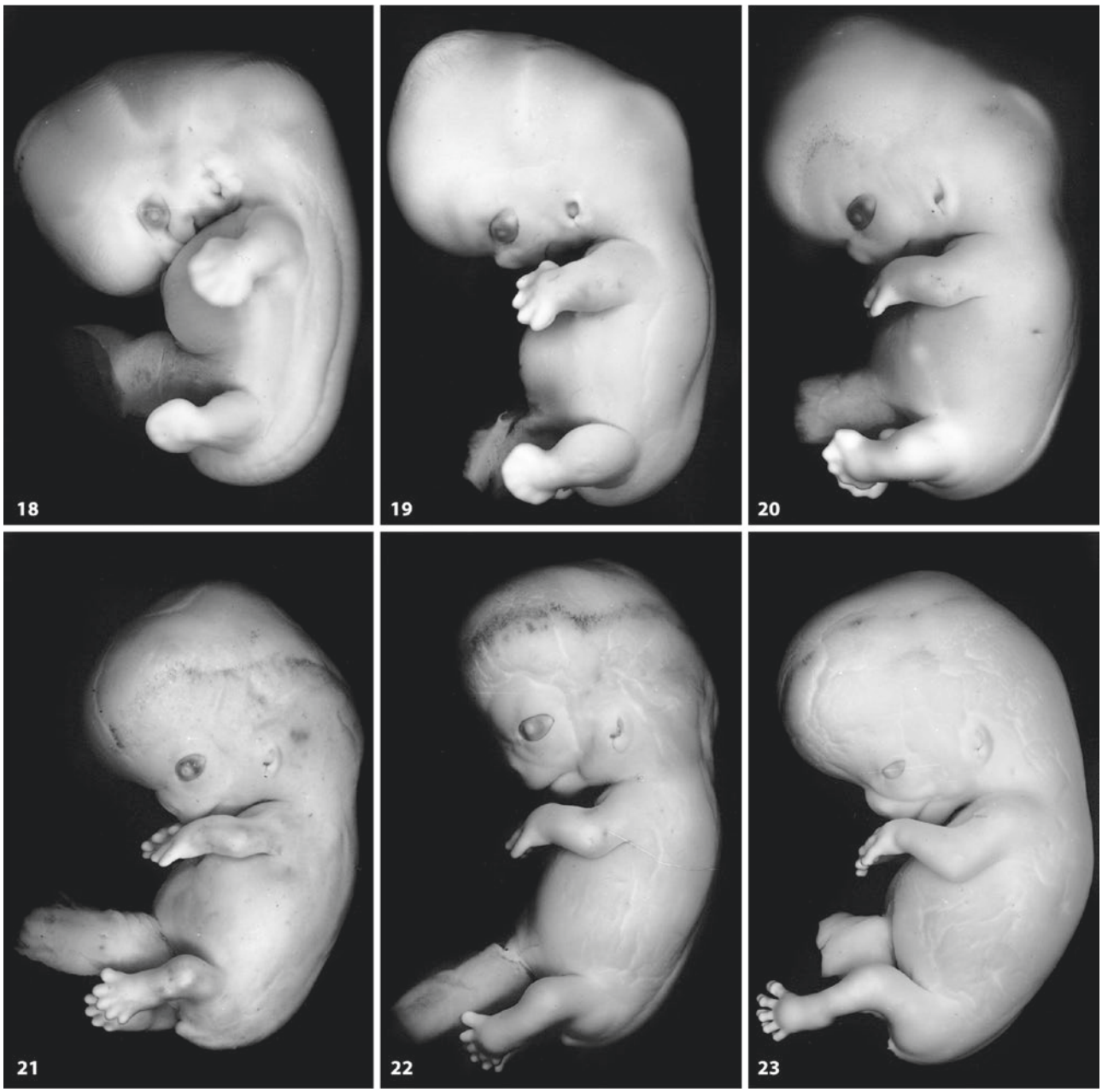

Fig. 1.2 (continued)

Table 1.1 Developmental stages and features of human embryos

Carnegie stages	Length (mm)	Age (days)	External features	Internal features (with emphasis on the nervous system)
1		1	Fertilization	
2		2–3	From 2 to about 16 cells	
3		4–5	Free blastocyst	Inner cell mass and trophoblast
4		6	Attaching blastocyst	Cytotrophoblast and syncytiotrophoblast distinguishable
5	0.1–0.2	7–12	Implantation; embryonic disc circular	Amniotic cavity; primary yolk sac; extra-embryonic mesoderm
6	0.2	17	Embryonic disk elongated	Chorionic villi; primitive streak and node; prechordal plate appears; secondary yolk sac
7	0.4	19	Embryonic disk oval	Notochordal process visible; haematopoiesis starts
8	1.0–1.5	23	Primitive pit appears; neural folds may begin to form	Notochordal and neurenteric canals detectable
9	1.5–2.5	25	First somites appear; mesencephalic flexure begins; otic disc forms	Neural groove evident; 3 major subdivisions of brain distinguishable; heart begins to develop
10	2–3.5	28	Neural folds begin to fuse; otic pit develops; 4–12 somites; pharyngeal arches 1 and 2 visible	Optic primordium begins to develop; cardiac loop appears; intermediate mesoderm
11	2.5–4.5	29	Rostral neuropore closes; 13–20 somites	Optic vesicles develop
12	3–5	30	Caudal neuropore closes; 21–29 somites; 4 pharyngeal arches visible; upper limb buds appearing	Secondary neurulation starts
13	4–6	32	Otic vesicle closed; lens disc not yet indented; 30 or more somites; 4 limb buds visible	Retinal and lens discs develop; primordium of cerebellum
14	5–7	33	Lens pit appears; upper limb buds elongated	Future cerebral hemispheres; pontine flexure; optic cup develops; adenohypophysial pouch defined
15	7–9	36	Lens pit closed; nasal pit appearing; hand plate forming	Future cerebral hemispheres become defined; retinal pigment visible
16	8–11	38	Retinal pigment visible; nasal sacs face ventrally; auricular hillocks beginning; foot plate appears	Pineal gland develops; neurohypophysial evagination; olfactory tubercle
17	11–14	41	Head relatively larger; trunk straighter; auricular hillocks distinct; finger rays	Internal and external cerebellar swellings; chondrification begins in humerus, radius and some vertebral centra
18	13–17	44	Body more cuboidal; elbow region and toe rays appearing	Oronasal membrane develops; 1–3 semicircular ducts in internal ear
19	16–18	46	Trunk elongating and straightening	Olfactory bulb develops; cartilaginous otic capsule; choroid plexus of fourth ventricle
20	18–22	49	Upper limbs longer and bent at elbows	Optic fibres reach optic chiasm; choroid plexus of lateral ventricle
21	22–24	51	Fingers longer; hands approach each other, feet likewise	Cortical plate becomes visible; optic tract and lateral geniculate body

Table 1.1 (continued)

Carnegie stages	Length (mm)	Age (days)	External features	Internal features (with emphasis on the nervous system)
22	23–28	53	Eyelids and external ear more developed	Olfactory tract; internal capsule; adenohypophysial stalk incomplete
23	27–31	56	Head more rounded; limbs longer and more developed	Insula indented; caudate nucleus and putamen recognizable; humerus presents all cartilaginous stages

After O'Rahilly and Müller (1987, 2001)

Table 1.2 Criteria for estimating age during the foetal period

Age (postconceptional weeks)	Average crown-rump length (mm)	Average foot length (mm)	Average weight (g)	Main external characteristics
Previable foetuses				
9	50	7	8	Eyes closing or closed; head large and more rounded; external genital not distinguishable as male or female; intestines in proximal part of umbilical cord; low-set ears
10	61	9	14	Intestines returned to abdomen; early fingernail development
12	87	14	45	Sex distinguishable externally; well-defined neck
14	120	20	110	Head erect; eyes face anteriorly; ears close to their definitive position; lower limbs well developed; early toenail development
16	140	27	200	External ears stand out from head
18	160	33	320	Vernix caseosa covers skin; quickening felt by mother
20	190	39	460	Head and body hair (lanugo) visible
Viable foetuses				
22	210	45	630	Skin wrinkled, translucent, pink to red colour
24	230	50	820	Fingernails present; lean body
26	250	55	1000	Eyes partially open; eyelashes present
28	270	59	1300	Eyes wide open; good head of hair may be present; skin slightly wrinkled
30	280	63	1700	Toenails present; body filling out; testes descending
32	300	68	2100	Fingernails reach finger tips; skin pink and smooth
36	340	79	2900	Body usually plump; lanugo hairs almost absent; toenails reach toe tips; flexed limbs; firm grasp
38	360	83	3400	Prominent chest; breasts protrude; testes in scrotum or palpable in inguinal canals; fingernails extend beyond finger tips

After Moore et al. (2000)

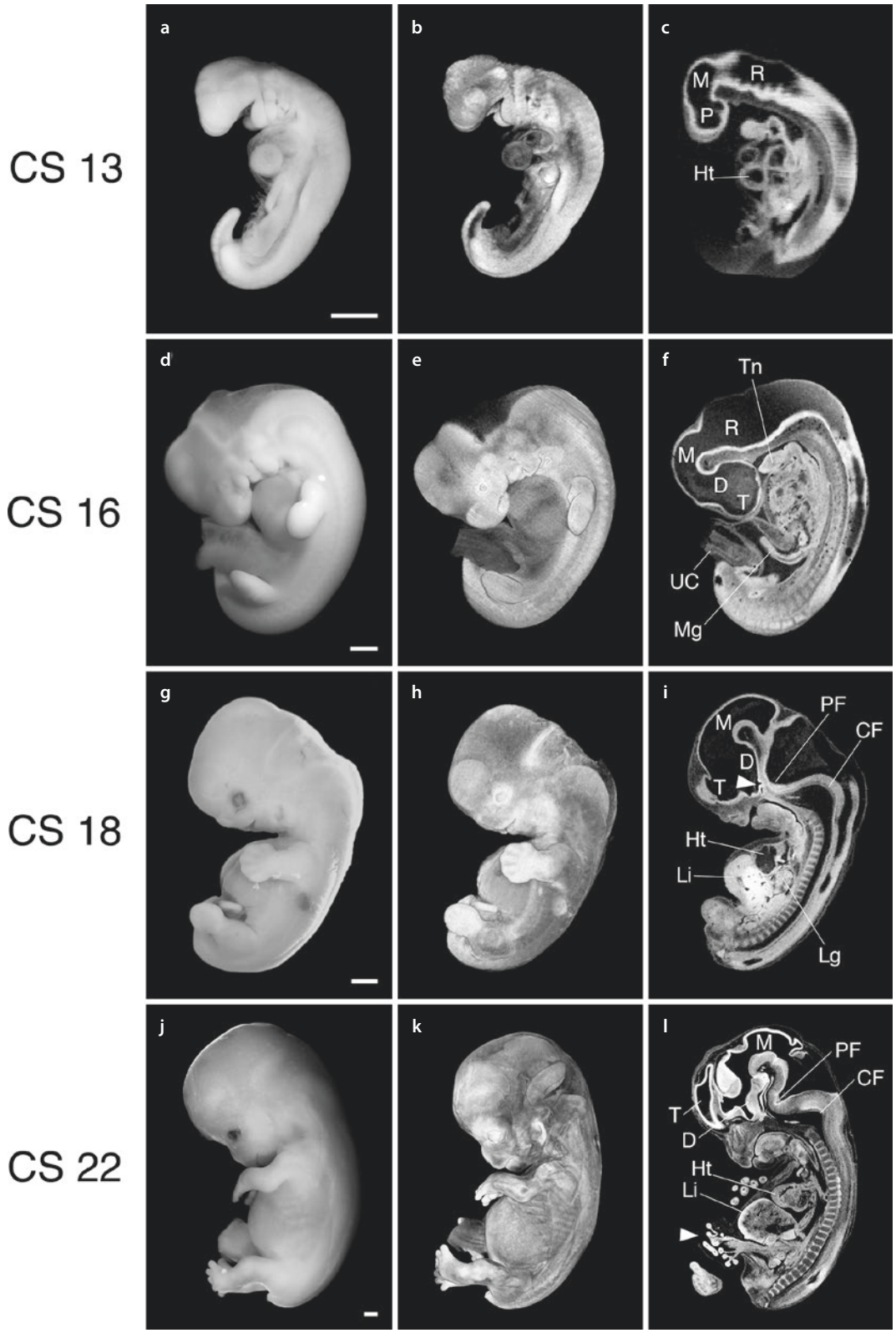
CS 13
CS 16
CS 18
CS 22
a
b
c
M
R
P
Ht
d
e
f
Tn
R
M
D
T
UC
Mg
g
h
i
M
PF
CF
D
T
Ht
Li
Lg
j
k
l
M
PF
CF
T
D
Ht
Li

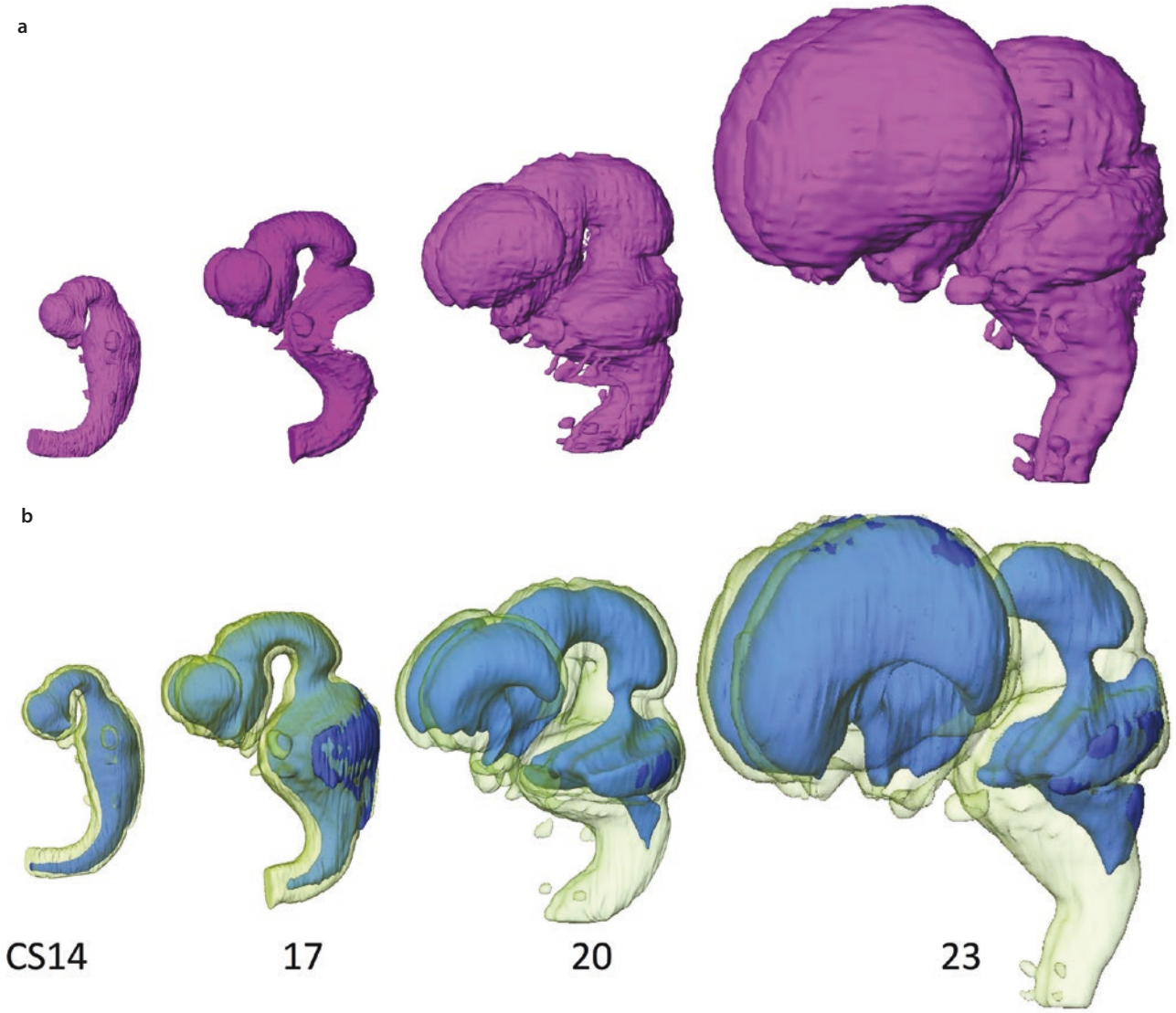

Fig. 1.4 3D reconstructions of the brain at Carnegie stages 14, 17, 20 and 23: **a** lateral view of the brain at same scale; **b** morphology of the ventricles observed through a transparent brain at same scale. (From Shiraishi et al. 2015, with permission; courtesy Tetsuya Takakuwa, Kyoto)

Fig. 1.3 Magnetic resonance (MR) microscopy of human embryos at different developmental stages. Human embryos at Carnegie stages (CS) 13, 16, 18 and 22 were imaged by MR microscopy. **a, d, g, j** Photographs of the embryos; **b, e, h, k** Three-dimensional (3D) reconstructions of the same embryos using MR images; **c, f, i, l** Two-dimensional (2D) MR images in the sagittal plane. At CS 13 **a–c**, limb buds are present and the prosencephalon (*P*), mesencephalon (*M*) and rhombencephalon (*R*) with rhombomeres can be seen. Also notable is the looped heart tube (*Ht*). At CS 16 **d–f**, the eye primordia and upper and lower limb buds with limb paddles are observed (*E*). In the abdominal cavity, the midgut (*Mg*) is invested in the umbilical cord (*UC*). At CS 18 **g–i**, anlagen for the digits are evident in the forelimb **g, h**. In the thoracic cavity, the heart and the lung (*Lg*) are clearly seen (**i**). At CS 22 **j–l** craniofacial and eye developments have advanced considerably and the digits in the fore- and hindlimbs are well developed **l**. At this stage of development, most of the abdominal cavity is occupied by the liver (*Li*) and physiological midgut herniation is present (*arrowhead* in **l**). *CF* cervical flexure, *D* diencephalon, *PF* pontine flexure, *T* telencephalon, *Tn* tongue; bars: 1 mm. (From Yamada et al. 2010, with permission; courtesy Shigehito Yamada, Kyoto)

Table 1.3 Major stages of human CNS development

Stage	Time of occurrence (weeks)	Major morphological events in brain	Main corresponding disorders
Embryonic period			
Formation and separation of germ layers	2	Neural plate	Enterogenous cysts and fistulas; split notochord syndrome
Dorsal induction: primary neurulation	3–4	Neural tube, neural crest and derivatives; closure of rostral and caudal neuropores; paired alar plates	Anencephaly, encephalocele, myeloschisis; myelomeningocele, Chiari malformations
Ventral induction: telencephalization	4–6	Development of forebrain and face; formation of cerebral vesicles; optic and olfactory placodes; rhombic lips appear; 'fusion' of cerebellar plates	Holoprosencephaly; Dandy-Walker malformation; craniosynostosis
Foetal period			
Neuronal and glial proliferation	6–16	Cellular proliferation in ventricular and subventricular zones; early differentiation of neuroblasts and glioblasts; cellular death (apoptosis); migration of Purkinje cells and external granular layer in cerebellum	Microcephaly, megalencephaly
Migration	12–24	Migration of cortical neurons; formation of corpus callosum	Neuronal migration disorders (lissencephalies, polymicrogyria, schizencephaly, heterotopia)
Perinatal period			
Organization	24 to postnatal	Late migration; organization and maturation of cerebral cortex; synaptogenesis; formation of internal granular layer in cerebellum	Minor cortical dysplasias
Myelination	24–2 years postnatally		Myelination disorders, destructive lesions (secondarily acquired injury of normally formed structures)

Based on Aicardi (1992)

1.3 The First Three Weeks of Development

During the first three weeks of development, the three germ layers (ectoderm, mesoderm and endoderm), the basis of the various organs and systems of the body, are established. During the first week of development (CS 2–4), the embryo develops from a solid mass of totipotent cells or blastomeres (the **morula**) into the blastocyst. This occurs when 16–32 cells are present. The **blastocyst** is composed of an inner cell mass or **embryoblast**, giving rise to the embryo, and the **trophoblast**, the peripherally situated cells, surrounding the blastocystic cavity and forming the developmental adnexa (Fig. 1.5). Embryoblast cells adjacent to this cavity form a new layer of flat cells, the **hypoblast**. This cell layer covers the blastocystic cavity from inside that is now called the **primitive umbilical vesicle** or **yolk sac**. The rest of the inner cell mass remains relatively undifferentiated and is known as the **epiblast**. Duplication of the inner cell mass is probably the basis for most cases of monozygotic twinning. Possibly, such divisions arise during 'hatching', the emergence of the blastocyst from the zona pellucida (O'Rahilly and Müller 2001). At approximately six days (CS 4b), the blastocyst becomes attached to the endometrium of the uterus.

1.3.1 Implantation

The second week is characterized by **implantation** (CS 5) and the formation of the primitive streak (CS 6). The trophoblast differentiates into the **cytotrophoblast** and the more peripherally situated **syncytiotrophoblast** that invades the endometrium. Blood-filled spaces, the **lacunae**, soon develop within the syncytiotrophoblast and communicate with endometrial vessels, laying the

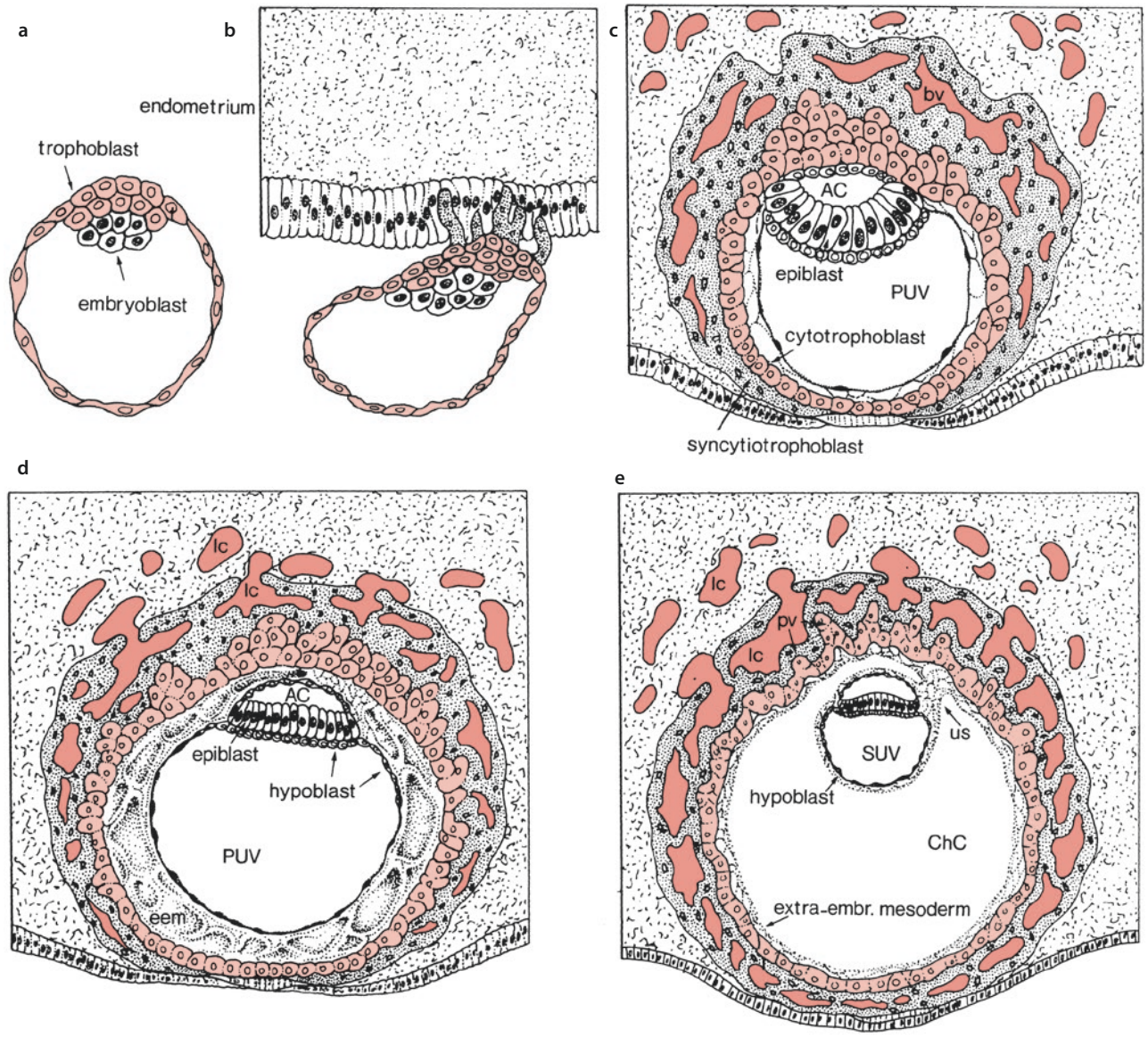

Fig. 1.5 Implantation and the formation of the bilaminar embryo: **a** 107-cell blastocyst; **b–e** blastocysts of approximately 4.5, 9, 12 and 13 days, respectively. The trophoblast and the cytotrophoblast are indicated in *light red*, the syncytiotrophoblast is *stippled* and maternal blood in lacunae is shown in *red*. *AC* amniotic cavity, *ChC* chorionic cavity, *eem* extra-embryonic mesoderm, *lc* lacuna, *pv* primary villi, *PUV* primary umbilical vesicle, *SUV* secondary umbilical vesicle (yolk sac), *us* umbilical stalk. (After Langman 1963)

basis for the placental circulation. Between the epiblast and the cytotrophoblast, the **amniotic cavity** appears. The embryonic disc is now known as the **bilaminar embryo**. Only the cylindric epiblast cells adjacent to the hypoblast form the embryo. The remaining flattened epithelial cells participate in the formation of the amnion (Fig. 1.5). The amniotic cavity is bounded ventrally by the epiblast and dorsally by a layer of amniotic ectoderm.

1.3.2 Gastrulation

During CS 6, in the slightly elongated embryonic disc caudally situated cells of the epiblast migrate ventralwards along the median plane, and form the **primitive streak** (Fig. 1.6). It probably appears between days 12 and 17 (Jirásek 1983, 2001; Moore et al. 2000; O'Rahilly and Müller 2001). The rostral, usually distinct, part of the primitive streak is known as the **primi-**

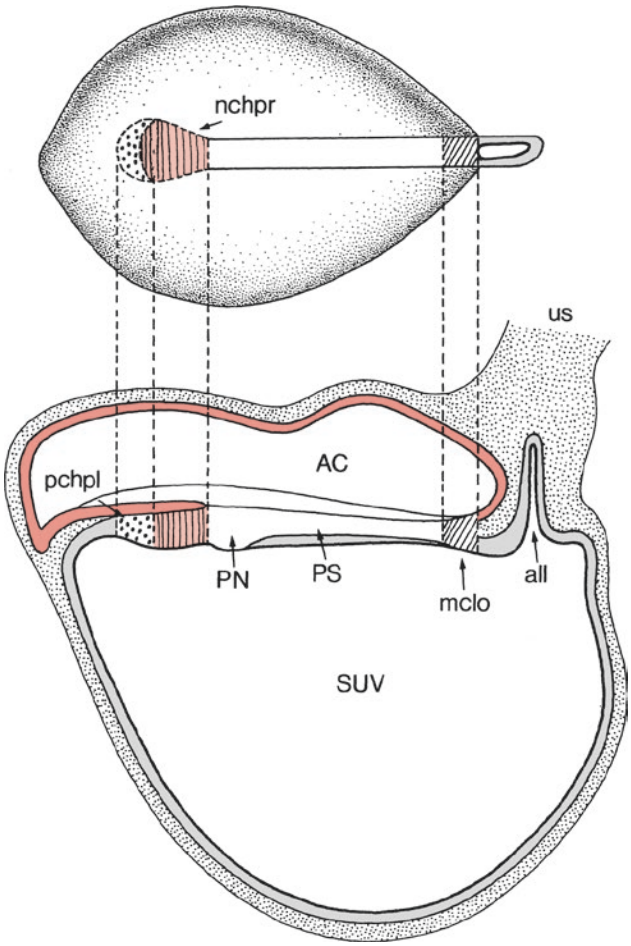

Fig. 1.6 Dorsal (*top*) and medial (*bottom*) views of a stage 7 embryo. The ectoderm is indicated in *red*, the notochordal process in *light red* and the endoderm in *grey*. *AC* amniotic cavity, *all* allantois, *mclo* membrana cloacalis, *nchpr* notochordal process, *pchpl* prechordal plate, *PN* primitive node, *PS* primitive streak, *SUV* secondary umbilical vesicle (yolk sac), *us* umbilical stalk. (After O'Rahilly 1973)

tive node of Hensen. The primitive streak is a way of entrance whereby cells invaginate, proliferate and migrate to subsequently form the extra-embryonic mesoderm, the endoderm and the intra-embryonic mesoderm. Remnants of the primitive streak may give rise to ***sacrococcygeal teratomas*** (▶ Chap. 4). The **endoderm** replaces the hypoblast. The remaining part of the epiblast is the **ectoderm**. For this process the term **gastrulation** is frequently used. Originally, the term referred to the invagination of a monolayered blastula to form a bilayered gastrula, containing an endoderm-lined archenteron as found in amphibians (▶ Chap. 2). Nowadays, the term gastrulation is more generally used to delimit the phase of development from the end of cleavage until the formation of an embryo possessing a defined axial structure (Collins and Billett 1995). Rostral to the primitive node, the endoderm appears thicker and is called the **prechordal plate**. Caudally, the epiblast is closely related to the endoderm, giving rise to the **cloacal membrane** (Fig. 1.6). The primitive streak is the first clear-cut indication of bilaterality, so the embryo now, apart from rostral and caudal ends, also has right and left sides. Genetic mutations expressed in the primitive streak may lead to duplication of the neural tube (▶ Chap. 6) or its partial or complete agenesis (Flores-Sarnat and Sarnat 2008).

The **extra-embryonic mesoderm** soon covers the trophoblast, the amniotic ectoderm and the yolk sac (Fig. 1.5). Extra-embryonic mesoderm at the caudal part of the embryo forms the **connecting** or **umbilical stalk** that anchors the embryo to the chorion. The **chorion** is composed of the trophoblast and the covering extra-embryonic mesoderm. Hypoblast cells and this extra-embryonic mesoderm form the wall of the yolk sac, whereas the amniotic epithelium and its mesodermal layer form the **amnion**. The **secondary umbilical vesicle** or **yolk sac** develops from the primary one, probably by collapse and disintegration of the latter (Luckett 1978). The yolk sac is involved in active and passive transport to the embryo, and is possibly associated with the relationship between metabolic disorders such as diabetes mellitus and congenital malformations (O'Rahilly and Müller 2001). The chorion encloses the **chorionic cavity**, in which the embryonic disc, now a **trilaminar embryo**, is located.

During the third and the fourth weeks, the somites, the heart, the neural folds, the three major divisions of the brain, the neural crest and the beginnings of the inner ear and the eye develop. At approximately 19 days (CS 7), rostral to the primitive streak, a prolongation below the ectoderm, the **notochordal process**, arises from the primitive node, and extends rostrally as far as the prechordal plate (Fig. 1.6). The floor of the notochordal process breaks down at CS 8, giving rise to the notochordal plate. The embryonic disc is now broader rostrally, and a shallow neural groove appears, which is the first morphological indication of the nervous system (O'Rahilly 1973; O'Rahilly and Gardner 1979; O'Rahilly and Müller 1981; Jirásek 2001, 2004). The primitive node may be hollowed by a **primitive pit**, which extends into the notochordal process as the **notochordal canal** (O'Rahilly 1973). The channel becomes intercalated in the endoderm, and its floor begins to disintegrate at once, allowing temporary communication between the amniotic cavity and the umbilical vesicle. The remnant of the notochordal canal at the level of the primitive pit is known as the **neurenteric canal** (Fig. 1.7a). It may be involved in the pathogenesis of ***enterogenous cysts*** (▶ Chap. 6). The **prechordal plate** is wider than the notochordal process, and is in close contact with the floor of the future forebrain. The prechordal plate is

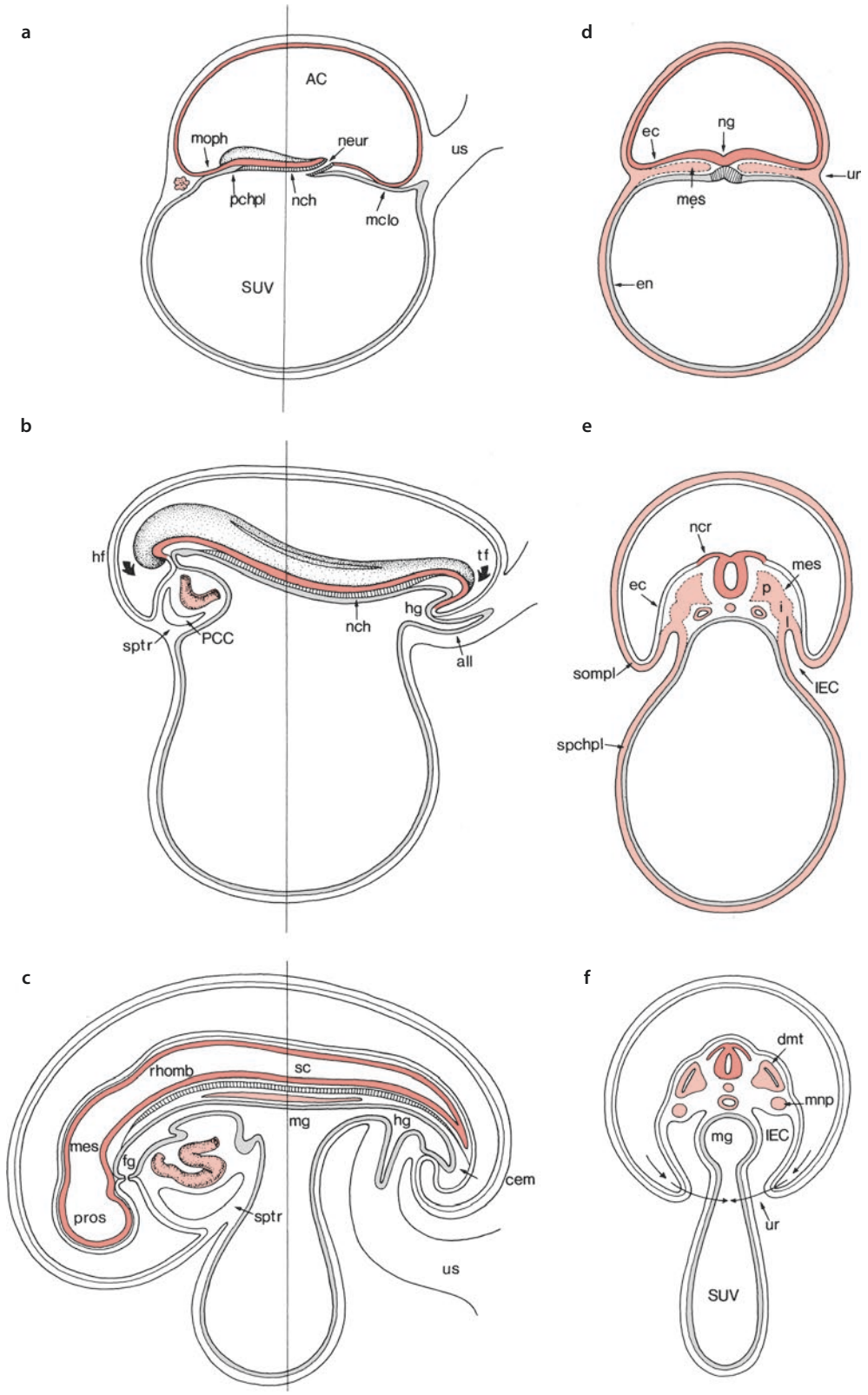

Fig. 1.7 The folding of the embryo: **a, d** Carnegie stage (CS) 8; **b, e** CS 10; **c, f** CS 11/12. The ectoderm (*ec*) and its derivates are indicated in *red*, derivates of the mesoderm (*mes*) in *light red* and the endoderm (*en*) in *grey*. *AC* amniotic cavity, *all* allantois, *cem* caudal eminence, *dmt* dermamyotome, *fg* foregut, *hf* head fold, *hg* hindgut, *i* intermediate mesoderm, *IEC* intra-embryonic coelom, *l* lateral plate of mesoderm, *mclo* membrana cloacalis, *mes* mesencephalon, *mg* midgut, *mnp* mesonephros, *moph* membrana oropharyngealis, *nch* notochord, *ncr* neural crest, *neur* neurenteric canal, *ng* neural groove, *p* paraxial mesoderm, *PCC* pericardiac cavity, *pchpl* prechordal plate, *pros* prosencephalon, *rhomb* rhombencephalon, *sc* spinal cord, *sompl* somatopleure, *spchpl* splanchnopleure, *sptr* septum transversum, *SUV* secondary umbilical vesicle (yolk sac), *tf* tail fold, *ur* umbilical ring, *us* umbilical stalk. (After Streeter 1951; Hamilton and Mossman 1972)

derived from the prechordal mesendoderm (de Souza and Niehrs 2000) and it is essential for the induction of the forebrain (▶ Chap. 9). The prechordal plate is usually defined as mesendodermal tissue underlying the medial aspect of the anterior neural plate just anterior to the rostral end of the notochord.

1.3.3 Folding of the Embryo

At approximately 25 days (CS 9), **folding** of the **embryo** becomes evident. Rostral or cephalic and caudal folds overlie the beginning foregut and hindgut, respectively (◘ Fig. 1.7). Caudal to the cloacal membrane, the allantois arises as a dorsal diverticle of the umbilical vesicle. On each side the mesoderm is arranged as three components (◘ Fig. 1.7e): (1) a longitudinal, **paraxial** band adjacent to the notochord, forming the somites; (2) **intermediate** mesoderm, giving rise to the urogenital system; and (3) a **lateral plate**, giving rise to two layers covering the body wall and the viscera, respectively. The first layer is known as the **somatopleure**, the other as the **splanchnopleure**. In the Anglo-Saxon literature, however, the terms somatopleure and splanchnopleure include the covering ectoderm and endoderm, respectively (O'Rahilly and Müller 2001). The space between the somatopleure and the splanchnopleure is the **coelom**. At first it is found outside the embryo (the **extraembryonic coelom**), later also within the embryo. This is the **intra-embryonic coelom** or body cavity, which develops in the lateral plate mesoderm (◘ Fig. 1.7e, f). For a discussion of body wall closure and its relevance to ***gastroschisis*** and other ventral body wall defects, see Sadler and Feldkamp (2008) and Hunter and Stevenson (2008).

Somites arise at CS 9 in longitudinal rows on each side of the neural groove. The first four pairs of somites belong to the occipital region. Within the next 10 days subsequently 8 cervical, 12 thoracic, 5 lumbar, 5 sacral and some 3–6 coccygeal somites are formed, but they are never visible together at one stage of development. Each somite divides into a ventromedial **sclerotome**, participating in the formation of the vertebral column (▶ Chap. 6), and a dorsolateral **dermamyotome** that forms a myotome and the overlying dermis (**dermatome**). Each **myotome** divides into two parts: (1) a dorsal **epimere**, giving rise to the erector spinae muscle, and (2) a ventral **hypomere**, from which the ventral vertebral muscles (**epaxial muscles**), the muscles of the lateral and ventral body wall (**hypaxial muscles**) and the muscles of the extremities arise. The derivatives of the epimeres become innervated by the dorsal rami of the spinal nerves, those of the hypomeres by the ventral rami (▶ Chap. 6).

The primitive streak becomes confined to a region known as the **caudal eminence**, or end-bud, which gives rise to the hindgut, adjacent notochord and somites, and the most caudal part of the spinal cord (O'Rahilly and Müller 2001). Malformations in this region may lead to the still poorly understood ***caudal regression syndrome*** that is discussed in ▶ Chap. 4. Rostrally, the ectoderm and the endoderm come together as the **oropharyngeal membrane**, which temporarily separates the gut from the amniotic cavity. Pharyngeal arches, clefts and pouches become visible. The **pharyngeal arches** are separated by the **pharyngeal clefts**, and appear ventrolaterally on the head and neck between four and five weeks. Four pairs are visible at CS 13 (◘ Fig. 1.2). More caudally, no clear-cut arrangement is found, but it is customary to distinguish a fifth and a sixth arch. The externally situated clefts have internal counterparts, the **pharyngeal pouches**. The development of the pharyngeal arches is closely related to that of the rhombomeres and the neural crest, and is controlled by *Hox* genes (Favier and Dollé 1997; Rijli et al. 1998). Each pharyngeal arch is characterized by a unique combination of *Hox* genes. Rostral to the somites, the paraxial mesoderm forms the **somitomeres** from which the external eye musculature and the muscles of the pharyngeal bars arise (Noden 1991; Noden and Trainor 2005; Trainor 2014; see ▶ Chap. 5). The sense organs of the head develop from interactions of the neural tube with a series of epidermal thickenings called the **cranial ectodermal placodes**. The olfactory placode forms the olfactory epithelium, the trigeminal placode forms the trigeminal ganglion, the otic placode forms the inner ear and the epibranchial placodes form the distal ganglia of the VIIth, IXth and Xth nerves (▶ Chap. 7). The lens placode forms the lens and induces the overlying ectoderm to form the transparent cornea (▶ Chap. 9).

1.4 Neurulation

The first indication of the neural plate in human embryos is a median sulcus around 23 days of development. At approximately 25 days (CS 9), this **neural groove** is deeper and longer. Its rostral half represents the forebrain, its caudal half mainly the hindbrain (◘ Fig. 1.8). The **neural folds** of the forebrain are conspicuous. The **mesencephalic flexure** appears, and allows a first subdivision of the brain into three major divisions in the still unfused neural folds (O'Rahilly 1973; O'Rahilly and Gardner 1979; Müller and O'Rahilly 1983, 1997; Jirásek 2001, 2004): the forebrain or **prosencephalon**, the midbrain or **mesencephalon**, and the hindbrain or **rhombencephalon** (◘ Fig. 1.9). The otic placodes, the first indication of the internal ears, can also be recognized. At CS 10, the two subdivisions of the forebrain, the **telencephalon** and the **diencephalon**, become evident (Müller and O'Rahilly 1985). An **optic sulcus** is the first indication of the developing eye. Closure of the neural

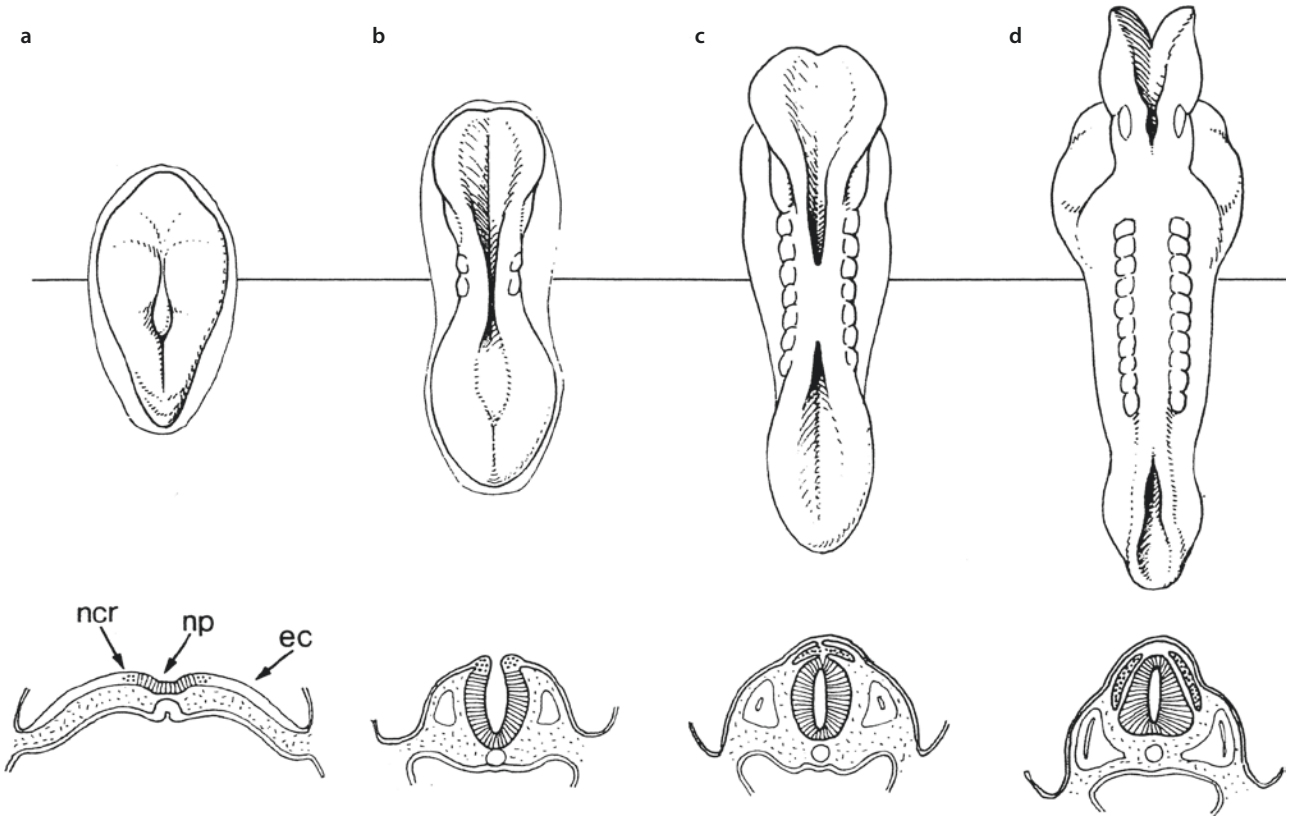

Fig. 1.8 The formation of the neural tube and neural crest. Dorsal views and transverse sections are shown for human embryos of CS 8 **a**, CS 9 **b**, CS 10 (**c**, seven somites) and CS 10 (**d**, ten somites). *ec* ectoderm, *ncr* neural crest, *np* neural plate

groove begins near the junction between the future brain and the spinal cord. Rostrally and caudally, the cavity of the developing neural tube communicates via the **rostral** and **caudal neuropores** with the amniotic cavity. The rostral neuropore closes at about 30 days (CS 11), and the caudal neuropore about one day later (CS 12). The site of final closure of the rostral neuropore is at the site of the embryonic lamina terminalis (O'Rahilly and Müller 1999). The closure of the neural tube in human embryos is generally described as a continuous process that begins at the level of the future cervical region, and proceeds both rostrally and caudally (O'Rahilly and Müller 1999, 2001; de Bakker et al. 2017). Nakatsu et al. (2000), however, provided evidence that neural tube closure in humans may initiate at multiple sites as in mice and other animals (see also Bassuk and Kibar 2009; Pyrgaki et al. 2010; Rifat et al. 2010; Massarwa and Niswander 2013). ***Neural tube defects*** are among the most common malformations (► Chap. 4).

When the surface ectodermal cells of both sides fuse, the similarly fusing neuroectodermal cells of the neural folds give off neural crest cells (Fig. 1.8). These cells arise at the neurosomatic junction. The **neural crest cells** migrate extensively to generate a large diversity of differentiated cell types (Le Douarin and Kalcheim 1999; Trainor 2014; ► Chap. 5), including (1) the spinal cranial and autonomic ganglia, (2) the enteric nervous system, (3) the medulla of the adrenal gland, (4) the melanocytes, the pigment-containing cells of the epidermis, and (5) many of the skeletal and connective tissue of the head. The final phase of primary neurulation is the separation of neural and surface ectoderm by mesenchyme. Failure to do so may lead to an encephalocele, at least in rats (O'Rahilly and Müller 2001). Malformations of the neural crest (***neurocristopathies***) may be accompanied by developmental disorders of the CNS (► Chap. 5).

Detailed **fate map** studies are available for amphibians and birds (► Chap. 2). The organization of vertebrate neural plates appears to be highly conserved. This conservation probably extends to mammals, for which detailed fate maps are more difficult to obtain. Nevertheless, available data (Rubenstein and Beachy 1998; Rubenstein et al. 1998; Inoue et al. 2000; Puelles et al. 2012; Puelles 2013) showed that in mice ventral parts of the forebrain such as the hypothalamus and the eye vesicles arise from the medial part of the rostral or prosencephalic part of the neural plate (Fig. 1.11c). Pallial as well as subpallial parts of the telencephalon arise from the lateral parts of the prosencephalic neural plate. The lateral border of this part of the neural plate forms the dorsal, septal roof of the telencephalon. The

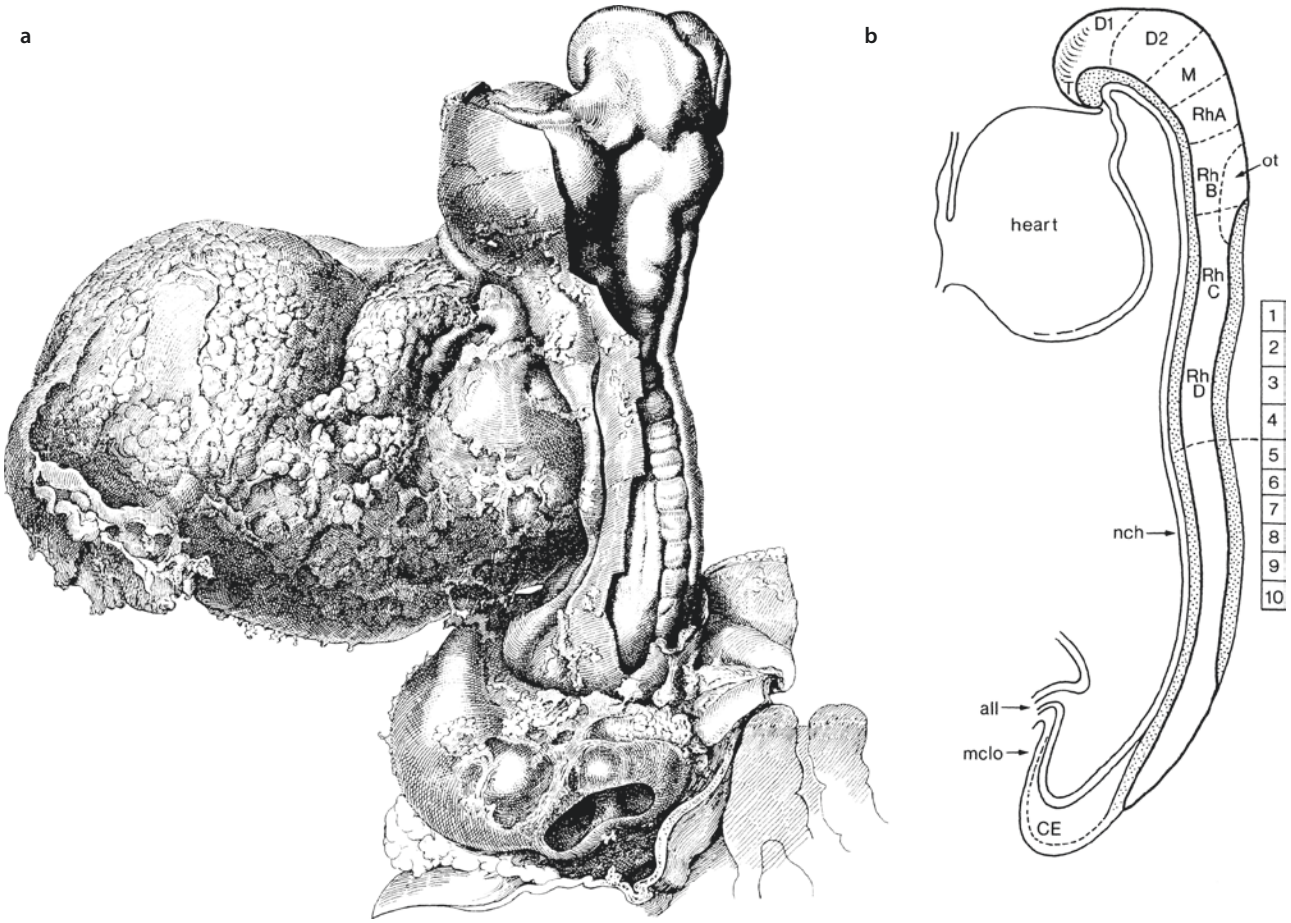

Fig. 1.9 Corner's ten-somite embryo **a**. **b** A median section, showing the subdivision of the brain into the primary neuromeres. *all* allantois, *CE* caudal eminence, *D1*, *D2* diencephalic neuromeres, *M* mesomere, *mclo* membrana cloacalis, *nch* notochord, *ot* otocyst, *RhA-RhD* primary rhombomeres, *T* telencephalic neuromere, *1–10* first ten somites. (**a**, illustration by James Didusch, from Corner 1929, with permission; **b**, after O'Rahilly and Müller 1987)

most rostral, median part of the neural plate gives rise to the commissural plate from which the anterior commissure and the corpus callosum arise.

Initially, the wall of the neural tube consists of a single layer of neuroepithelial cells, the **germinal neuroepithelium** or **matrix layer**. As this layer thickens, it gradually acquires the configuration of a pseudostratified epithelium. Its nuclei become arranged in more and more layers, but all elements remain in contact with the external and internal surface. Mitosis occurs on the internal, ventricular side of the cell layer only (▶ Chap. 2), and migrating cells form a second layer around the original neural tube. This layer, the **mantle layer** or **intermediate zone**, becomes progressively thicker as more cells are added to it from the germinal neuroepithelium that is now called the **ventricular zone**. The cells of the intermediate zone differentiate into neurons and glial cells. Radial glial cells are present during early stages of neurogenesis. Most radial glial cells transform into astrocytes (▶ Chap. 2). The neurons send axons into an outer layer, the **marginal zone**. The mantle layer, containing the cell bodies, becomes the **grey matter**, and the axonal, marginal layer forms the **white matter**. In the spinal cord, this three-zone pattern is retained throughout development.

Secondary proliferative compartments are found elsewhere in the brain. The **external germinal** or **granular layer** is confined to the cerebellum. It develops from the ventricular zone of the rostral part of the rhombic lip, a thickened germinal zone in the rhombencephalic alar plate, and gives rise to the granule cells of the cerebellum. The **subventricular zone** is found in the lateral and basal walls of the telencephalon. This zone gives rise to a large population of glial cells and to the granule cells of the olfactory bulb. A special role for the outer subventricular zone as a proliferative compartment for neurons has been demonstrated (Kriegstein and Alvarez-Buylla 2009; Lui et al. 2011; ▶ Chaps. 2 and 10).

1.5 Development of the Spinal Cord

After neurulation, the **spinal cord** can be divided into dorsal **alar plates** derived from lateral parts of the neural plate, and ventral **basal plates** derived from its medial parts (◘ Fig. 1.10). The alar and basal plates are separated by the **limiting sulcus (sulcus limitans)** of His (His 1880). The alar plates are united by a small roof plate, and the basal plates by a thin floor plate. The alar plates and incoming dorsal roots form the afferent or sensory part of the spinal cord, whereas the basal plate and its exiting ventral root form the efferent or motor part. The spinal ganglia arise from the neural crest. The development of the alar and basal plates is induced by **extracellular signalling molecules**, secreted by the notochord and the adjacent ectoderm (◘ Fig. 1.10). The protein SHH of the *SHH* gene in the notochord induces the formation of the floor plate. In its turn, the floor plate induces the formation of motoneurons in the basal plate. Bone morphogenetic proteins (BMPs) from the ectoderm induce the formation of the alar and roof plates and of the neural crest. BMP4 and BMP7 induce the expression of the transcription factor 'Slug' in the neural crest and the expression of certain *Pax* transcription factors in the alar plates. SHH suppresses these dorsal *Pax* genes in the ventral half of the spinal cord. Many other genes are involved in the specification of the various progenitor zones and the types of neurons derived from them in the spinal cord (▶ Chap. 6). Motoneurons are the first neurons to develop (Windle and Fitzgerald 1937; Bayer and Altman 2002). They appear in the uppermost spinal segments at approximately embryonic day 27 (about CS 13/14). At this time of development also dorsal root ganglion cells are present. Dorsal root fibres enter the spinal grey matter very early in development (Windle and Fitzgerald 1937; Konstantinidou et al. 1995; ▶ Chap. 6). The first synapses between primary afferent fibres and spinal motoneurons were found in a CS 17 embryo (Okado et al. 1979; Okado 1981). Ascending fibres in the dorsal funiculus have reached the brain stem at CS 16, i.e. at about 37 postovulatory days (Müller and O'Rahilly 1989). The first descending supraspinal fibres from the brain stem have extended into the spinal cord at CS 14 (Müller and O'Rahilly 1988b). Even the late developing pyramidal tract extends as far caudally as the spinomedullary junction at the end of the embryonic period (Müller and O'Rahilly 1990c; ten Donkelaar 2000). The spinal cord then still reaches the end of the vertebral canal. During the foetal period, it 'ascends' to lumbar levels (▶ Chap. 6).

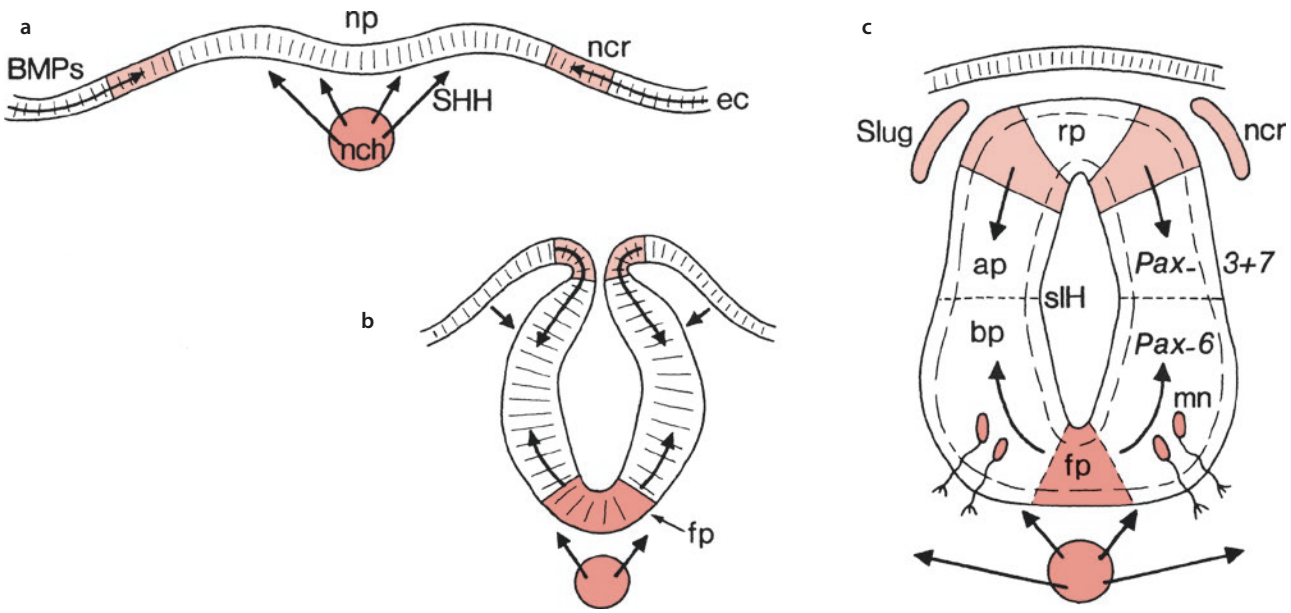

◘ **Fig. 1.10** The development of the spinal cord and the dorsalizing (bone morphogenetic proteins, *BMPs*) and ventralizing (Sonic hedgehog, *SHH*) factors involved. **a** SHH in the notochord (*nch*, *red*) induces the formation of the floor plate (*fp*), after which SHH in the floor plate induces the formation of motoneurons **b, c**. BMP4 and BMP7 (*light red*) from the ectoderm (*ec*) induce Slug in the neural crest (*ncr*) and support the expression of *Pax3* and *Pax7* in the dorsal part of the spinal cord. SHH suppresses the expression of these transcription factors. *ap* alar plate, *bp* basal plate, *mn* motoneurons, *np* neural plate, *rp* roof plate, *slH* sulcus limitans of His. (After Carlson 1999)

1

1.6 Pattern Formation of the Brain

Prospective subdivisions of the brain are specified through **pattern formation**, which takes place in two directions: from medial to lateral, and from rostral to caudal (Lumsden and Krumlauf 1996; Rubenstein and Beachy 1998; ◘ Fig. 1.11). Mediolateral or ventrodorsal pattern formation generates longitudinal areas such as the alar and basal plates, and rostrocaudal pattern formation generates transverse zones (one or more neuromeres). Most likely, the rostrocaudal regionalization of the neural plate is induced already during gastrulation (Nieuwkoop and Albers 1990). In amphibians, the first mesoderm to ingress gives rise to the anterior head mesoderm. The mesoderm that follows will form the chordamesoderm and more lateral mesodermal structures. The anterior mesoderm differs from the chordamesoderm also in the genes that it expresses. Signals from both the anterior mesoderm and the chordamesoderm initiate neural development by inducing neural tissue of an anterior type, i.e. forebrain and midbrain, in the overlying ectoderm along its entire anteroposterior length. A second signal from chordamesoderm alone converts the overlying neuroectoderm induced by the first signal into a posterior type of neural tissue, i.e. hindbrain and spinal cord (► Chap. 2). Endodermal signalling molecules also play an important role in the induction of the rostral part of the CNS (de Souza and Niehrs 2000).

Developmental gene-expression studies show that the vertebrate CNS can be divided into three regions. The anterior region comprises the forebrain and the midbrain, and is characterized by expression of the **homeobox genes** *Emx* and *Otx*. The middle division comprises the isthmic rhombomere (rhombomere 0 or r0; see ► Sect. 1.7.2) and the first rhombomere (r1). It is known as the **midbrain–hindbrain boundary** (**MHB**) or

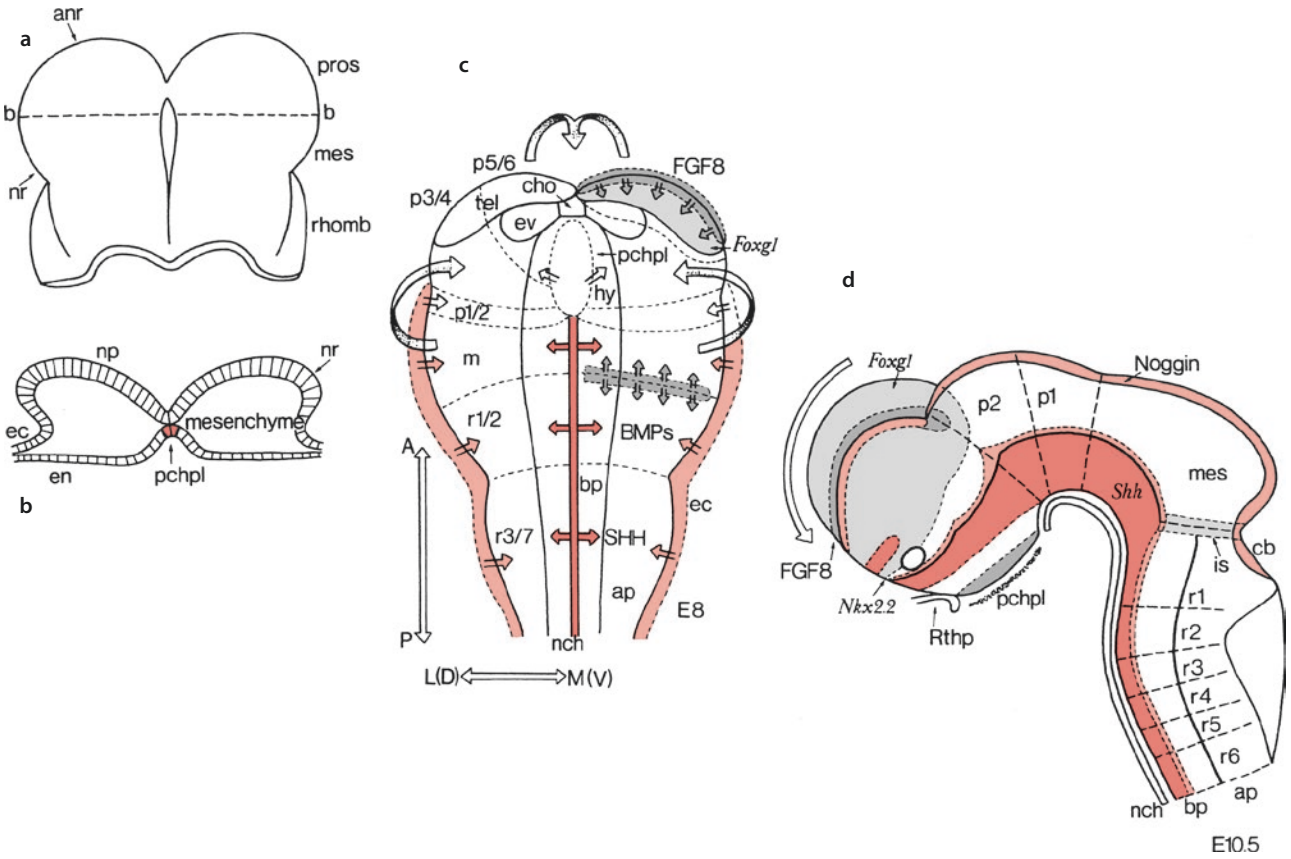

◘ **Fig. 1.11** Bauplan and pattern formation of the mouse brain. **a** The dorsal view of the rostral part of the neural plate (*np*) shows the approximate locations of the prosencephalon (*pros*), mesencephalon (*mes*) and rhombencephalon (*rhomb*), and **b** the transverse section shows the structures involved. The expression of some genes involved in the patterning of the brain is shown in a dorsal view of the neural plate of an E8 mouse **c** and in a median section through the neural tube at E10.5 **d**. The *arrows* indicate the morphogenetic processes involved in the closure of the neural tube. The expression of lateralizing (*L*) or dorsalizing (*D*) signalling molecules such as BMPs is indicated in *light red*, the medializing (*M*) or ventralizing (*V*) factor SHH in *red*, the fibroblast growth factor 8 (*FGF8*) in *dark grey* and brain factor 1 (*Foxg1*) in *grey*. Medial signals induce the basal plate (*bp*), whereas lateral signals induce the alar plate (*ap*). *anr* anterior neural ridge, *cb* cerebellum, *cho* chiasma opticum, *ec* ectoderm, *en* endoderm, *ev* eye vesicle, *hy* hypothalamus, *is* isthmus, *m* mesencephalon, *nch* notochord, *nr* neural ridge, *pchpl* prechordal plate, *p1*, *p6* prosomeres, *Rthp* Rathke's pouch, *r1–r7* rhombomeres, *tel* telencephalon. (After Rubenstein and Beachy 1998; Rubenstein et al. 1998)

isthmocerebellar region. The third region comprises most of the rhombencephalon (r2–r11) and the spinal cord, and is characterized by *Hox* gene expression. **Longitudinal patterning centres** are present along the ventral (notochord and prechordal plate, and later the floor plate) and dorsal (epidermal–neuroectodermal junction, and later the roof plate) aspects of the neural plate and early neural tube. Medial, i.e. **ventralizing**, signals such as SHH play an important role during the formation of the primordia of the basal plate. SHH induces the formation of motoneurons in the spinal cord and brain stem (▶ Chaps. 6 and 7). Lateral, i.e. **dorsalizing**, signals such as BMPs from the adjacent ectoderm induce the formation of the alar plate and the dorsal part of the forebrain. SHH is not only responsible for dorsoventral patterning in the CNS, but also plays a role during the specification of oligodendrocytes, the proliferation of neural precursors and the control of axon growth (Marti and Bovolenta 2002). The BMPs also have a variety of functions (Mehler et al. 1997). ***Holoprosencephaly***, a defect in brain patterning, is the most common structural anomaly of the developing forebrain (Golden 1998; Muenke and Beachy 2000; Sarnat and Flores-Sarnat 2001; Monuki and Golden 2018; ▶ Chap. 9).

Specialized, **transverse patterning centres** are present at specific anteroposterior locations of the neural plate such as the anterior neural ridge, the intrathalamic limiting zone and the already mentioned MHB (◘ Fig. 1.11). They provide a source of secreted factors that establish the regional identity in adjacent domains of the neural tube. The posterior limit of *Otx2* expression marks the anterior limit of the MHB, whereas the anterior limit of *Gbx2* expression marks its posterior limit. In *Otx2* knockout mice, the rostral neuroectoderm is not formed, leading to the absence of the prosencephalon and the midbrain (Acampora et al. 2001; Wurst and Bally-Cuif 2001). In *Gbx2* knockouts, all structures arising from the first two rhombomeres (r0, r1), such as the cerebellum, are absent. Cells in the MHB (the **isthmic organizer**) secrete fibroblast growth factors (FGFs) and Wnt proteins, which are required for the differentiation and patterning of the midbrain and hindbrain (Rhinn and Brand 2001). The **intrathalamic limiting zone** (**zona limitans intrathalamica**) of Rendahl (1924) is important for the establishment of regional identity in the diencephalon (Kiecker and Lumsden 2012). It separates the (dorsal) thalamus from the ventral thalamus or prethalamus (▶ Chaps. 2 and 9). Signals from the **anterior neural ridge** including FGF8 regulate the expression of *Foxg1* (earlier known as *brain factor 1*, *BF1*), a transcription factor that is required for normal telencephalic and cortical morphogenesis (Rubenstein and Beachy 1998; Monuki and Walsh 2001). For structural brain anomalies in patients with *FOXG1* syndrome and in *Foxg1*+/– mice, see Pringsheim et al. (2019) and ▶ Chap. 10. Although much of our insight into these patterning mechanisms relies on studies in mice, humans are subject to a wide variety of naturally occurring mutations (▶ Chap. 9).

1.7 Early Development of the Brain

Lateral and medial views of the developing brain are shown in ◘ Figs. 1.12 and 1.13. The neural tube becomes bent by three flexures: (1) the **mesencephalic flexure** at the midbrain level, already evident before fusion of the neural folds; (2) the **cervical flexure**, situated at the junction between the rhombencephalon and the spinal cord; and (3) the **pontine flexure** in the hindbrain. The three main divisions of the brain (the forebrain or prosencephalon, the midbrain or mesencephalon and the hindbrain or rhombencephalon) can already be recognized when the neural tube is not yet closed. The forebrain soon divides into an end portion, the **telencephalon**, and the **diencephalon**, and the optic vesicles can be identified (◘ Fig. 1.13). With the development of the **cerebellum**, the division of the hindbrain into a rostral part, the **rostral hindbrain**, colloquially called the **'pons'**, and a caudal part, the **caudal hindbrain** (**medulla oblongata** or **myelencephalon**), becomes evident. The junction between the hindbrain and midbrain is relatively narrow and is known as the **rhombencephalic isthmus** (**isthmus rhombencephali**). The first part of the telencephalon that can be recognized is the **telencephalon medium** or **impar**. By CS 15, the future cerebral hemispheres can be recognized. The **cerebral hemispheres** enlarge rapidly so that by the end of the embryonic period they completely cover the diencephalon. Frontal, temporal and occipital poles and the insula become recognizable (◘ Fig. 1.12), whereas an olfactory bulb becomes visible on the ventral surface. Nakashima et al. (2011) used MR microscopic imaging for a morphometric analysis of the brain vesicles during the embryonic period.

1.7.1 Imaging of the Embryonic Brain

The introduction of the ultrasound method has opened new possibilities for studying the human embryonic brain. The use of the transvaginal route has so greatly improved the image quality that a detailed description of the living embryo and early foetus has become possible (◘ Fig. 1.14). Ultrasound data show agreement with the developmental time schedule described in the Carnegie staging (CS) system (Blaas et al. 1994, 1995a, b; Blaas and Eik-Nes 1996, 2009; van Zalen-Sprock et al. 1996; Blaas 1999; Pooh 2009; Pooh et al. 2003, 2011). Human development and possible maldevelopment can be followed in time. Three-dimensional (3D) ultrasound tech-

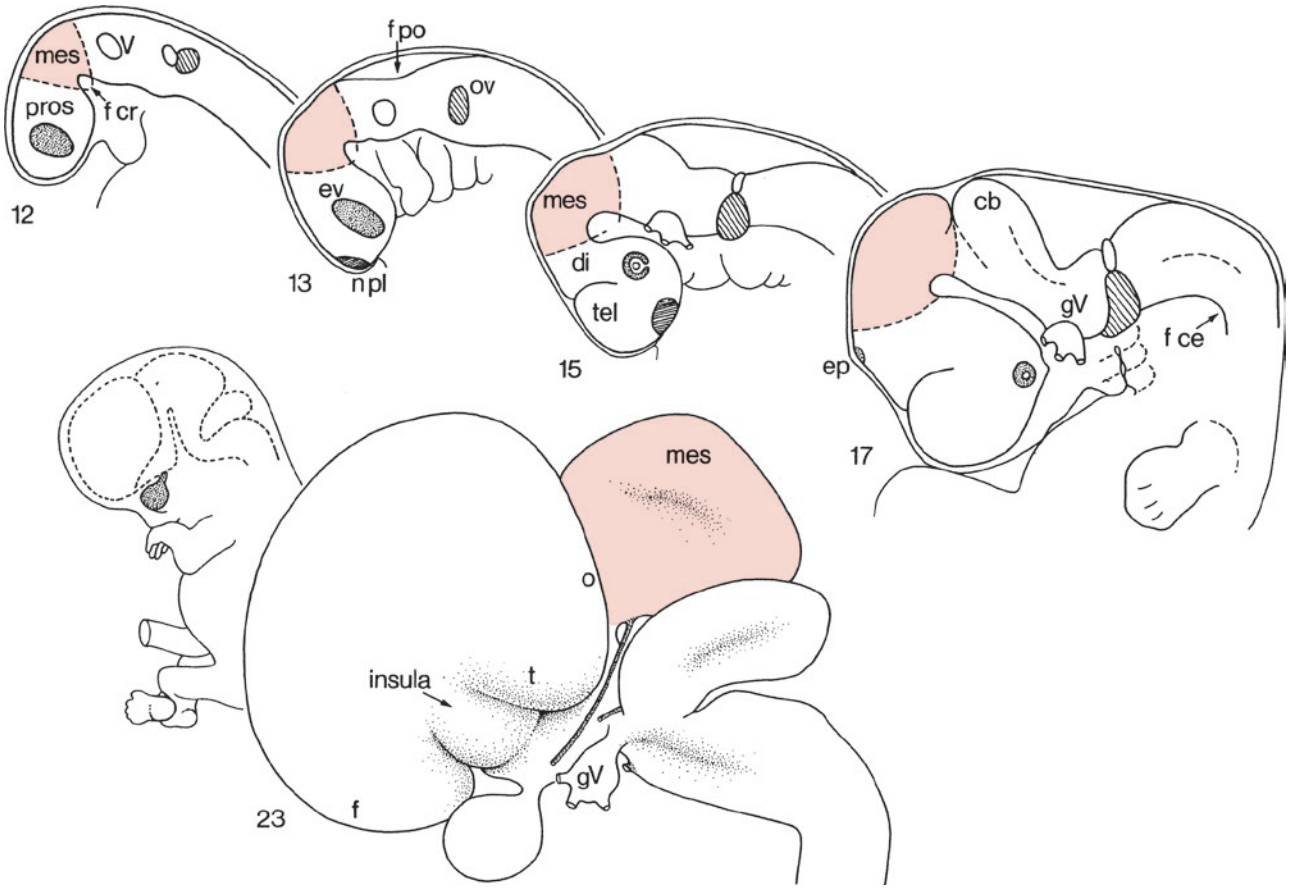

Fig. 1.12 Lateral views of the developing brain in CS 12, 13, 15, 17 and 23. The mesencephalon is indicated in *light red*. *cb* cerebellum, *di* diencephalon, *ep* epiphysis, *ev* eye vesicle, *f* frontal lobe, *f ce* flexura cervicalis, *f cr* flexura cranialis, *f po* flexura pontina, *gV*, *V* trigeminal ganglion, *mes* mesencephalon, *n pl* nasal placode, *o* occipital lobe, *pros* prosencephalon, *t* temporal lobe, *tel* telencephalon. (After O'Rahilly and Müller 1999)

niques have made it possible to reconstruct the shape of the brain ventricles and to measure their volumes (Blaas et al. 1995a, b; Blaas 1999; Blaas and Eik-Nes 2002). Anomalies of the ventricular system such as diverticula are rare (Hori et al. 1983, 1984a). Accessory ventricles of the posterior horn are relatively common and develop postnatally (Hori et al. 1984b; Tsuboi et al. 1984).

1.7.2 Neuromeres

Morphological segments or neuromeres of the brain were already known to von Baer (1828), and described for the human brain by Bartelmez (1923) and Bergquist (1952), and for many other vertebrates (Nieuwenhuys 1998). **Neuromeres** are segmentally arranged transverse bulges along the neural tube, particularly evident in the hindbrain (Fig. 1.15). Only more recently, interest in neuromeres was greatly renewed owing to the advent of gene-expression studies on development, starting with the homeobox genes. The expression of *HOX* genes in the developing human brain stem is directly comparable to that of *Hox* genes in mice (Vieille-Grosjean et al. 1997). Each rhombomere is characterized by a unique combination of *Hox* genes, its *Hox* code. The timing and sequence of appearance of neuromeres and their derivatives were studied in staged human embryos (Müller and O'Rahilly 1997; Fig. 1.16). In the human brain, they are usually abbreviated with a capital (M1, P1, Rh1), in all other vertebrates without (m1, p1, r1). The neuromeres of the forebrain, midbrain and hindbrain were determined morphologically on the basis of sulci, mitotic activity in the walls and fibre tracts. Six **primary neuromeres** appear already at CS 9 when the neural folds are not fused (Fig. 1.8b): prosencephalon, mesencephalon and four rhombomeres (A–D). Sixteen **secondary neuromeres** can be recognized from about CS 11. They gradually fade after CS 15 (Fig. 1.13). Eight **rhombomeres** (**Rh1–8**), an **isthmic neuromere** (**I**), two **mesomeres** (**M1, M2**) of the midbrain, two **diencephalic neuromeres** (**D1, D2**) and one **telencephalic neuromere** (**T**) have been distinguished. The diencephalic neuromere D2 can be further subdivided into the **synencephalon**, the **caudal parencephalon** and the **rostral**

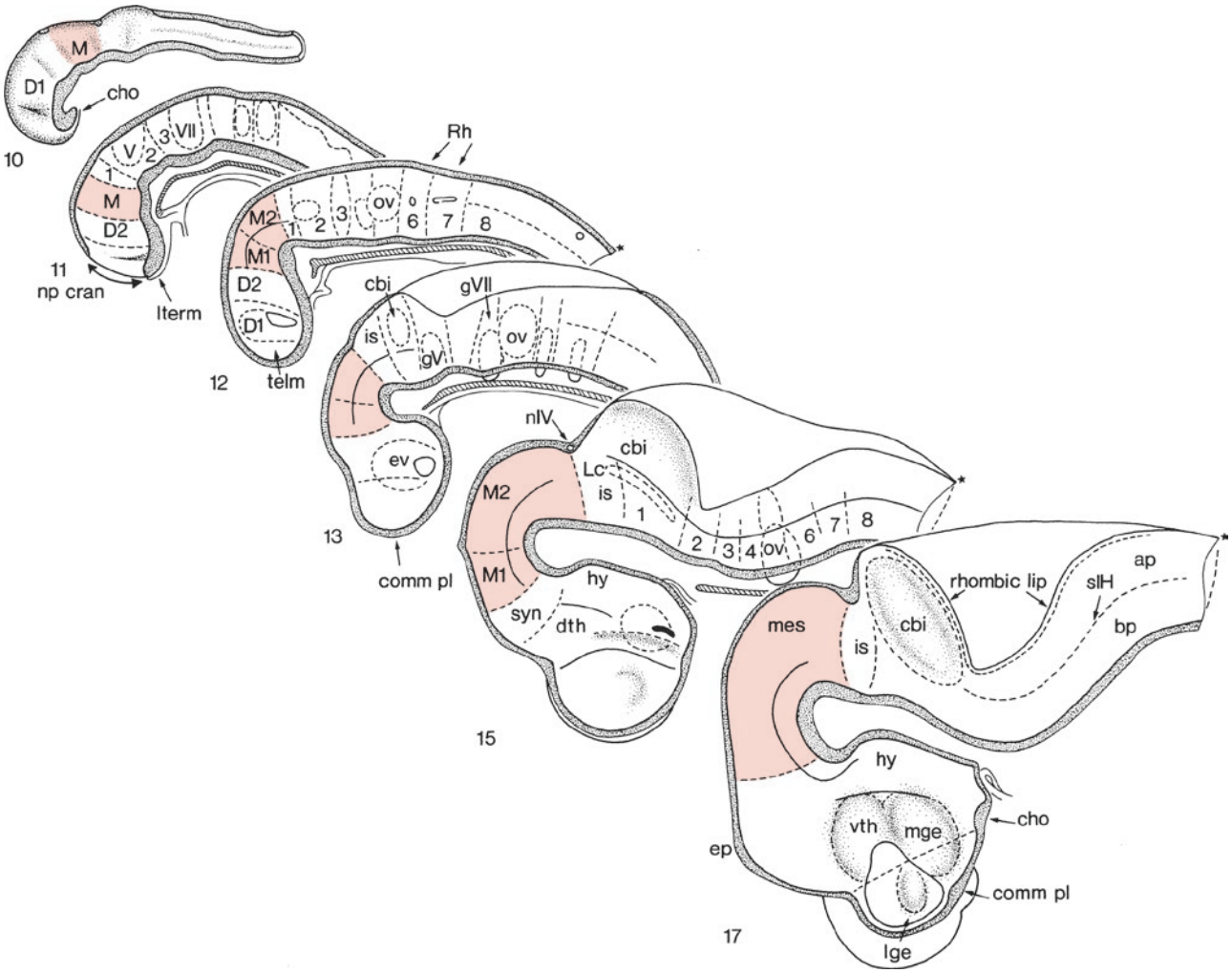

Fig. 1.13 Medial views of the developing brain in CS stages 10–13, 15 and 17. The mesomeres (*M*, *M1*, *M2*) and the mesencephalon (*mes*) are indicated in *light red*. *Asterisks* indicate the spinomedullary junction. *ap* alar plate, *bp* basal plate, *cbi* internal cerebellar bulge, *cho* chiasma opticum, *comm pl* commissural plate, *D1*, *D2* diencephalic neuromeres, *dth* dorsal thalamus, *ep* epiphysis, *ev* eye vesicle, *gV* trigeminal ganglion, *gVII* facial ganglion, *hy* hypothalamus, *is* isthmus, *Lc* locus coeruleus, *lge* lateral ganglionic eminence, *lterm* lamina terminalis, *mge* medial ganglionic eminence, *np* cran cranial neuropore, *nIV* nervus trochlearis, *ov* otic vesicle, *1–8* rhombomeres, *slH* sulcus limitans of His, *syn* synencephalon, *telm* telencephalon medium, *vth* ventral thalamus. (After O'Rahilly and Müller 1999)

parencephalon. Neuromere D1 was suggested to give rise to the optic vesicles and the medial ganglionic eminences (Müller and O'Rahilly 1997; O'Rahilly and Müller 2008). It should be emphasized, however, that Müller and O'Rahilly's subdivision of the prosencephalon is rather arbitrary. The prosomere D1 is defined as a far too large neuromere extending to the rostral border of the chiasmatic plate. It seems more likely that the **prosomeric model** developed by Puelles and Rubenstein (2003) can also be applied to human embryos. In this model, the primary prosencephalon becomes divided into the **caudal prosencephalon**, giving rise to the prosomeres P1–P3 (the **diencephalon**), and the **secondary prosencephalon**, giving rise to the hypothalamus, the eye vesicles, the neurohypophysis and the entire telencephalon including the medial and lateral ganglionic eminences (Fig. 1.17). In fact, the human prosomeres D1 and T together form the secondary prosencephalon. Consequently, the medial ganglionic eminence and the hypothalamus arise from the secondary prosencephalon. A recent version of the prosomeric model is shown in Fig. 1.18.

Each neuromere has **alar** (dorsal) and **basal** (ventral) components. In the developing spinal cord and brain stem, the **limiting sulcus** of His divides the proliferative compartments into alar and basal plates. The mesencephalic part of the sulcus is not continuous with a more rostral, diencephalic sulcus (Keyser 1972; Gribnau and Geijsberts 1985; Müller and O'Rahilly 1997; Fig. 1.13). Studies in mice (Bulfone et al. 1993; Puelles and Rubenstein 1993; Shimamura et al. 1995; Rubenstein et al. 1998; Martínez et al. 2012; Medina and Abellán 2012; Puelles et al. 2012) showed that some

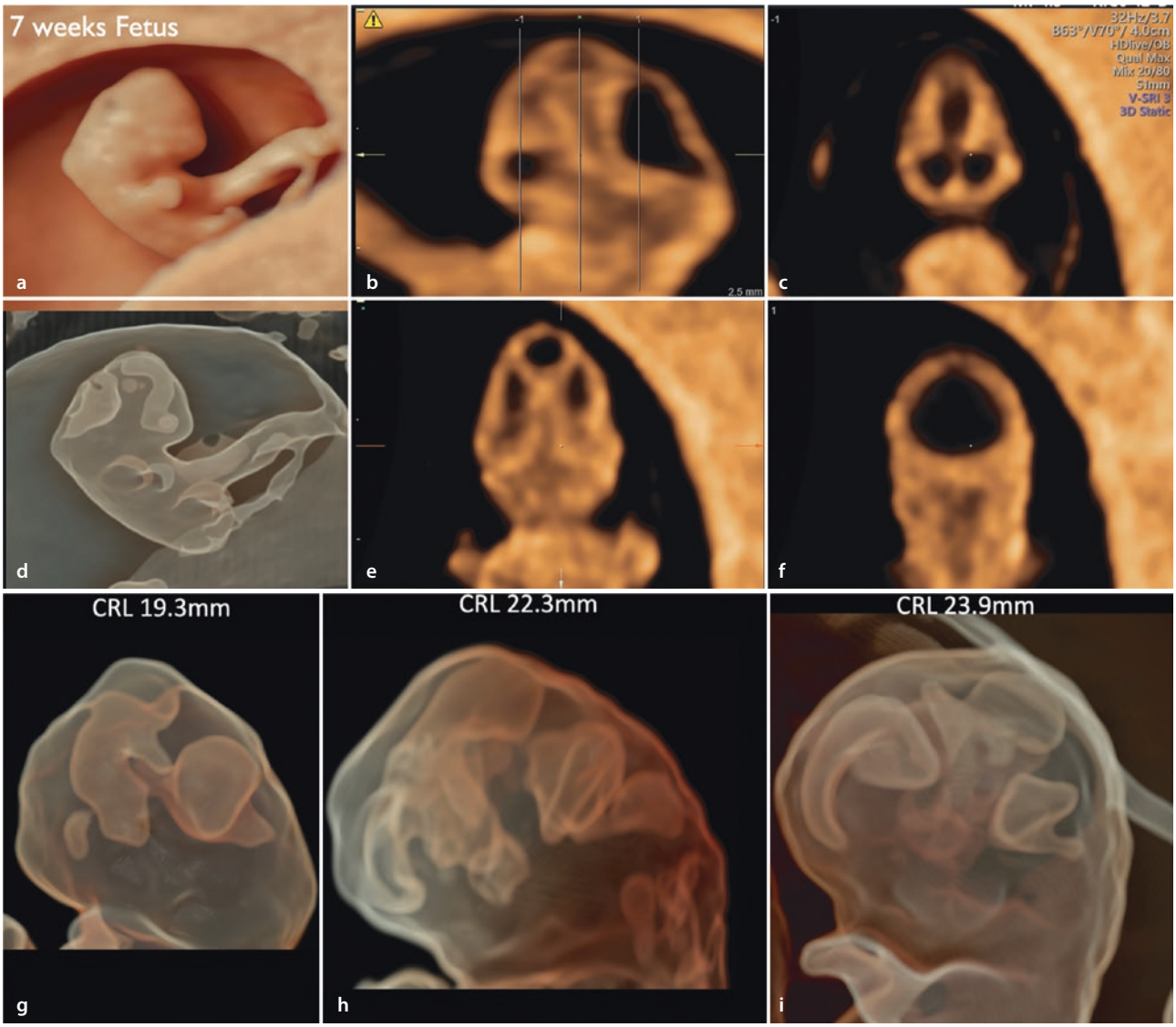

Fig. 1.14 Ultrasound images in human embryos of seven **a–f** and seven to eight gestational weeks (GW; **g–i**). In the upper set of figures **a–f**, surface rendering image **a** and silhouette ultrasound image **b** showing forebrain, midbrain and hindbrain. In **c–f**, tomographic ultrasound images, a sagittal section **c** showing the level of the coronal sections in **d–f**. In the lower set of figures **g–i**, silhouette ultrasound images at GW 7–8; crown-rump length: 19.3 mm (**g**), 22.3 mm (**h**) and 23.9mm (**i**). These ultrasound images show the rapid development of the telencephalon (*arrows*). These images were kindly provided by Ritsuko Pooh (Osaka)

genes are expressed in the alar plate only, others only in the basal plate (Fig. 1.11). One gene, *Nkx2.2*, is expressed along the longitudinal axis of the brain, ending in the chiasmatic region. Based on these findings, in all murine prosomeres alar and basal parts are distinguished (Rubenstein et al. 1998; Puelles et al. 2000; Puelles and Rubenstein 2003; Martínez et al. 2012; Puelles 2013; Fig. 1.18). Puelles and Verney (1998) applied the prosomeric subdivision to the human forebrain. The prosomeric model of the vertebrate forebrain was implemented in the HUDSEN Atlas (▶ http://www.hudsen.org), a three-dimensional spatial framework for studying gene expression in the developing human brain (Kerwin et al. 2010).

In mice (▶ Chap. 2), the prosencephalon has been divided into six **prosomeres**, numbered p1–p6 from caudal to rostral. Prosomeres p1–p3 form the diencephalon. The prosomeres p4–p6, together known as a protosegment, form the **secondary prosencephalon** (Rubenstein et al. 1998; Puelles et al. 2000, 2012, 2013; Puelles and Rubenstein 2003; Martínez et al. 2012; Puelles 2013, 2019), from which the hypothalamus, both eye vesicles, the neurohypophysis and the telencephalon arise. The basal part of the secondary prosencephalon gives rise to the basal part of the hypothalamus, whereas from the alar part, the alar part of the hypothalamus and the entire telencephalon, i.e. the cerebral cortex and the subcortical centres, such as the basal ganglia, arise. The eye

Fig. 1.15 Dorsal view of a malformed embryo (CS 14) showing the bulging of several rhombomeres. (Kindly provided by Kohei Shiota, Kyoto)

vesicles and the neurohypophysis arise from the most rostral part of the secondary prosencephalon, i.e. the **acroterminal region**. More recently, Puelles et al. (2012) subdivided the secondary prosencephalon into two hypothalamic 'prosomeres' (hp2 and hp1) and the acroterminal region (Fig. 1.18; ▶ Chaps. 2 and 9).

The **diencephalon** in its classic, **columnar view** (Herrick 1910; Droogleever Fortuyn 1912) was divided into four dorsoventrally arranged columns separated by ventricular sulci, i.e. the epithalamus, the dorsal thalamus, the ventral thalamus and the hypothalamus. Extensive embryological studies by the Swedish school of neuroembryologists (Bergquist and Källén 1954) and a more recent Spanish school initiated by Luis Puelles (1995) made it clear that the thalamic 'columns' are derived from transversely oriented zones, the prosomeres. The prosomeres p1–p3 form the diencephalon: p1 is the synencephalon, p2 the caudal parencephalon and p3 the rostral parencephalon. These three segmental units contain in their alar domains (Fig. 1.18; Puelles et al. 2008; Puelles et al. 2012, 2013; Puelles 2019), from caudal to rostral, the pretectum with the pretectal nuclei and the posterior commissure (p1), the epithalamus with the habenular nuclei, and the thalamus (p2), and the prethalamus with the prethalamic reticular nucleus and the zona incerta, and the eminentia prethalami (p3). The diencephalic basal plate contains the diencephalic part of the substantia nigra–ventral tegmental area (VTA) complex, the interstitial nucleus of Cajal and related nuclei and the fields of Forel, collectively described as the prerubral or diencephalic tegmentum (TNA 2017). In several aspects, the diencephalic basal region shares characteristics with the midbrain, so 'mesodiencephalic' may also be a useful descriptor. The entire hypothalamus arises from the alar and basal components of the secondary prosencephalon. The secondary prosencephalon is currently divided into three parts: (1) the **hypothalamic and telencephalic prosomere 1** (hp1), from which the caudal or peduncular hypothalamus derives; (2) the **hypothalamic and telencephalic prosomere 2** (hp2), from which the rostral or terminal hypothalamus derives; and (3) the **acroterminal region**, from which the eye vesicle and the neurohypophysis derive (Fig. 1.18). The entire telencephalon, pallium and subpallium derive from the alar components of the secondary prosencephalon.

A relatively small set of genes is sufficient to establish the rostrocaudal general plan of the CNS (Puelles 2013, 2019; Watson et al. 2019). Those vital to brain stem development include the *Pax* group, *Otx2*, *Wnt1*, *Gbx2*, *Fgf8*, *Shh* and the family of the *Hox* genes. *Pax6* establishes the boundary between the diencephalon and the midbrain; *Otx2* is expressed in the forebrain and midbrain, but not in the hindbrain; *Gbx2* is expressed in the most rostral part of the hindbrain (isthmus and r1); *Fgf8* is selectively expressed in the isthmus; and the *Hox* genes are expressed from r2 to the end of the spinal cord. Since the cerebellum is a developmental dorsal alar derivative of the isthmus and the first rhombomere, it is also an intrinsic part of the hindbrain. There is now need to harmonize the parts of the neuromeric hindbrain with the older subdivision into pons and medulla oblongata. Watson et al. (2019) proposed to group the region from the isthmus to the sixth rhombomere as the **rostral hindbrain** and rhombomeres 7–11 as the **caudal hindbrain**. As a consequence, several structures traditionally included within the caudal mesencephalon in fact arise from the isthmic rhombomere and should be included within the isthmic region of the prepontine tegmentum (Fig. 1.19). Based on the distribution of the *Otx2* gene, Puelles (2019) argued that the midbrain belongs to the forebrain as it was already suggested by His (1893, 1895).

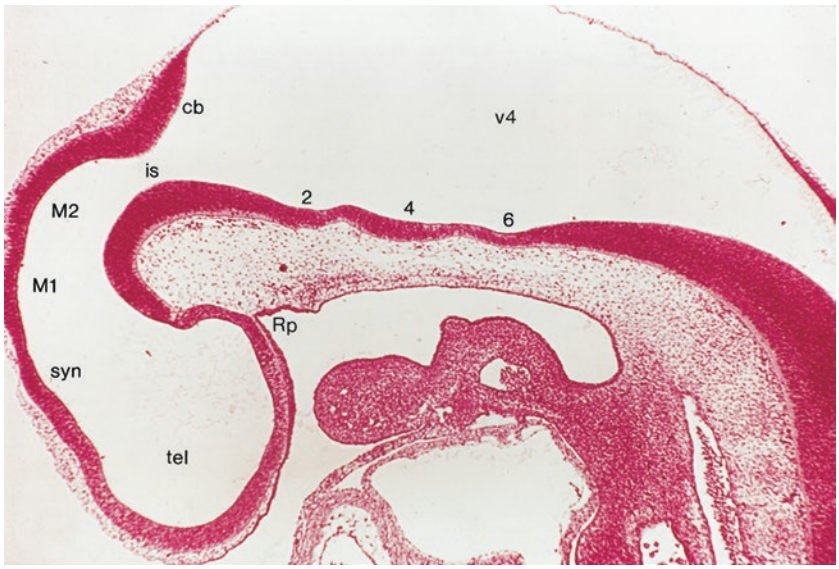

Fig. 1.16 Median section of a CS 13 embryo. Rhombomeres *2*, *4* and *6* can be recognized by ventral bulges. *cb* cerebellum, *is* isthmus, *M1*, *M2* mesomeres, *Rp* Rathke's pouch, *syn* synencephalon, *tel* telencephalon, *v4* fourth ventricle. (From O'Rahilly 1975, with permission)

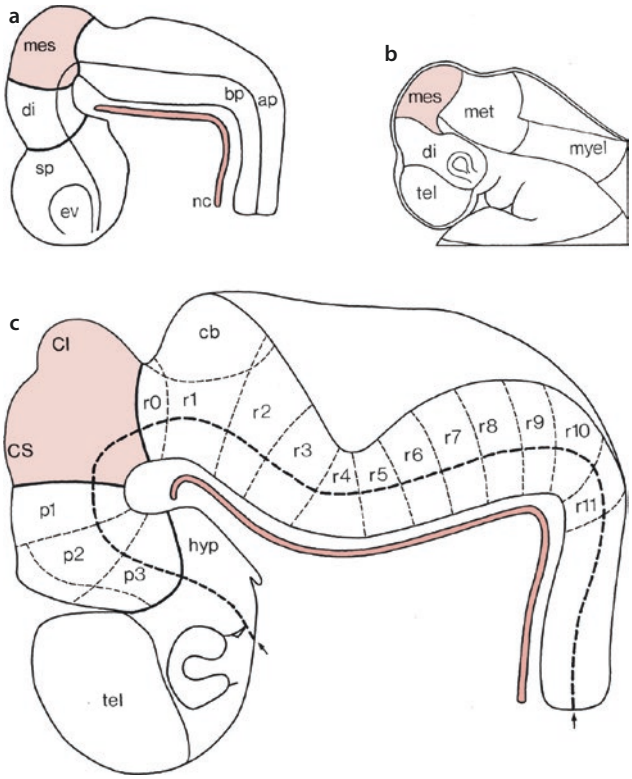

Fig. 1.17 **a, c** Segmentation of the human brain; **b** shows the classic O'Rahilly and Müller subdivision. *ap* alar plate, *bp* basal plate, *cb* cerebellum, *CI* colliculus inferior, *CS* colliculus superior, *di* diencephalon, *ev* eye vesicle, *hyp* hypothalamus, *mes* mesencephalon (in *light red*), *met* metencephalon, *myel* myelencephalon, *nc* notochord (in *medium red*), *p1–p3* prosomeres, *r0–r11* rhombomeres, *sp* secondary prosencephalon, *tel* telencephalon (see text for further explanation). (After Puelles et al. 2008)

The subdivision of the **mesencephalon** into two, almost even large, **mesomeres** has also been questioned. Fate mapping and gene expression data showed that only a very small caudal mesomere 2 can be distinguished, the large remainder of the mesencephalon arising from the rostral mesomere 1 (Martínez et al. 2012; Fig. 1.19; ▶ Chap. 7). With the site-specific recombinase technique, by which transient developmental expression can trigger persistent expression of a reporter gene, the *Fgf8–Cre* lineage, it was possible to sharply define the presumptive isthmic territory (Watson et al. 2017). The **isthmic region** so defined contains the trochlear nucleus, the dorsal raphe nucleus, the dorsal nucleus of the lateral lemniscus and the vermis of the cerebellum. The cerebellar hemispheres arise from the first rhombomere that lacks *Fgf8* expression. Other characteristics of the isthmus are: (1) it contains **serotonergic raphe neurons**, whereas such neurons are not generated in the midbrain (Alonso et al. 2013); the rostral part of the dorsal raphe nucleus extends into the caudal midbrain as a result of migration from the isthmus; and (2) it houses the hindbrain **cholinergic neurons**, the parabigeminal nucleus (Ch8), the laterodorsal nucleus (Ch6) and the pedunculopontine or pedunculotegmental nucleus (Ch5). It should also be emphasized that the decussation of the superior cerebellar peduncles lies across the floor of the isthmus as already described by His (1895), not in the newly defined midbrain.

In colloquial neuroanatomy, the term **pons** is used for the region that extends from the midbrain to the myelencephalon. In a transverse section through the pons at the level of the abducens nucleus, the trape-

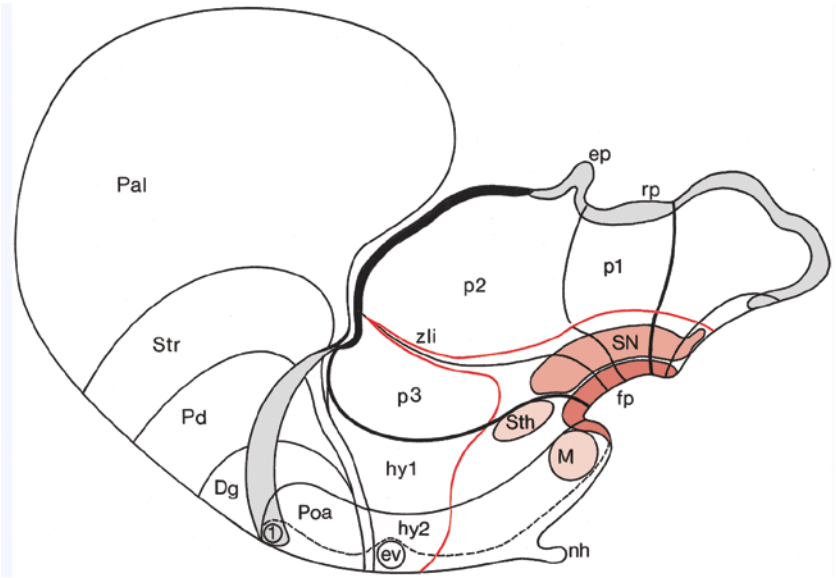

Fig. 1.18 Prosomeric model of the mouse brain. The roof plate (*rp*) has been indicated in *light grey*, in between the two parts, the choroid plexus of the third ventricle is shown in *black*. The *red line* separates the alar and basal parts. The floor plate (*fp*) is shown in *red*, the substantia nigra (*SN*) in *medium red* and the subthalamic nucleus (*Sth*) and the mammillary body (*M*), both derivatives of the hypothalamic basal plate, in *light red*. *Dg* diagonal band, *ep* epiphysis, *ev* eye vesicle, *hy1*, *hy2* hypothalamic prosomeres, *nh* neurohypophysis, *Pal* pallium, *Pd* pallidum, *Poa* preoptic area, *p1–p3* diencephalic prosomeres, *Str* striatum, *zli* zona limitans intrathalamica. (After Puelles et al. 2012; see text for further explanation)

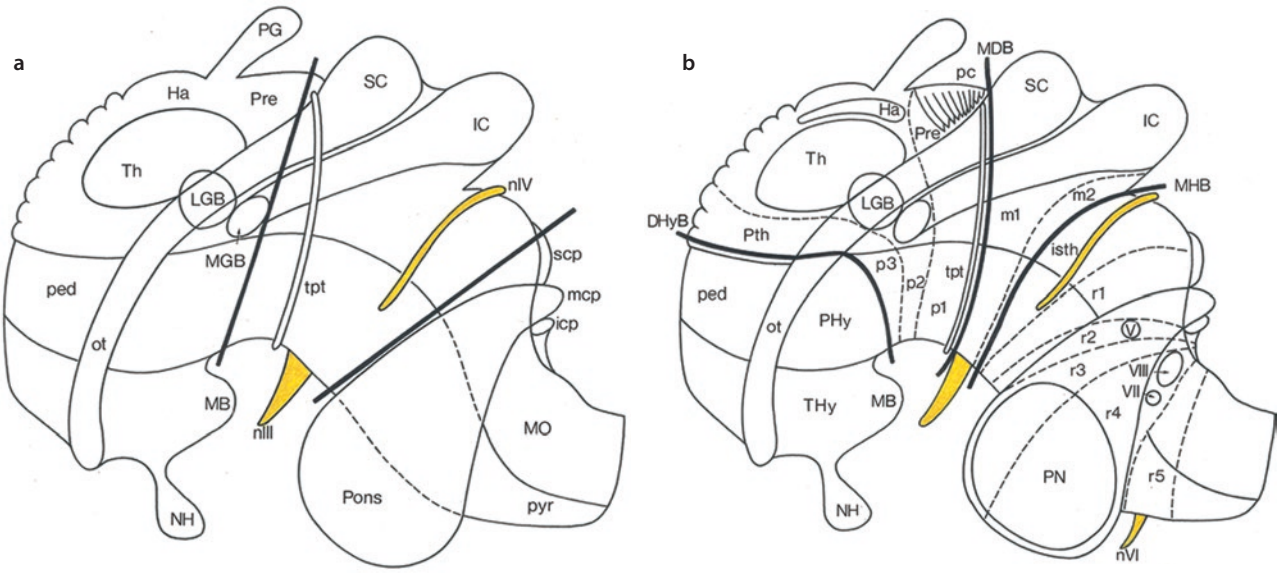

Fig. 1.19 Diagrams showing **a** the traditional view of the mesencephalon and **b** the new, prosomeric view (modified after Puelles 2019 Front Neuroanat 13:20; with permission, courtesy Luis Puelles, Murcia; see text for explanation; from ten Donkelaar 2020). In the prosomeric model, part of the caudal mesencephalon is included in the rostral hindbrain, whereas the pretectum and related tegmentum are included in the diencephalon. The diencephalohypothalamic boundary (*DHyB*) marks the border between the hypothalamus and the diencephalon, the midbrain–diencephalic boundary (*MDB*) that between the diencephalon and the midbrain and the midbrain–hindbrain boundary (*MHB*) that between the midbrain and the rostral hindbrain. *Ha* habenula, *IC* inferior colliculus, *icp* inferior cerebellar peduncle, *isth* isthmocerebellar rhombomere (r0), *LGB* lateral geniculate nucleus, *MB* mammillary body, *mcp* middle cerebellar peduncle, *MGB* medial geniculate nucleus, *MO* medulla oblongata, *NH* neurohypophysis, *ot* optic tract, *m1*, *m2* mesomeres, *pc* posterior commissure, *ped* cerebral peduncle, *PG* pineal gland, *PHy* peduncular hypothalamus, *PN* pontine nuclei, *Pre* pretectum, *Pth* prethalamus, *pyr* pyramid, *p1–p3* diencephalic prosomeres, *r1–r5* rhombomeres, *SC* superior colliculus, *scp* superior cerebellar peduncle, *Th* thalamus, *Thy* terminal hypothalamus, *tpt* transverse peduncular tract, *nIII* oculomotor nerve, *nIV* trochlear nerve, *V* trigeminal nerve root, *nVI* abducens nerve, *VII* facial nerve, *VIII* vestibulocochlear nerve

zoid body separates the pontine tegmentum from the basilar part of the pons. The term **pons**, however, as **pons Varolii**, means the large protrusion with the pontine nuclei and associated fibre pathways. In fact, the pontine nuclei arise from the lower rhombic lip in r6 and r7, and migrate to the ventral margin of r3 and r4. Therefore, the term 'pons' as a regional descriptor of a zone ventral to the cerebellum reaching from the midbrain to the medulla oblongata should be abandoned, although this will take a long time, especially in clinical terms. From an ontological point of view, the terms **prepontine**, **pontine** and **retropontine** (or **pontomedullary**) **tegmentum** are preferred (Puelles et al. 2013; Watson et al. 2019; ◘ Fig. 1.20). The term pons can be properly applied to the nuclei and crossing fibres of the traditional basilar part of the pons. The substantial prepontine tegmentum includes the isthmus (r0) and rhombomere 1, and contains the trochlear nucleus, the parabigeminal nucleus, the pedunculopontine or pedunculotegmental nucleus, the locus coeruleus, the interpeduncular nucleus and the parabrachial nuclei. The pontine tegmentum (r2–4) includes among others the motor trigeminal nucleus. Other structures, such as the trapezoid body, the superior olivary complex and the abducens nucleus, are strictly retropontine (r5, r6) and associated with rhombomere 5.

Currently, the **hindbrain** is subdivided into 12 **rhombomeres** (r0–r11), counting the isthmus as r0 (Martínez et al. 2012; Watson 2012; Watson et al. 2019; ◘ Fig. 1.20). The rostral hindbrain corresponds to the part influenced by the isthmic organizer and can be divided into the isthmus or r0 and rhomobomere 1. The large remainder of the hindbrain is marked by the expression of *Hox* genes and can be divided into ten segments (r2–r11). Rhombomeres r2–r6 can be recognized as overt bulges separated by constrictions in the embryonic hindbrain. The caudal hindbrain was first subdivided into two rhombomeres, r7 and r8 (Lumsden and Krumlauf 1996). Fate mapping and differential *Hox* gene expression in the avian medulla oblongata (Marín et al. 2008) suggested a further subdivision into rhombomeres r7–r11. Rodent data also suggest such a subdivision (Watson 2012; Puelles et al. 2013; Tomás-Roca et al. 2016; Watson et al. 2019).

1.7.3 The Ganglionic Eminences

At first, each cerebral hemisphere consists of a thick basal part, the **subpallium**, giving rise to the basal ganglia, and a thin part, the **pallium**, that becomes the future cerebral cortex. The subpallium appears as medial and lateral elevations, known as the **ganglionic** (*Ganglionhügel* of His 1889) or **ventricular eminences** (◘ Fig. 1.21). The caudal part of the ventricular eminences is also known as the *c***audal ganglionic eminence**, and gives rise to the subpallial parts of the amygdala. The **medial ganglionic eminence** is involved in the formation of the globus pallidus, whereas the larger **lateral ganglionic eminence** gives rise to the caudate nucleus, the putamen and olfactory bulb interneurons (▶ Chap. 9). As the internal capsule develops, its fibres separate the caudate nucleus

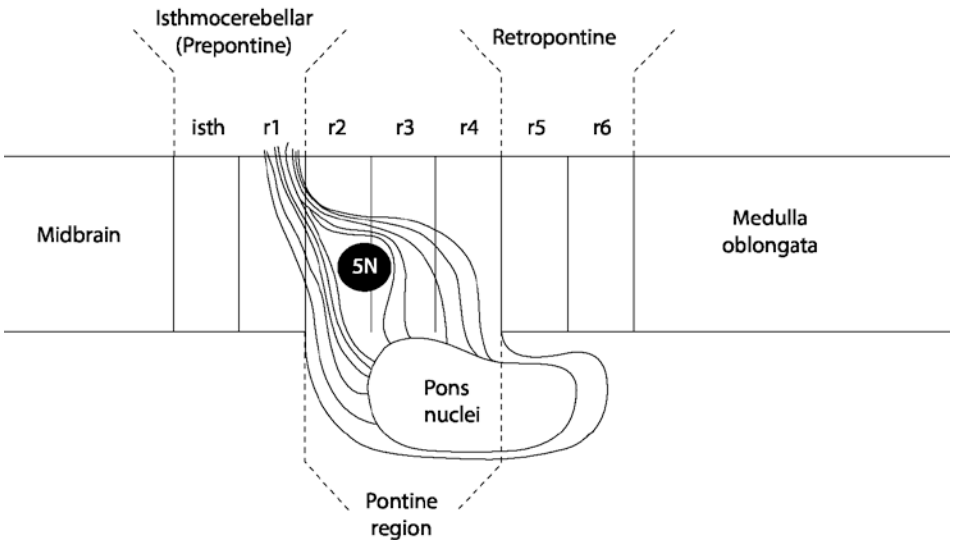

◘ **Fig. 1.20** New view on the hindbrain organization (from Watson C, Bartholomaeus C, Puelles L 2019 *Time for radical changes in brain stem nomenclature – applying the lessons from developmental gene patterns.* Front Neuroanat 13:10; with permission; courtesy Charles Watson, Perth). The diagram shows the current subdivision of the rostral hindbrain into prepontine or isthmocerebellar, pontine and retropontine regions. The prepontine part arises from the isthmic rhombomere (*isth*) or r0 and the rhombomere r1, the pontine part from the rhombomeres r2–r4 and the retropontine part from the rhombomeres r5 and r6. The caudal hindbrain or medulla oblongata arises from the rhombomeres 7–11

from the putamen, and the thalamus and the subthalamus from the globus pallidus. The three ventricular eminences are also involved in the formation of the cerebral cortex. The pyramidal cells of the cerebral cortex arise from the ventricular zone of the pallium, but the cortical GABAergic interneurons arise from the three ganglionic eminences, the medial and caudal eminence in particular (Parnavelas 2000; Anderson et al. 2001; Marín and Rubenstein 2001; Clowry 2015; Alzu'bi et al. 2017a, b; Clowry et al. 2018; Alzu'bi and Clowry 2019; ▶ Chap. 9). In the human forebrain, cortical interneurons were assumed to arise in the ventricular and subventricular zones of the dorsal telencephalon as well (Letinić et al. 2002; Rakic 2009). More recent studies (Hansen et al. 2013; Ma et al. 2013; Alzu'bi and Clowry 2019), however, suggest that intracortical interneurogenesis arises from dorsal progenitors or from ventral progenitors that have migrated dorsally and continue dividing. The caudal part of the ganglionic eminence also gives rise to a contingent of GABAergic neurons for thalamic association nuclei such as the pulvinar through a transient foetal structure, the **gangliothalamic body** (Rakić and Sidman 1969; Letinić and Kostović 1997; Letinić and Rakic 2001).

1.8 Foetal Development of the Brain

The most obvious changes in the foetal period are (1) the outgrowth of the cerebellar hemispheres and the formation of its median part, the vermis; (2) the continuous expansion of the cerebral hemispheres, the formation of the temporal lobe and the formation of sulci and gyri; and (3) the formation of commissural connections, the corpus callosum in particular. The foetal period has been extensively illustrated in Bayer and Altman's *Atlas of Human Central Nervous System Development* (Bayer and Altman 2003, 2005, 2006, 2007). More recently, Ivica Kostović and co-workers focussed on the transient zones, the subplate in particular, and their role in brain

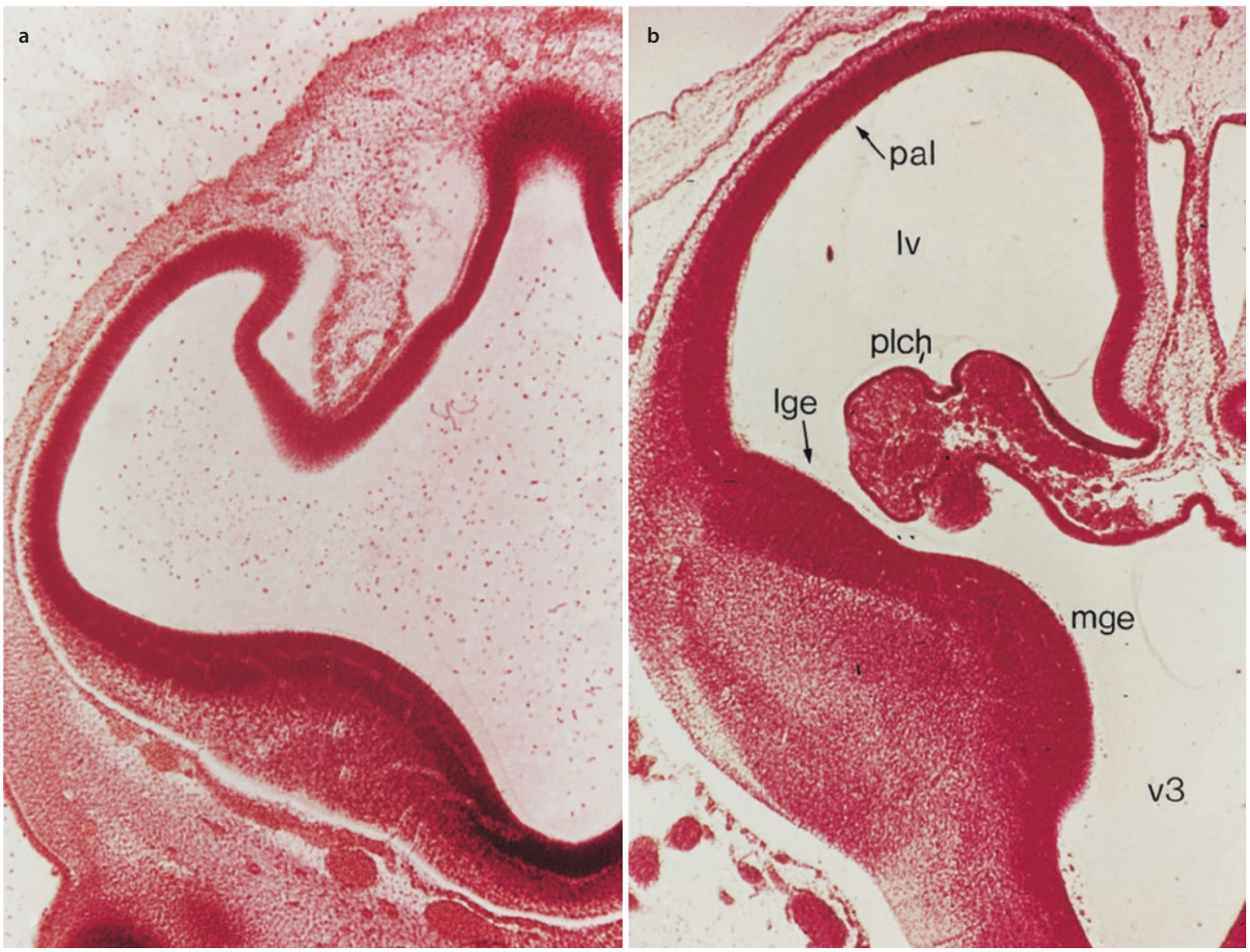

Fig. 1.21 Transverse sections through the human forebrain, showing the developing ganglionic or ventricular eminences at stages 17 **a** and 20 **b**, respectively. *lge* lateral ganglionic eminence, *lv* lateral ventricle, *mge* medial ganglionic eminence, *pal* pallium, *plch* plexus choroideus, *v3* third ventricle. (From O'Rahilly 1975, with permission)

development (Kostović et al. 2019a, b). For a quantitative approach to brain growth, gyrus formation and myelination, see Gilles and Nelson (2012).

Takakuwa et al. (2021) assessed sequential morphological and morphometric changes in the foetal brain using high-resolution T1-weighted MRI scans from 21 cases preserved at Kyoto University. MRI sectional views and 3D reconstructions of the whole brain revealed the following changes in its external morphology and internal structures (◘ Figs. 1.22 and 1.23). The cerebrum's gross morphology, lateral ventricle and choroid plexus, cerebral wall, basal ganglia, thalamus and corpus callosum were assessed. The development of the cerebral cortex, white matter structure and basal ganglia can be well characterized using MRI scans (see also Terashima et al. 2021). The insula became apparent and deeply impressed as brain growth progressed. A thick, densely packed cellular ventricular/subventricular zone and ganglionic eminence became apparent at high signal intensity. The corpus callosum was first detected at crown-rump length (CRL) of 62 mm. A primary sulcus on the medial part of the cortex (the cingulate sulcus) became evident in the sample with CRL 114 mm.

1.8.1 The Cerebellum

The development of the **cerebellum** takes place largely in the foetal period (◘ Fig. 1.24). The cerebellum arises bilaterally from the alar layers of the isthmic rhombomere (r0) and the first rhombomere (◘ Fig. 1.13). Early in the foetal period, the two cerebellar primordia are said to unite dorsally to form the vermis. Sidman and Rakic (1982), however, advocated Hochstetter's (1929) view that such a fusion does not take place, and suggested one cerebellar primordium (the **cerebellar tubercle** or **tuberculum cerebelli**). The tuberculum cerebelli consists of a band of tissue in the dorsolateral part of the alar plate that straddles the midline in the shape of an inverted V (◘ Fig. 1.24). The arms of the V are directed caudally as well as laterally, and thicken enormously, accounting for most of the early growth of the cerebellum. The rostral, midline part of the V, however, remains small and relatively inconspicuous. The further morphogenesis of the cerebellum can be summarized as follows: (1) the caudally and laterally directed limbs of the tuberculum cerebelli thicken rapidly during the sixth postovulatory week and bulge downwards into the fourth ventricle (on each side the internal cerebellar bulge or *innerer Kleinhirnwulst* of Hochstetter, which together form the **cerebellar body** or **corpus cerebelli**); (2) during the seventh week, the rapidly growing cerebellum bulges outwards as the external cerebellar bulges (*äusserer Kleinhirnwulst* of Hochstetter) that represent the **flocculi**, which are delineated by the posterolateral fissures; (3) during the third month of development, i.e. early in the foetal period, growth of the midline component accelerates and begins to fill the gap between the limbs of the V, thereby forming the **vermis**; and (4) by the 12th–13th weeks of development, outward, lateral and rostral growth processes have reshaped the cerebellum to a transversely oriented bar of tissue overriding the fourth ventricle. At the 12th week, fissures begin to form transverse to the longitudinal axis of the brain, first on the vermis and then spreading laterally into the hemispheres. By CS 18 (about 44 days), the internal cerebellar swellings contain the dentate nuclei, the first sign of the superior cerebellar peduncles can be seen around CS 19 (about 48 days) and the cerebellar commissures appear at the end of the embryonic period (Müller and O'Rahilly 1990b). In ◘ Fig. 1.25, a 3D analysis of the cerebellum in the early foetal period is presented (Takakuwa et al. 2021).

The **histogenesis** of the cerebellum is summarized in ◘ Fig. 1.26. The main cell types of the cerebellum arise at different times of development and at different locations. GABAergic cerebellar neurons, including the Purkinje cells, most neurons of the cerebellar nuclei and later the Golgi, stellate and basket cells, arise from the ventricular zone of the rostral hindbrain alar plate, expressing the bHLH factor Pff1a. The glutamatergic granule cells and a glutamatergic subpopulation of the neurons of the cerebellar nuclei arise from the rhombic lip, expressing the bHLH factor Atoh1 (for reviews, see Hoshino 2012; Millen et al. 2014; Leto et al. 2016; Lowenstein et al. 2022, and ▶ Chap. 8). The **Purkinje cells** and the **cerebellar nuclei** arise from the ventricular zone of the rostral rhombencephalic alar plate. Bayer et al. (1995) estimated that in humans the cerebellar nuclei as well as the Purkinje cells are generated from the early fifth to sixth weeks of development. Towards the end of the embryonic period, **granule cells** are added from the rhombic lip. The **rhombic lip** (*Rautenleiste* of His 1890) is the dorsolateral part of the alar plate, and it forms a proliferative zone along the length of the hindbrain. Cells from its rostral part, the **upper rhombic lip**, reach the superficial part of the cerebellum, and form the **external germinal** or **granular layer** at the end of the

◘ **Fig. 1.22** 3D reconstructions of the human foetal brain at the same scale: **a** lateral view with cerebrum in *green*, 'interbrain' (diencephalon and hypothalamus) in *orange*, midbrain in *blue*, rostral hindbrain and cerebellum in *yellow* and caudal hindbrain in *purple*; **b** ventricle (in *blue*) and choroid plexus (in *purple*) of the lateral ventricle. The standard line was defined as the tangential line of the frontal lobe, which goes through the pituitary gland (*red circle*). Numbers indicate the crown-rump length (CRL) of the samples. (From Takakuwa et al. 2021, with permission; courtesy Tetsuya Takakuwa, Kyoto)

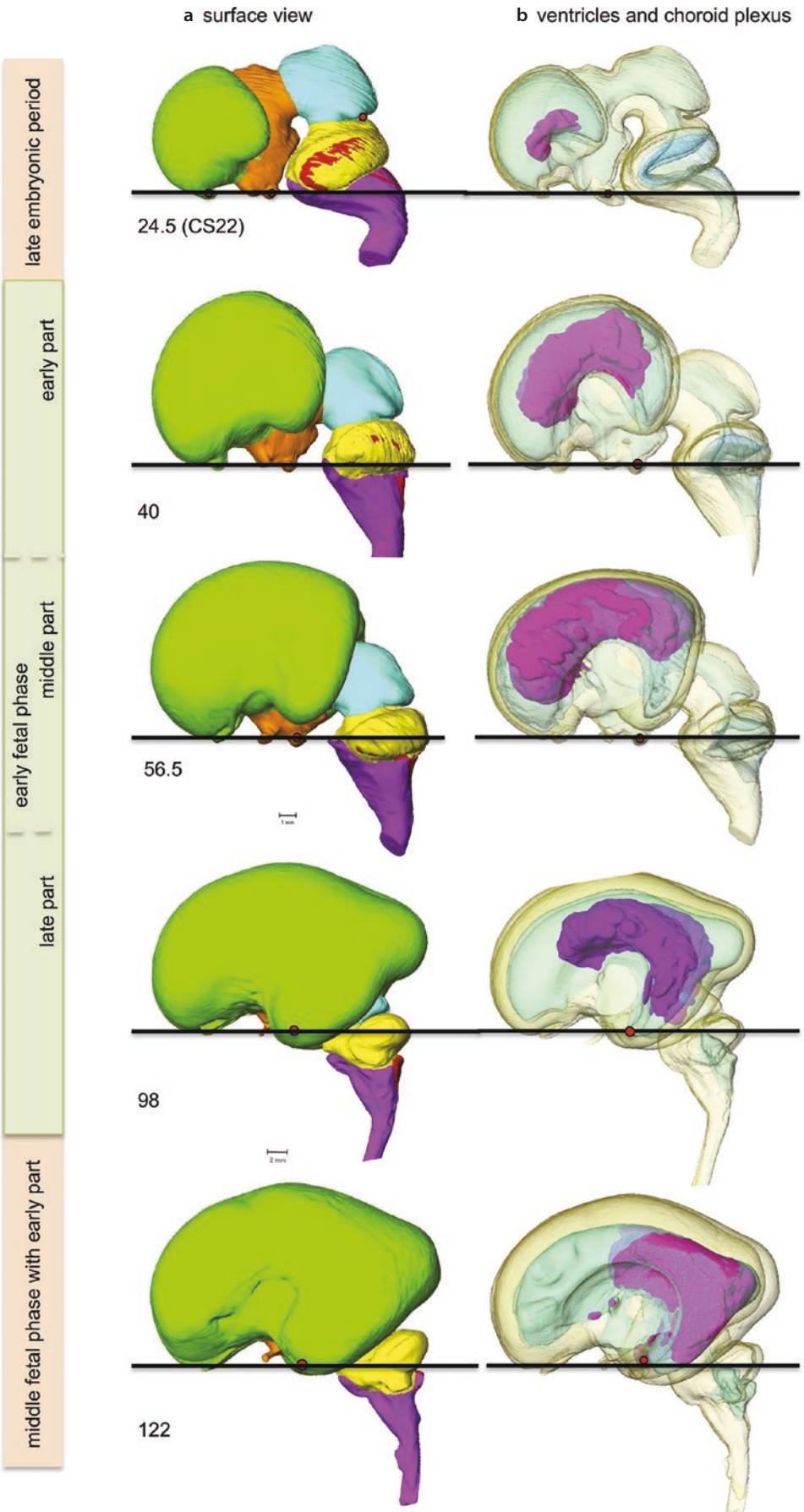
a surface view
b ventricles and choroid plexus
late embryonic period
early fetal phase
early part
middle part
late part
middle fetal phase with early part
24.5 (CS22)
40
56.5
98
122

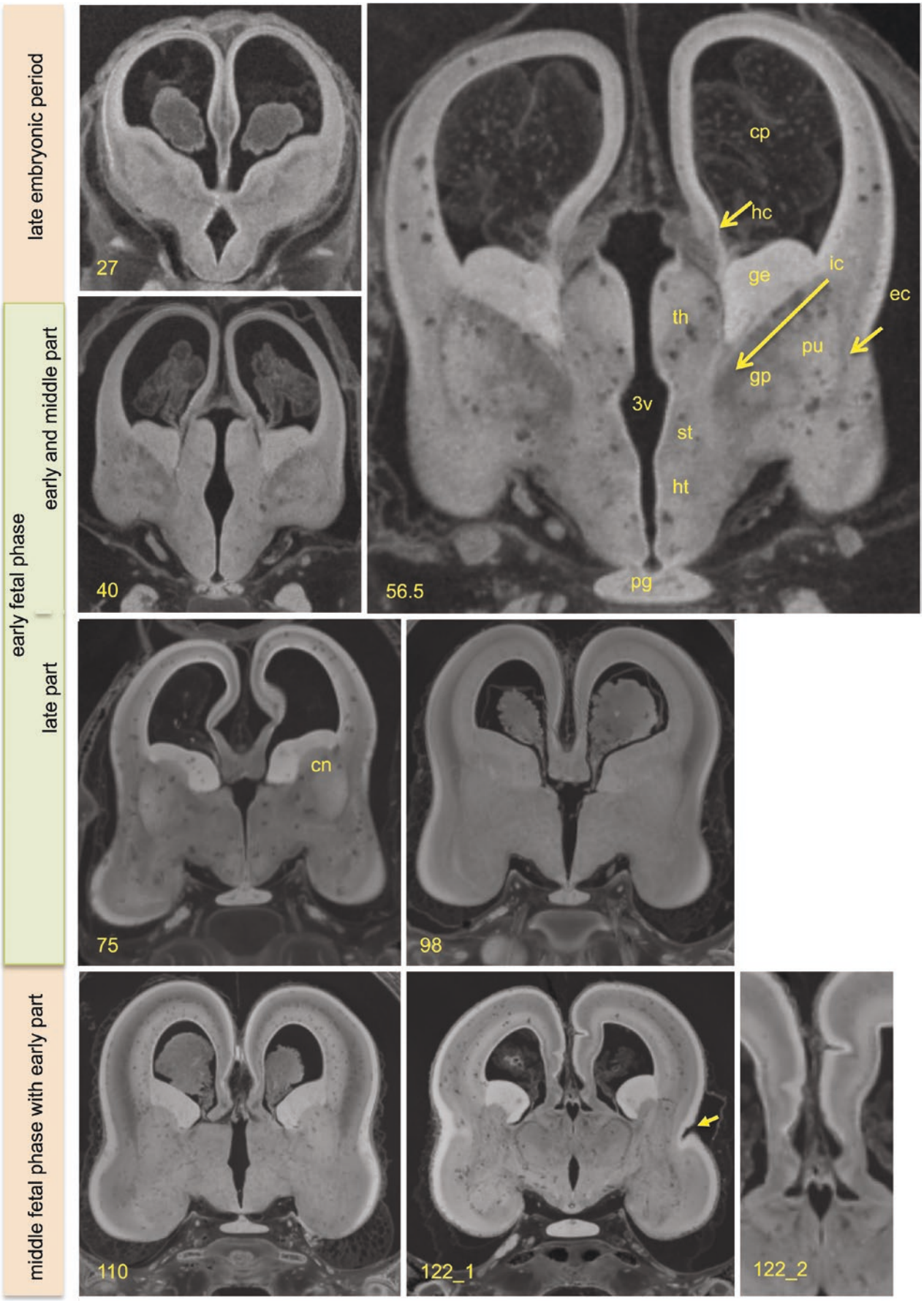
late embryonic period
early fetal phase
early and middle part
late part
middle fetal phase with early part
27
40
56.5
75
98
110
122_1
122_2
cp
hc
ge
ic
ec
th
pu
gp
3v
st
ht
pg
cn

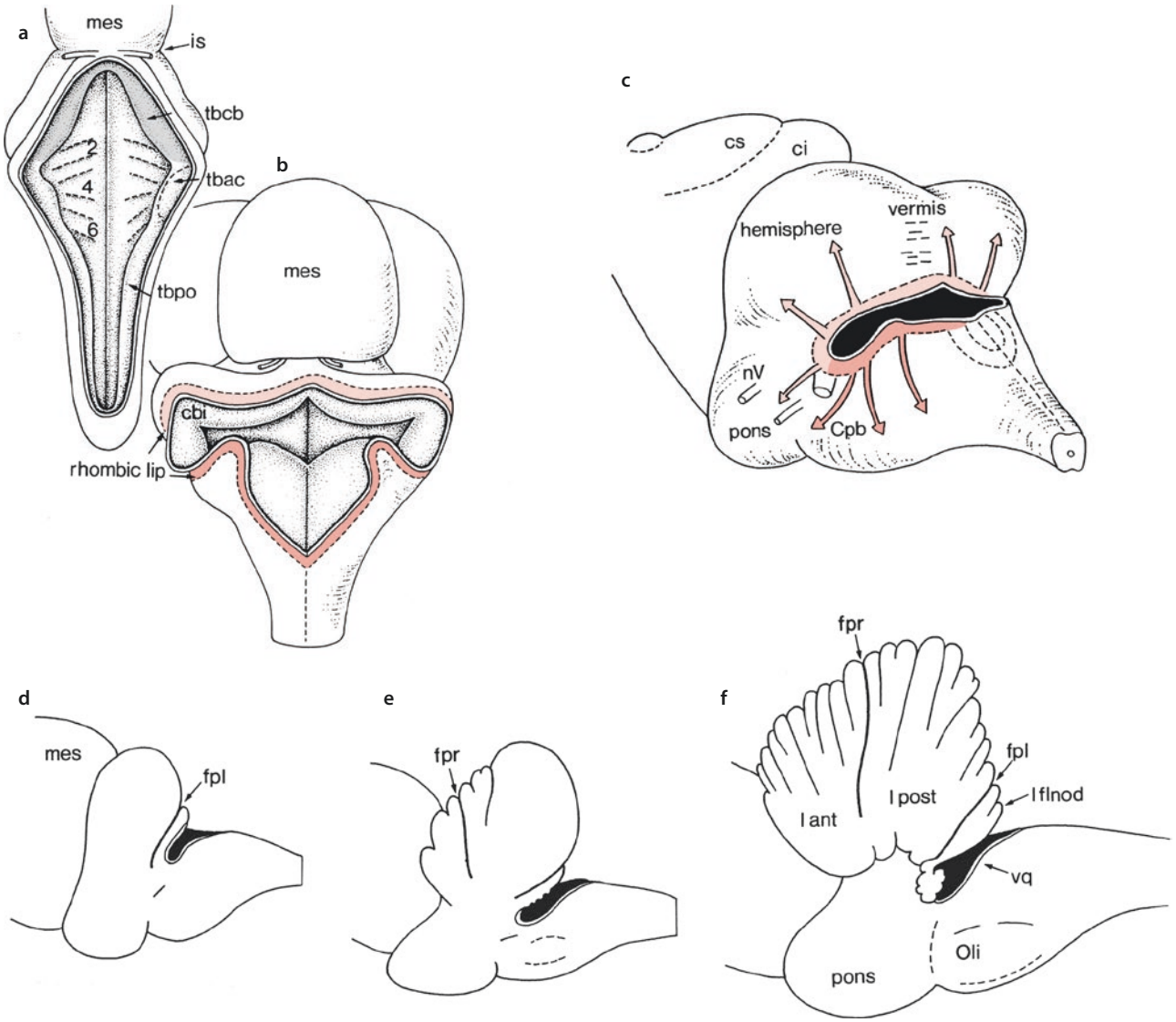

Fig. 1.24 Embryonic **a, b** and foetal (**c–f** development of the human cerebellum: **a** approximately 4 weeks; **b** at the end of the embryonic period; **c–f** at 13 weeks **c, d**, and 4 **e** and 5 **f** months of development. The V-shaped tuberculum cerebelli (*tbcb*) is indicated in *grey*, and the upper and lower rhombic lips in *light red* and *red*, respectively. *cbi* internal cerebellar bulge, *ci* colliculus inferior, *Cpb* corpus pontobulbare, *cs* colliculus superior, *fpl* fissura posterolateralis, *fpr* fissura prima, *is* isthmus, *l ant* lobus anterior, *l flnod* lobus flocculonodularis, *l post* lobus posterior, *mes* mesencephalon, *nV* trigeminal nerve, *Oli* oliva inferior, *tbac* tuberculum acusticum, *tbpo* tuberculum ponto-olivare, *vq* ventriculus quartus, *2*, *4*, *6* rhombomeres. (**a**, after Streeter 1911, 1912; Jakob 1928; **b**, after Hochstetter 1929; **c–f,** after Streeter 1911, 1912)

embryonic period. Granule cells are formed in the external germinal layer. The granule cells that arise from it migrate along the processes of Bergmann glia cells to their deeper, definitive site. Adhesion molecules such as TAG1, L1 and astrotactin play a role in this migration (Hatten et al. 1997). In the foetal period, the **internal granular layer** is formed by further proliferation and migration of the external germinal cells. This layer, situated below the layer of Purkinje cells, is the definitive granular layer of the cerebellar cortex. A transient layer, the **dissecting layer** (**lamina dissecans**), separates the internal granular layer from the Purkinje cells. It is filled

Fig. 1.23 MRI coronal sections at the level of the pituitary gland. The coronal plane was defined vertical to the AC–PC line; *cn* caudate nucleus, *cp* choroid plexus, *ec* external capsule (*yellow arrow* at sample CRL 56.5), *fo* fornix, *ge* ganglionic eminence, *gp* globus pallidus, *hc* hippocampus (*yellow arrow* at sample CRL 56.5), *ht* hypothalamus, *ic* internal capsule (*large yellow arrow* at sample CRL 56.5), *in* insula (*yellow arrow* at sample CRL 122 indicates initial sulcus formation), *pg* pituitary gland, *put* putamen, *st* subthalamus, *th* thalamus, *v3* third ventricle. (From Takakuwa et al. 2021, with permission; courtesy Tetsuya Takakuwa, Kyoto)

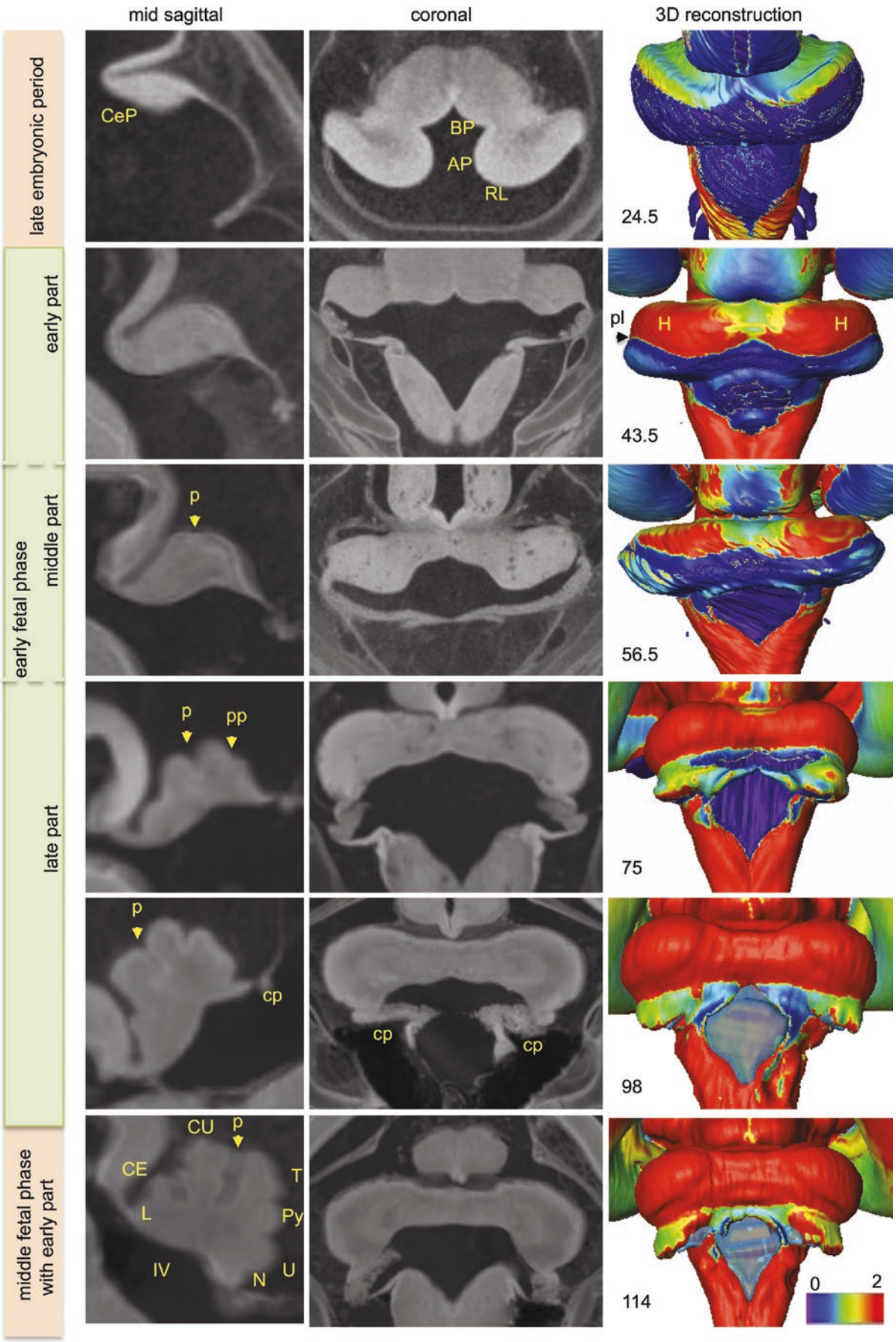
mid sagittal
coronal
3D reconstruction
late embryonic period
early part
early fetal phase
middle part
late part
middle fetal phase with early part
CeP
BP
AP
RL
24.5
pl
H
H
43.5
p
56.5
p
pp
75
p
cp
cp
cp
98
CU
p
CE
T
L
Py
IV
N
U
114
0
2

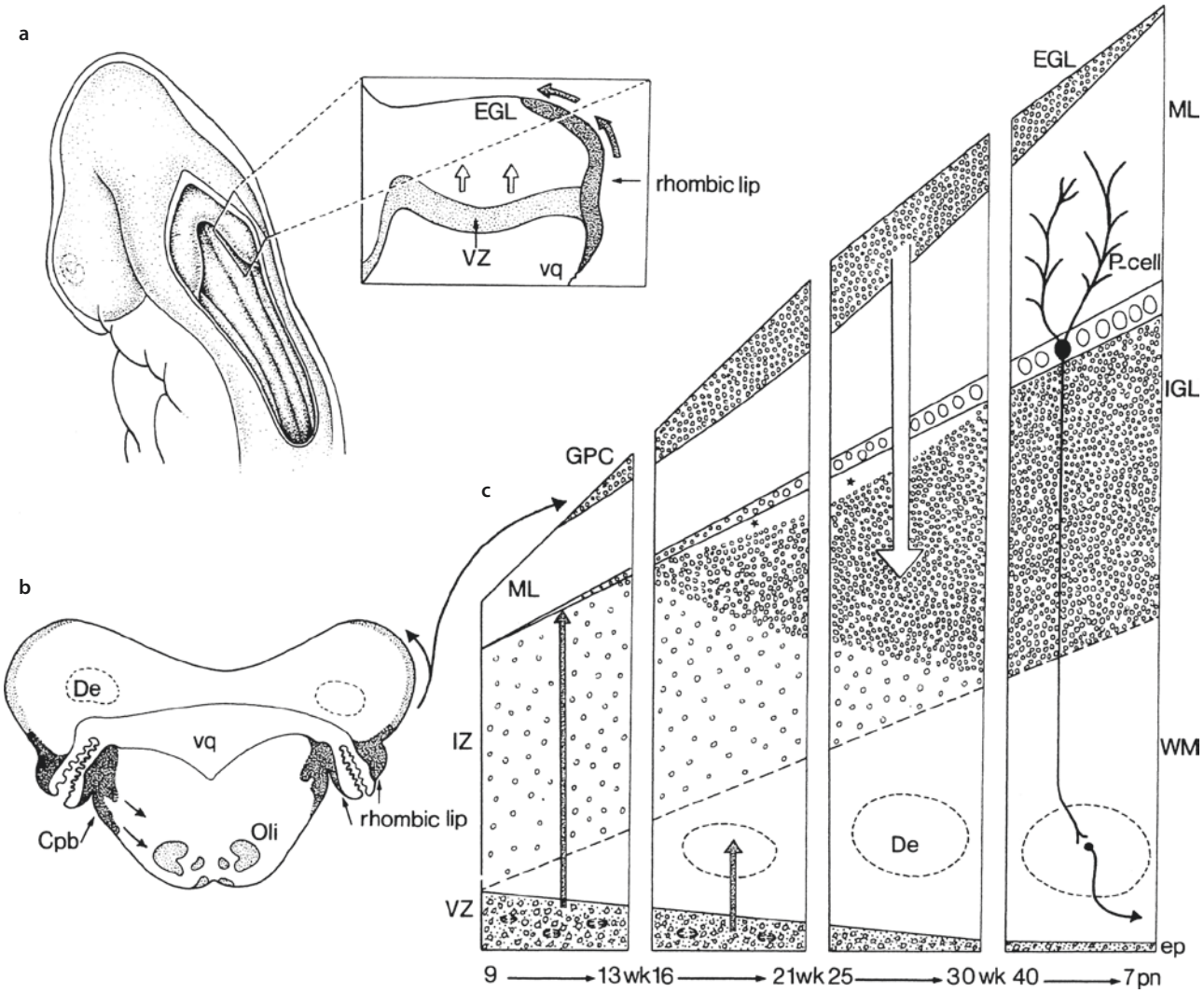

Fig. 1.26 Overview of the histogenesis of the cerebellum. **a** A dorsolateral view of a human embryo and part of the tuberculum cerebelli enlarged, showing the two proliferative compartments: the ventricular zone (*VZ*), giving rise to Purkinje cells and the deep cerebellar nuclei, and the external germinal or granular layer (*EGL*), giving rise to the granule cells. **b** The position of the rhombic lip in a transverse section at the level of the lateral recess of the fourth ventricle. The upper rhombic lip is found lateral to the lateral recess, and the lower rhombic lip medial to the recess. **c**) The formation of the layers of the cerebellum in four periods from the early foetal period until seven weeks postnatally. The lamina dissecans is indicated with *asterisks*. The *arrows* in **a–c** show the migration paths. *Cpb* corpus pontobulbare, *De* dentate nucleus, *ep* ependyma, *GPC* granule precursor cells, *IGL* internal granular layer, *IZ* intermediate zone, *Ml* molecular layer, *Oli* oliva inferior, *P-cell* Purkinje cell, *vq* ventriculus quartus, *WM* white matter. (After Sidman and Rakic 1982, Hatten et al. 1997, and O'Rahilly and Müller 2001; from ten Donkelaar et al. 2003, with permission)

by migrating granule cells and disappears (Rakic and Sidman 1970). At the same time as the postmitotic granule cells migrate inwards (16–25 weeks), the Purkinje cells enlarge and develop dendritic trees. In humans, the external granular layer appears at the end of the embryonic period and persists for several months to one to two years after birth (Lemire et al. 1975). The caudal part of the rhombic lip, the **lower rhombic lip**, gives rise to the pontine nuclei and the inferior olivary nucleus (Essick 1912; Wingate 2001; ◘ Fig. 1.26c). Neurons of these precerebellar nuclei migrate along various pathways, the **pontobulbar body** (**corpus pontobulbare**) in particular, to their ultimate position in the brain stem (Altman and Bayer 1997).

Fig. 1.25 Cerebellar growth shown in MRI midsagittal and coronal sections, and 3D reconstructions with surface colour mapping of dorsal view of cerebellum. The thickness of brain tissue changes was visualized using a rainbow colour scale (range: 0–2 mm). *CE* central lobule, *CU* culmen, *CP* choroid plexus, *L* lingula, *N* Nodule, *P* primary fissure, *PL* posterolateral fissure, *PP* prepyramidal fissure, *Py* pyramis, *T* tuber, *U* uvula. (From Takakuwa et al. 2021, with permission; courtesy Tetsuya Takakuwa, Kyoto)

Several genes have marked impact upon cerebellar development. In mice, knockouts of the *Wnt1* and *En1* genes largely or totally eliminate the cerebellum, whereas in *En2* knockouts the lobular pattern of the posterior vermis is disrupted (Hatten et al. 1997; Millen et al. 1999; Wang and Zoghbi 2001). The *Atoh1* (also known as *Math1*) gene is expressed in the rhombic lip (Ben-Arie et al. 1997). In *Atoh1* knockout mice, no granular layer is formed. SHH is expressed in migrating and settled Purkinje cells, and acts as a potent mitogenic signal to expand the granule cell progenitor population (Wechsler-Reya and Scott 1999). ***Medulloblastoma***, a brain stem tumour of childhood, is thought to originate in malignant external granule cells (see ▶ Chap. 8). **Developmental malformations** of the cerebellum are mostly bilateral and may be divided into (1) malformations of the vermis and (2) malformations of the vermis as well as of the hemispheres (Lemire et al. 1975; Norman et al. 1995; Kollias and Ball 1997; Ramaekers et al. 1997; ten Donkelaar et al. 2003; Barkovich et al. 2009; ten Donkelaar and Lammens 2009; Boltshauser and Schmahmann 2012; Barkovich and Raybaud 2018). ***Agenesis*** or ***hypoplasia*** of the ***vermis*** may occur in a great variety of disorders, most frequently in the ***Dandy-Walker malformation*** (▶ Chap. 8). ***Pontocerebellar hypoplasia*** forms a large group of disorders, characterized by a small pons and a varying degree of hypoplasia of the cerebellum (Barth 1993; Ramaekers et al. 1997; Boltshauser and Schmahmann 2012), up to its near-total absence (Gardner et al. 2001).

1.8.2 The Cerebral Cortex

The outgrowth of the **cerebral cortex** and the proliferation and migration of cortical neurons largely take place in the foetal period. Each hemisphere first grows caudalwards, and then bends to grow into ventral and rostral directions (◘ Figs. 1.27 and 1.28). In this way the temporal lobe arises. The outgrowth of the caudate nucleus, the amygdala, the hippocampus and the lateral ventricle occurs in a similar, C-shaped way. During the foetal period, the complex pattern of sulci and gyri arises. On the lateral surface of the brain, the **lateral sulcus** and the **central sulcus** can be recognized from four months onwards. Owing to the development of the prefrontal cortex, the central sulcus gradually moves caudalwards. On its medial surface, first the **parieto-occipital** and **cingulate sulci** appear, followed by the **calcarine** and **central sulci**. The formation of sulci and gyri in the right hemisphere usually precedes that in the left one. It should be noted that the morphology of cortical gyri and sulci is complex and variable among individuals with an established asymmetry appearing very early on (Dubois et al. 2008a, b, 2010; Habas et al. 2012). The **choroid plexus** of the lateral ventricle arises in the lower part of the medial wall of the telencephalic vesicle (◘ Figs. 1.21 and 1.23).

Usually, the **pallium** is divided into a **medial pallium** or **archipallium**, a **dorsal pallium** or **neopallium** and a **lateral pallium** (◘ Fig. 1.29). More recently, an additional **ventral pallium** was added (Puelles et al. 2000; Marín and Rubenstein 2002; Schuurmans and Guillemot

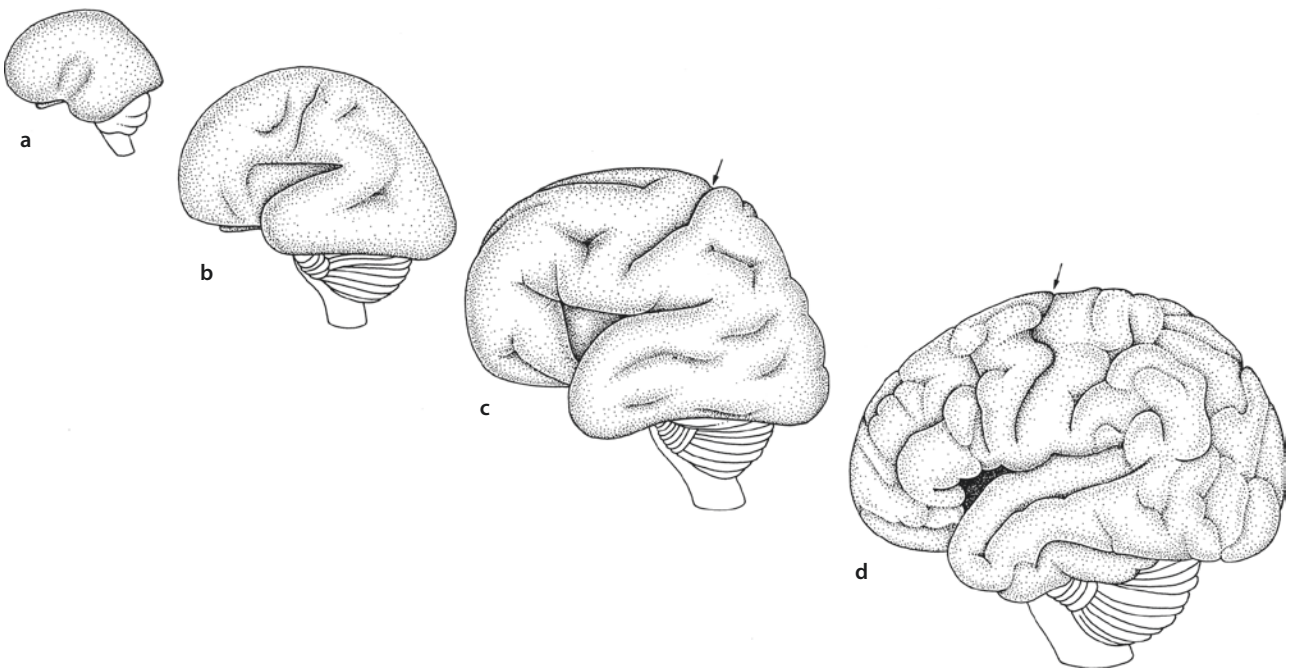

◘ **Fig. 1.27** Lateral views of the developing human brain in the fourth **a**, sixth **b** and eighth **c** gestational months, and in a neonate **d**. The *arrows* indicate the central sulcus. (After Kahle 1969; O'Rahilly and Müller 1999)

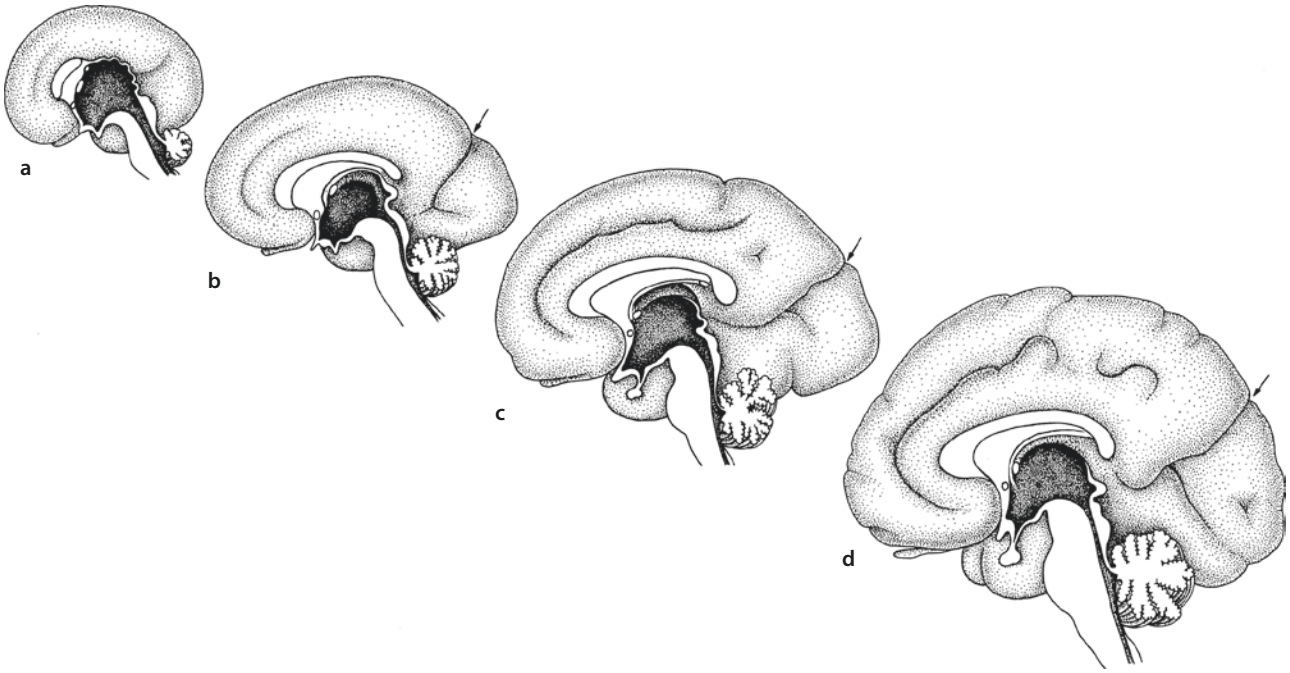

Fig. 1.28 Medial views of the developing human brain in the fourth **a**, sixth **b** and eighth **c** gestational months, and in a neonate **d**. The *arrows* indicate the parieto-occipital sulcus. (After Macchi 1951, Kahle 1969 and Feess-Higgins and Larroche 1987)

2002). The medial pallium forms the hippocampal cortex, the three-layered **allocortex**. Parts of the surrounding transitional cingulate and entorhinal cortex, the four- to five-layered **mesocortex**, may have the same origin. The dorsal pallium forms the six-layered **isocortex** or **neocortex**. Watson and Puelles (2016) provided gene expression data that the claustrum and the insula derive from the lateral pallium, and that the ventral pallium gives rise to the pallial amygdala and the olfactory cortex, which so far were considered to arise from the lateral pallium (see Wullimann 2017, for a critical comment).

The **subpallium** consists of two progenitor domains, the lateral and medial ganglionic eminences, generating the striatum and the pallidum, respectively. Dorsal and ventral domains of the developing telencephalon are distinguished by distinct patterns of gene expression, reflecting the initial acquisition of regional identity by progenitor populations (Puelles et al. 2000; Schuurmans and Guillemot 2002; ▶ Chap. 9).

The **hippocampal formation** or **formatio hippocampi** comprises the dentate gyrus, the hippocampus and the subiculum. These structures develop from the medial pallium and are originally adjacent to cortical areas (◘ Fig. 1.30). During the outgrowth of the cerebral hemispheres, first caudalwards and subsequently ventralwards and rostralwards, the **retrocommissural part** of the hippocampal formation becomes situated in the temporal lobe (Stephan 1975; Duvernoy 1998; Meyer et al. 2019). This part is also known as the ventral hippocampus. Rudiments of the **supracommissural part** of the hippocampus (or dorsal hippocampus) can be found on the medial side of the hemisphere on top of the corpus callosum: the **indusium griseum**, a thin cell layer, flanked by the **medial longitudinal stria** and the **lateral longitudinal stria** of Lancisi (▶ Chap. 10). The dorsal hippocampus forms at gestational week 10 (GW 10), when it develops a rudimentary Ammon horn, but transforms into the indusium griseum by GW 14–17. The ventral hippocampus forms at GW 11 in the temporal horn (Meyer et al. 2019).

At the beginning of the foetal period, the hippocampal formation contains four layers (Humphrey 1966; Kahle 1969; Arnold and Trojanowski 1996): a ventricular zone, an intermediate layer, a hippocampal plate composed of bipolar-shaped neurons, and a marginal zone. At GW 15–19, individual subfields can be distinguished. A distal-to-proximal gradient of cytoarchitectonic and neuronal maturity is found, with the subiculum appearing more developed than the ammonic subfields (CA1–CA3). The dentate gyrus is the latest area to develop. Most pyramidal cells in the cornu ammonis fields are generated in the first half of pregnancy and no pyramidal neurons are formed after GW 24 (Seress et al. 2001). Granule cells of the dentate gyrus proliferate at a decreasing rate during the second half of pregnancy and after birth but still occur at a low percentage during the first postnatal year (Seress et al. 2001). The postnatal development of the human hippocampus has been described by Insausti et al. (2010; ▶ Chap. 10).

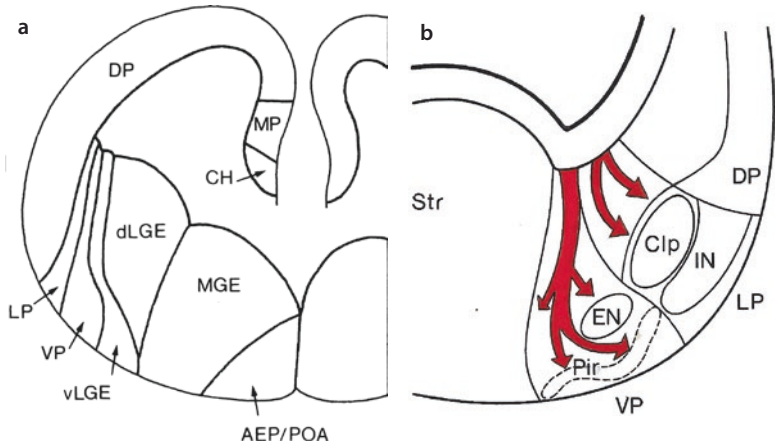

Fig. 1.29 Subdivision of the forebrain: **a** Subdivision into the medial pallium (*MP*), dorsal pallium (*DP*), lateral pallium (*LP*) and ventral pallium (*VP*) and subpallium. *AEP/POA* anterior entopeduncular/preoptic area, *CH* cortical hem, *dLGE* dorsal part of lateral ganglionic eminence, *MGE* medial ganglionic eminence, *vLGE* ventral part of lateral ganglionic eminence (after Puelles et al. 2000; Schuurmans and Guillemot 2002); **b** current view of the derivatives of the lateral and ventral pallium, proposing that the newly defined lateral pallium gives rise to the claustrum (*Clp*) and the insula (*IN*) and the ventral pallium, among others, to the piriform cortex (*Pir*; after Watson and Puelles 2016)

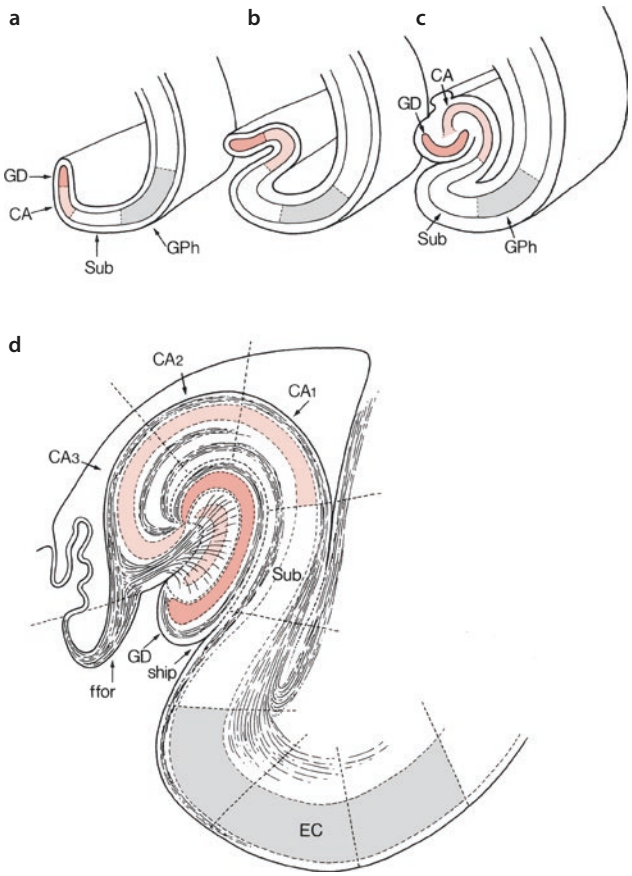

Fig. 1.30 Development **a–c** and structure **d** of the human hippocampal formation. The cornu ammonis (*CA*) is indicated in *light red*, the dentate gyrus (*GD*) in *red* and the entorhinal cortex (*EC*) in *grey*. *CA1-3* cornu ammonis subfields, *ffor* fimbria fornicis, *GPh* gyrus parahippocampalis, *ship* sulcus hippocampi, *Sub* subiculum

Reciprocal entorhinal–hippocampal connections are established by foetal midgestation (Hevner and Kinney 1996). Fibres connecting the entorhinal cortex, hippocampus and subiculum are present by about GW 19. The perforant path, connecting the entorhinal cortex with the dentate gyrus, and all connections with the isocortex are only beginning at GW 22.

The **histogenesis** of the six-layered isocortex is shown in Fig. 1.31. The developing cerebral wall contains several transient embryonic zones: (1) the ventricular zone, which is composed of dividing neural progenitor cells; (2) the subventricular zone, which acts early in corticogenesis as a secondary neuronal progenitor compartment and later in development as the major source of glial cells; (3) the intermediate zone, through which migrating neurons traverse along radial glial processes; (4) the subplate, thought to be essential in orchestrating thalamocortical connectivity and pioneering corticofugal projections (▶ Chap. 2); (5) the cortical plate, the initial condensation of postmitotic neurons that will become layers II–VI of the mature cortex; and (6) the marginal zone, the superficial, cell-sparse layer that is important in the establishment of the laminar organization of the cortex.

This terminology largely goes back to the Boulder Committee (1970), although the preplate and subplate were not known then. In the last decennia, a wealth of studies have advanced our knowledge of the timing, sequence and complexity of cortical histogenesis, and also emphasized important inter-species differences. Bystron et al. (2008) proposed a revision of the terminology of the Boulder Committee. New types of transient neurons and proliferative cells outside the classic neuroepithelium, new routes of cellular migration and additional cellular compartments were found (Smart

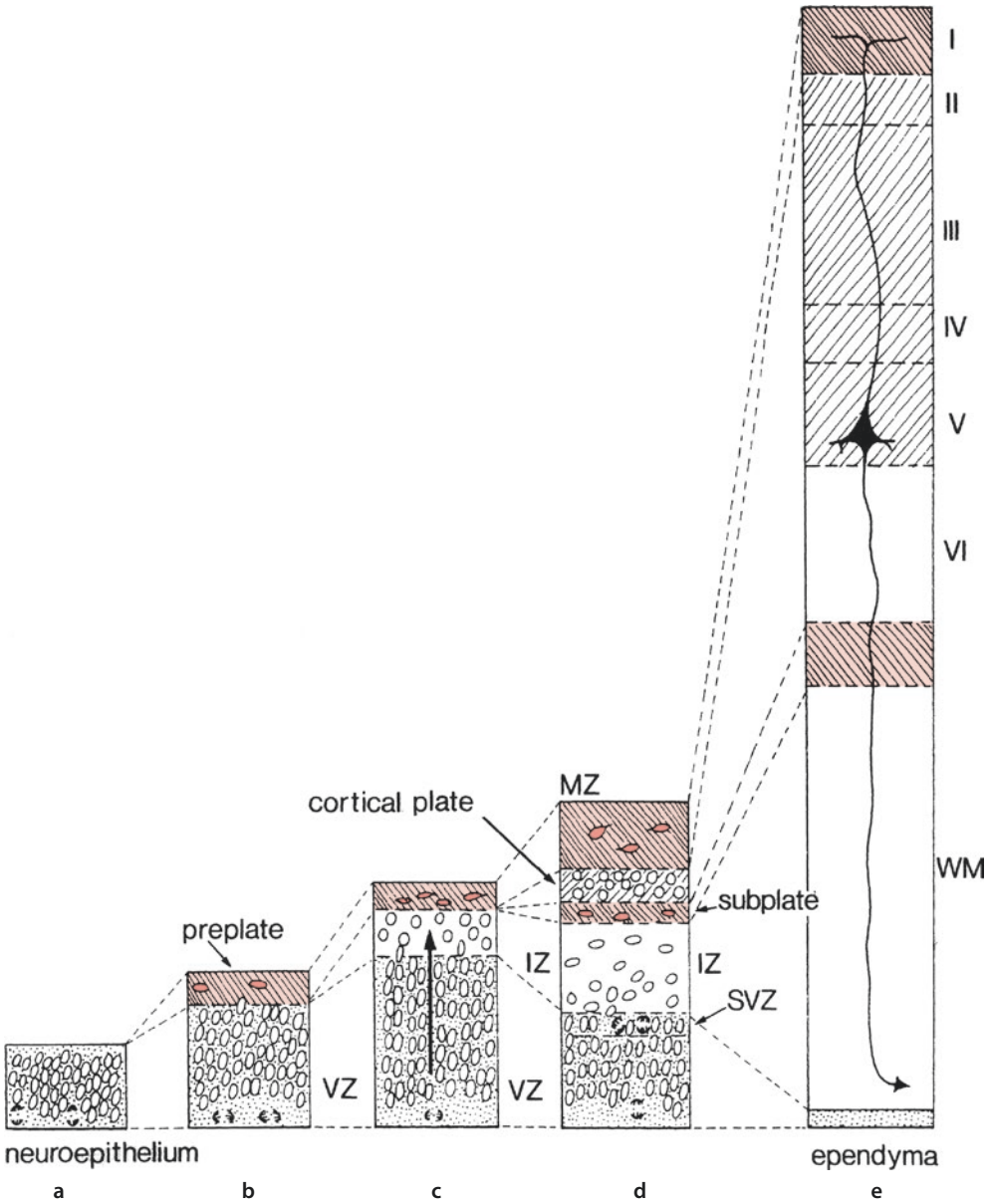

Fig. 1.31 Histogenesis of the cerebral cortex. **a–c** The neuroepithelium forms three zones: the ventricular zone (*VZ*), the intermediate zone (*IZ*) and the preplate. During the 8–18th weeks of development, neurons migrate from the ventricular zone and form the cortical plate **d**. The preplate becomes divided into the marginal zone (*MZ*) and the subplate. A second compartment for cell division, the subventricular zone (*SVZ*), is mainly involved in the production of glial cells. Finally **e**, the marginal zone forms the molecular layer (layer *I*) and the cortical plate layers *II–VI*. The intermediate zone forms the subcortical white matter (*WM*). The subplate disappears. (After O'Rahilly and Müller 1999)

et al. 2002; Zecevic et al. 2005, 2011; Bystron et al. 2006; Carney et al. 2007; Hansen et al. 2010, 2013; Lui et al. 2011; Ma et al. 2013; Alzu'bi and Clowry 2019; Molnár et al. 2019). The revisions of the Boulder model include:

(1) A transient layer with predecessor neurons and Cajal-Retzius cells forms between the neuroepithelium and the pial surface before the appearance of the cortical plate. The term **preplate** is already widely used for this layer.

(2) The **subventricular zone** appears as a distinctive proliferative layer *before* the emergence of the cortical plate, earlier than previously recognized. It has increased in size and complexity during evolution and its cellular organization in primates is different from that in rodents.

(3) Since there is no distinct cell-sparse layer under the pial surface before the cortical plate forms, the term **marginal zone** should be used only to refer to the residual superficial part of the preplate *after* the

appearance of the cortical plate. The marginal zone becomes the layer I of the mature cortex.

(4) The term **intermediate zone** should be reserved for the heterogeneous compartment that lies between the proliferative layers and the postmigratory cells above. The intermediate zone contains radially and tangentially migrating cells and a thickening layer of extrinsic axons that eventually constitutes the white matter.

(5) The **subplate** is a distinctive and functionally important transient layer, located directly below the cortical plate. In rodents and carnivores, most subplate neurons are born before the first cortical plate cells. In humans, preplate cells also contribute to the subplate but its substantial thickening at later stages probably involves the addition of later-born neurons.

Cortical neurons are generated in the ventricular zones of the cortical walls and ganglionic eminences, and reach their destination by radial and tangential migration, respectively. The first postmitotic cells form the **preplate** or **primordial plexiform layer** (Marín-Padilla 1998; Meyer and Goffinet 1998; Supèr et al. 1998; Zecevic et al. 1999; Meyer et al. 2000, 2019; Meyer 2007, 2010). Then, cells from the ventricular zone migrate to form an **intermediate zone** and, towards the end of the embryonic period, the **cortical plate**. This plate develops within the preplate, thereby dividing the preplate into a minor superficial component, the marginal zone and a large deep component, the subplate. The **marginal zone** is composed largely of **Cajal-Retzius neurons** (Meyer et al. 1999; Meyer 2007, 2010), secreting the extracellular protein Reelin, and the subplate contains pioneer projection neurons. Reelin is required for the normal inside-to-outside positioning of cells as they migrate from the ventricular zone. Another source of Cajal-Retzius cells is the **cortical hem**, a putative signalling centre at the interface of the future hippocampus and the choroid plexus (Meyer 2010; Meyer et al. 2019; ▶ Chap. 10). The formation of the cortical plate takes place from approximately weeks 7 to 16. The first cells to arrive will reside in the future layer VI. Cells born later migrate past the already present cortical cells to reside in progressively more superficial layers. In this way, the cortical layers VI–II are subsequently formed. The marginal zone becomes layer I, i.e. the molecular or plexiform layer. The subplate gradually disappears. The ventricular zone becomes the ependyma and the intermediate zone the subcortical white matter. A transient cell layer, the **subpial granular layer** (SGL) of Ranke (1910), originates from the basal periolfactory subventricular zone (Brun 1965; Gadisseux et al. 1992; Meyer and Wahle 1999; Meyer and González-Gómez 2018). It migrates tangentially beneath the pia to cover the isocortical marginal zone from GW 14 onwards. The SGL provides a constant supply of Reelin-producing cells during the critical period of cortical migration, keeping pace with the dramatic growth and surface expansion during corticogenesis. Naturally occurring cell death is an active mechanism contributing to the disappearance of the SGL (Spreafico et al. 1999).

Primate corticogenesis is distinguished by the appearance of a large **subventricular zone** that has inner and outer regions (Smart et al. 2002; Zecevic et al. 2005). Recent observations in human, non-human primate, carnivore and marsupial embryos and foetuses reveal how differences in neural progenitor cell populations can result in neocortices of variable size and shape (Lui et al. 2011; ▶ Chap. 10). Increases in isocortical volume and surface area are related to the expansion of progenitor cells in the outer subventricular zone during development (Smart et al. 2002; Fietz et al. 2010; Hansen et al. 2010; Lui et al. 2011).

The **subplate** is a largely transient zone containing precocious neurons involved in several key stages of corticogenesis (Kostović and Rakic 1990; Kostović and Jovanov-Milošević 2006; Kostović and Judaš 2007, 2010; Judaš et al. 2010; ◘ Fig. 1.32). In rodents, the majority of subplate neurons form a compact layer (Allendoerfer and Shatz 1994; Kanold and Luhmann 2010; Wang et al. 2010), but they are dispersed throughout a much larger zone in primates including humans. In rodents, subplate neurons are among the earliest born isocortical cells, whereas in primates, neurons are added to the subplate throughout cortical neurogenesis. Histochemical studies and MRI data (◘ Figs. 1.23, 1.36, and 1.37) show that the human subplate grows in size until the end of the second trimester (Kostović and Jovanov-Milošević 2006; Prayer et al. 2006; Radoš et al. 2006; Kostović and Vasung 2009; Kostović et al. 2019a, b; Terashima et al. 2021). **Transient layers** containing circuitry elements (synapses, postsynaptic neurons and presynaptic axons) appear in the cerebral wall from PCW 8 and disappear with the resolution of the subplate after the sixth postnatal month (Kostović and Jovanov-Milošević 2006; Kostović and Judaš 2007, 2010). The monolayer in the early foetal period, the **presubplate**, undergoes dramatic bilaminar transformation between PCW 13 and PCW 15, followed by sublamination into three 'floors' (Kostović et al. 2019b): (1) the deep subplate, the entrance zone for ingrowing thalamocortical fibres; (2) the intermediate subplate or 'proper' subplate for navigation of the thalamocortical fibres; and (3) the superficial subplate, a zone for axonal accumulation and target selection. Transient neuronal circuitry underlies transient functions during the foetal, perinatal and early postnatal life, determines developmental plasticity of the cerebral cortex and moderates effects of lesions of the developing brain (Kostović and Jovanov-Milošević 2006; Kostović and Judaš 2007, 2010). Krsnik et al. (2017) studied the growth of thalamocortical fibres to the somatosensory cortex in the

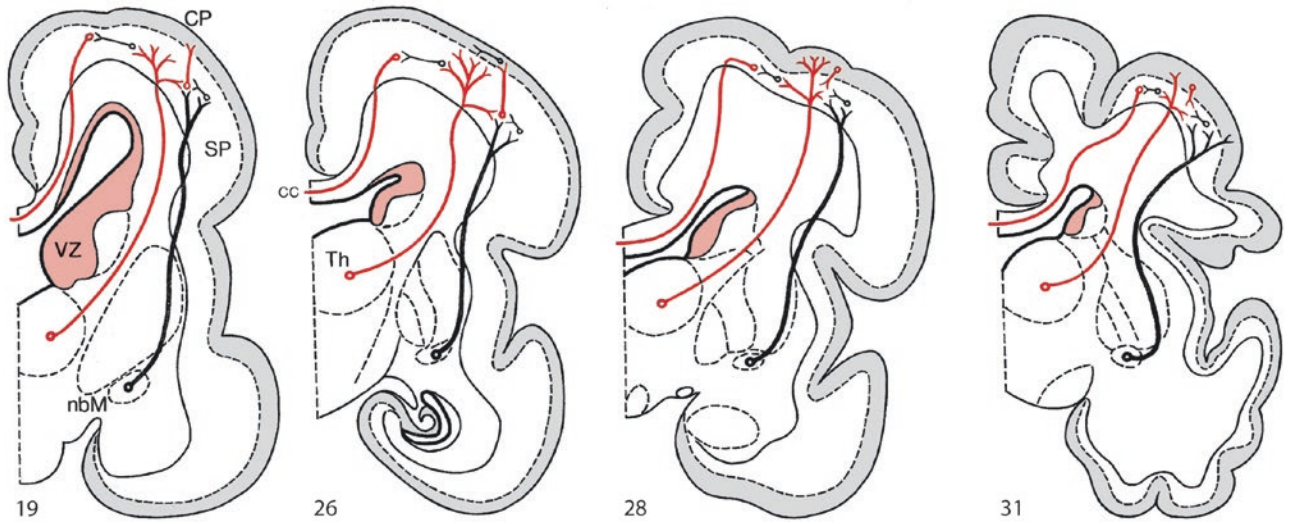

Fig. 1.32 The organization of afferent systems and transient cortical circuitry in human foetuses and preterm infants (19, 26, 28 and 31 postconceptional weeks). Glutamatergic projections arising in the thalamus (*Th*) and the contralateral hemisphere, passing via the corpus callosum (*cc*), are indicated in *red*, GABAergic fibres in *black* and cholinergic projections from the basal nucleus of Meynert (*nbM*) in *thick black lines*. The cortical afferents initially synapse in the large subplate (*SP*) before reaching the cortical plate. *CP* cortical plate (in *light grey*), *nbM* nucleus basalis of Meynert, *VZ* ventricular zone (in *medium red*). (After Kostović and Judaš 2010)

human foetal brain (Fig. 1.32). As early as PCW 7.5, outgrowth of thalamocortical fibres was found from the ventrolateral part of the thalamic anlage. After passing the pallial–subpallial boundary, they will be 'waiting' in the subplate to penetrate the cortical plate not before PCW 23 (for further discussion, see ▶ Chaps. 2 and 10).

In the telencephalon, **radial migration** is the primary mechanism by which developing neurons arrive at their final position (Rakic 1972). The newly born neuroblasts associate with specialized glial cells known as the radial glial cells. **Radial glial cells** are bipolar cells with one short process extended to the adjacent ventricular surface and a second projecting to the pial surface (▶ Chap. 2). A two-way signalling process between the migrating neuron and the radial glial fibre permits the neuroblast to migrate, and provides a signal to maintain the structure of the radial glial fibre (Hatten 1999). This process requires known receptors and ligands such as neuregulin and Erb4, cell adhesion molecules, putative ligands with unknown receptors such as astrotactin, and extracellular matrix molecules and their surface receptors. Blocking any of these components can slow or prevent radial cell migration (Pilz et al. 2002). More recent data have shown a much more prominent role for radial glial cells as **primary progenitors** or **neural stem cells** (reviewed by Kriegstein and Alvarez-Buylla 2009; ▶ Chap. 2). In development and in the adult brain, many neurons and glial cells are not the direct progeny of neural stem cells, but instead originate from transit amplifying **intermediate progenitor cells (IPCs)**. IPCs can generate neurons (nIPCs) or generate glial cells, including oligodendrocytes (oIPCs) or astrocytes (aIPCs; ▶ Chap. 2).

Cell migration perpendicular to the radial axis, i.e. **tangential migration** (Fig. 1.33), differs from radial cell migration in the direction of movement and in the mechanism of cell guidance. Instead of radial glia, axons appear to be the substrate for at least some non-radial cell migration (Pearlman et al. 1998). Non-radial cell migration provides most, if not all, GABAergic interneurons of the cerebral cortex. This population of cortical neurons migrates from the ganglionic eminences along non-radial routes to reach the cerebral cortex (Anderson et al. 1999, 2001; Lavdas et al. 1999; Marín and Rubenstein 2001). In rodents, the medial ganglionic eminence is the source of most cortical interneurons, and is also a major source of striatal interneurons (Marín et al. 2000). The tangential migration of postmitotic interneurons from the ganglionic eminences to the isocortex occurs along multiple paths, and is directed in part by members of the Slit and semaphorin families of guidance molecules (Marín et al. 2001). Later, it has been suggested that in the human forebrain (Fig. 1.34) interneurons arise both in the ganglionic eminences and locally in the ventricular and subventricular zones of the dorsal telencephalon under the isocortex (Letinić et al. 2002; Zecevic et al. 2005, 2011; Fertuzinhos et al. 2009; Rakic 2009; ▶ Chaps. 9, 10). Recent studies (Hansen et al. 2013; Ma et al. 2013; Alzu'bi and Clowry 2019), however, challenged that most cortical interneurons are derived from the dorsal pallium (for further discussion, see ▶ Chap. 10). In the human brain, a predominant role for the caudal ganglionic eminence in cortical interneurogenesis has been shown (Alzu'bi and Clowry 2019).

Malformations of cortical development may be divided into several categories, based on the stage of

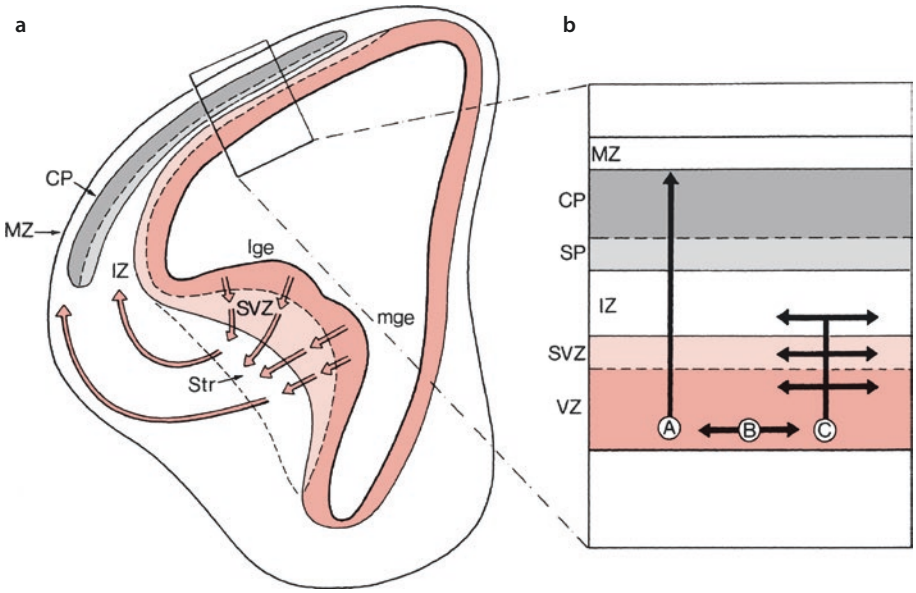

Fig. 1.33 Radial and tangential migration of cortical neurons. **a** The proliferative compartments of the murine telencephalon are shown: the ventricular zone (*VZ*, *red*) and the subventricular zone (*SVZ*, *light red*). Postmitotic GABAergic neurons leave the lateral (*lge*) and medial (*mge*) ganglionic eminences and reach the striatum (*Str*) and through tangential migration the marginal zone (*MZ*) and the intermediate zone (*IZ*). **b** Part of the cortex is enlarged in which radial migration of neurons (*A*) through the subplate (*SP*) to the cortical plate (*CP*) and tangential migration, occurring in the ventricular, subventricular and intermediate zones (*B*, *C*), are indicated. (After Pearlman et al. 1998)

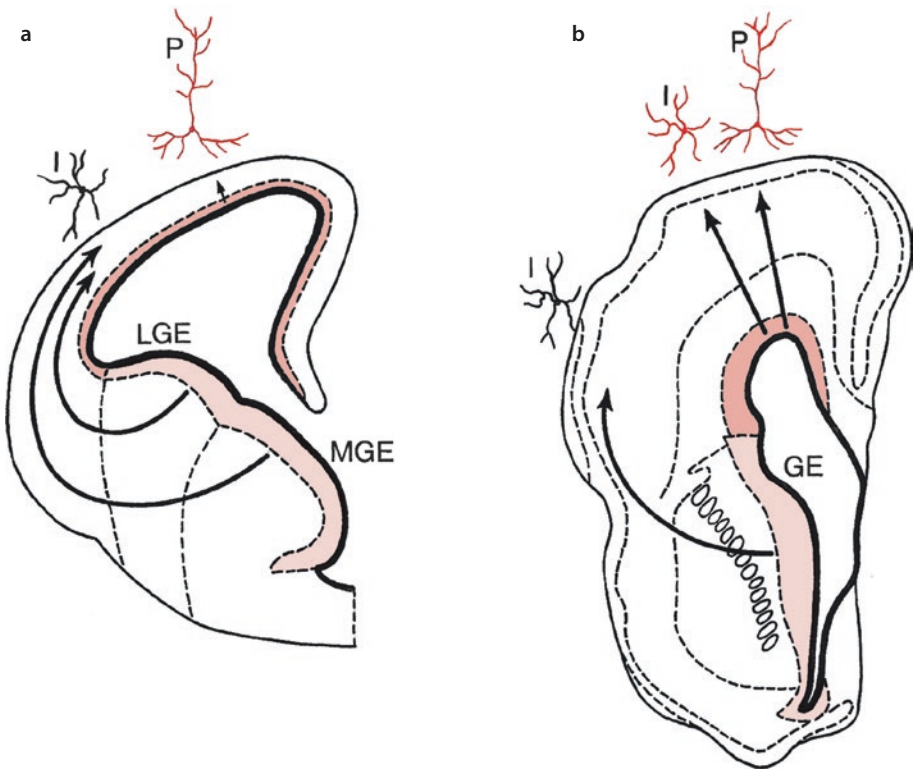

Fig. 1.34 Rodent **a** and human **b** foetal forebrains at the peak of corticogenesis, showing the sources of cortical interneurons. In rodents, projection neurons (*P*) arise in the ventricular and subventricular zones (in *medium red*), and cortical interneurons (*I*) in the lateral (*LGE*) and medial (*MGE*) ganglionic eminences (in *light red*). In the human brain, cortical interneurons may arise not only from the ganglionic eminence (*GE*) but also from the dorsal ventricular and subventricular zones (into *medium red*). (After Rakic 2009)

development (cell proliferation, neuronal migration, cortical organization) at which cortical development was first affected (Barkovich et al. 2001, 2012; Desikan and Barkovich 2016; ▶ Chap. 10). Malformations due to abnormal proliferation or apoptosis may lead to extreme microcephaly. Malformations due to abnormal migration, i.e. ***neuronal migration disorders***, have been extensively studied (Gleeson and Walsh 2000; Barkovich et al. 2001, 2012; Olson and Walsh 2002; Pilz et al. 2002; Desikan and Barkovich 2016; Barkovich and Raybaud 2018). Malformations due to abnormal cortical organization include the polymicrogyrias and schizencephalies (Barkovich et al. 2001, 2012).

The **olfactory bulbs** evaginate after olfactory fibres penetrate the cerebral wall at the ventrorostral part of the hemispheric vesicles (Pearson 1941). By the end of the sixth week, several bundles of fibres arising in the olfactory placodes have reached the forebrain vesicles. A few days later, a shallow protrusion appears at the site of contact, and between 8 and 13 weeks, the cavity of the evagination enlarges and becomes the olfactory ventricle. The olfactory bulbs gradually elongate rostralwards along the base of the telencephalon. Mitral cells arise from the surrounding ventricular zone. As the olfactory bulbs form, future granule and preglomerular cells are generated in the subventricular zone of the lateral ganglionic eminences, and migrate into each bulb along a rostral migratory stream (Hatten 1999). These neurons move rapidly along one another in chain formations, independent of radial glia or axonal processes. In rats and primates, this migration persists into adulthood (Doetsch et al. 1997; Kornack and Rakic 2001; Brazel et al. 2003). Numerous cells of the **piriform cortex** originate close to the corticostriatal boundary (Bayer and Altman 1991). They reach the rostrolateral telencephalon via a lateral cortical stream (de Carlos et al. 1996; ▶ Chap. 2).

1.8.3 Cerebral Commissures

Cerebral commissures arise in a thin plate, the **embryonic terminal plate** (**lamina terminalis**), i.e. the median wall of the telencephalon rostral to the chiasmatic plate. It is also known as the lamina reuniens or *Schlussplatte* (His 1889, 1904; Hochstetter 1919; Rakic and Yakovlev 1968; Paul et al. 2007; Raybaud 2010a; ▶ Chap. 10). At approximately five weeks (CS 16), the **commissural plate** appears as a thickening in the embryonic terminal plate. The remainder of the lamina then constitutes the adult terminal plate (*Endplatte* of His 1889, 1904). The commissural plate gives rise to (◘ Fig. 1.35) (1) the **anterior commissure**, which appears at the end of the embryonic period and connects the future temporal lobes, (2) the **hippocampal commissure** (or **psalterium**), which appears several

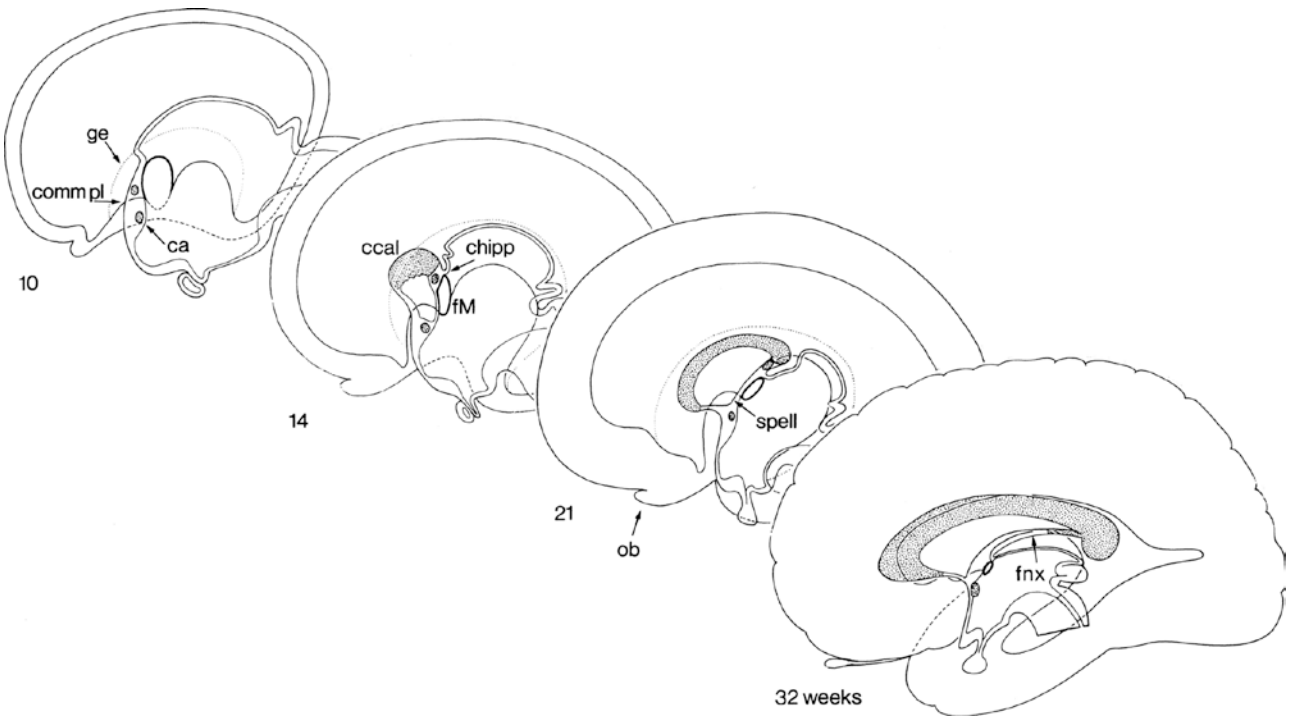

◘ **Fig. 1.35** Development of the cerebral commissures at the 10th, 14th, 21st and 32nd weeks of development. *ca* commissura anterior, *ccal* corpus callosum, *chipp* commissura hippocampi, *comm pl* commissural plate, *fM* foramen of Monro, *fnx* fornix, *ge* ganglionic eminence, *ob* olfactory bulb, *spell* septum pellucidum. (After Streeter 1911, 1912)

weeks later and connects the crura of the fornix, and (3) the corpus callosum, which appears early in the foetal period and connects the cerebral hemispheres. The **corpus callosum** is first identified at 11–12 weeks after ovulation, and gradually extends considerably caudalwards. The overlying part of the commissural plate becomes thinned to form the septum pellucidum. Within the septum the narrow cavum septi pellucidi appears. The corpus callosum appears to be fully formed by the middle of prenatal life. Mechanisms of the formation of the corpus callosum are discussed in ▶ Chap. 2. Partial or complete ***absence*** of the ***corpus callosum*** is not uncommon (Lemire et al. 1975; Aicardi 1992; Norman et al. 1995; Kollias and Ball 1997; Paul et al. 2007; Raybaud 2010a; Edwards et al. 2014; Barkovich and Raybaud 2018). Every disorder that influences the development of the commissural plate may lead to this malformation. Dysgenesis of the corpus callosum occurs in approximately 20% as an isolated disorder, but in about 80% of cases in combination with other disorders of the brain (▶ Chap. 10).

1.8.4 Imaging of the Foetal Brain

Foetal magnetic resonance images at 20 and 35 weeks of development are shown in ◘ Figs. 1.36 and 1.37, respectively. At 20 weeks of development, cortical layers, the hypodense subplate in particular, can be easily distinguished in the smooth cerebral cortex. Germinal zones are hyperdense. A 35-week-old brain shows the extensive changes that appear in the cerebrum in the second half of pregnancy. Garel's (2004) MRI atlas presents the foetal brain in detail from 20 weeks of development until birth. Kostović and Vasung (2009) analysed in vitro foetal magnetic resonance imaging of cerebral development. MRI data in the early foetal brain are shown in ◘ Figs. 1.23 and 1.25 (Takakuwa et al. 2021). With 7.0 Tesla MRI, Meng et al. (2012) displayed the development of subcortical brain structures in postmortem foetuses from GW 12 onwards. For ultrasound data on the foetal brain, see Monteagudo and Timor-Tritsch (2009), Pooh and Kurjak (2009) and Guimarães Gonçalves and Hwang (2021).

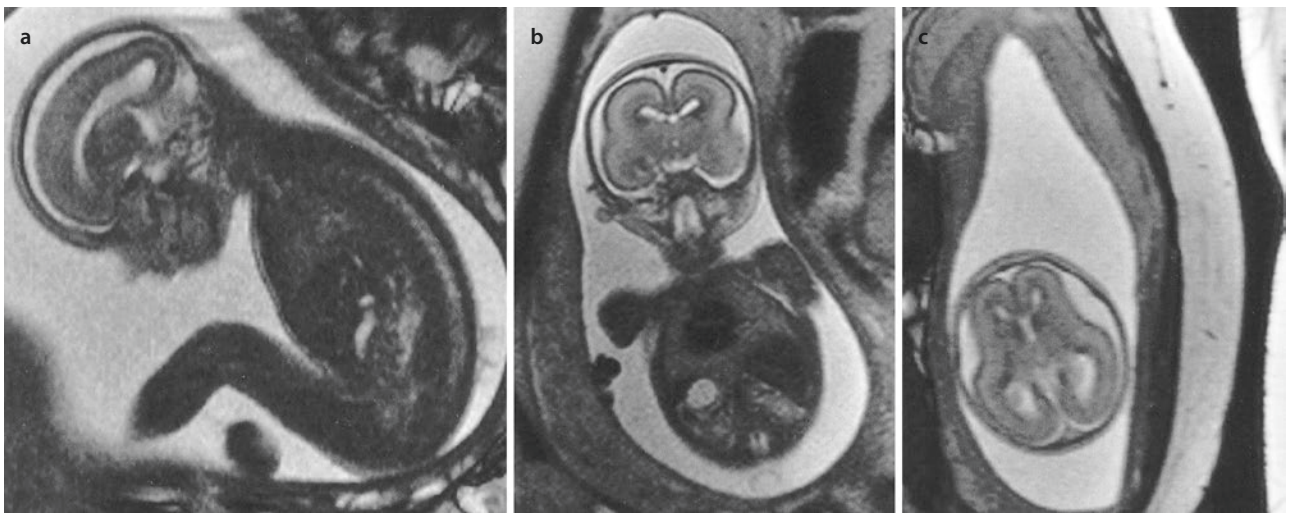

◘ **Fig. 1.36** Foetal T2-weighted MRI taken at the 20th week of development: **a** sagittal section; **b** frontal (or coronal) section; and **c** horizontal (or axial) section. There is a smooth cerebral surface without gyration. The thick periventricular germinal layer has a low-signal intensity. A thin cortical layer is present, below which the large subplate can be recognized. (Courtesy of Ton van der Vliet, Groningen)

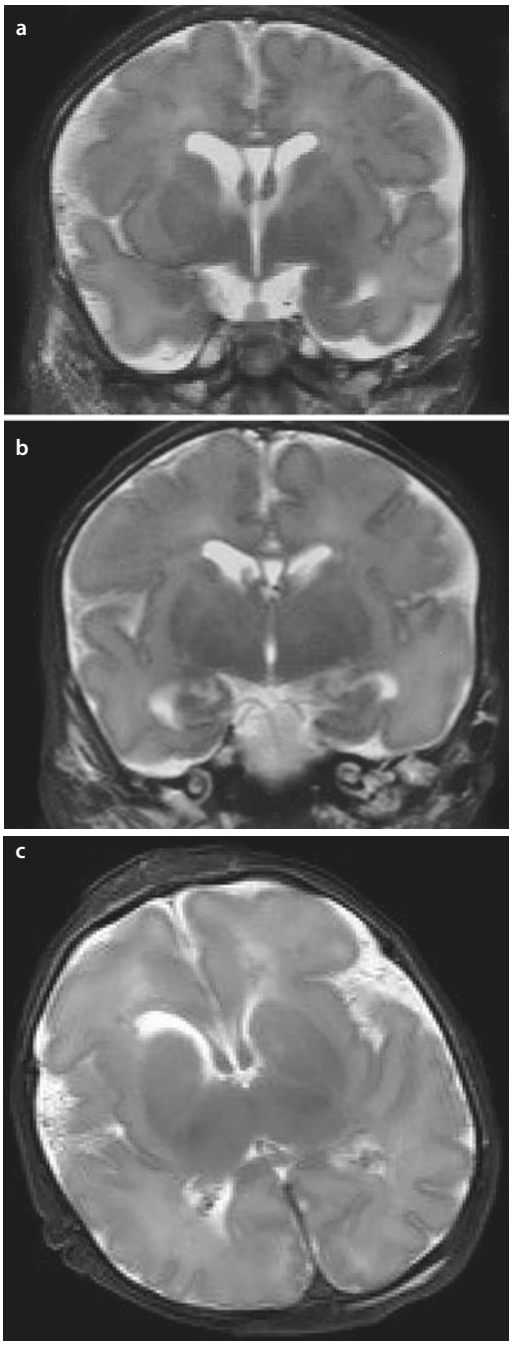

Fig. 1.37 Foetal T2-weighted MRI taken at the 35th week of development. Two frontal (or coronal: **a**, **b**) and one axial **c** sections show increasing development of the insulae and lateral fissures, and an increasing number of gyri and sulci. The basal ganglia (in **a**), the amygdala (in **a**) and the hippocampal region (in **b**) are easily recognized. Note the large cavum septi pellucidi and the prominent fornices (in **a** and **b**). The corpus callosum is visible in **a** and **b**, whereas in **c** the development of the insula can be observed. (Courtesy of Ton van der Vliet, Groningen)

1.9 Development of the Meninges and Choroid Plexuses

The **cranial meninges** originate from several sources such as the prechordal plate, the parachordal mesoderm and the neural crest (O'Rahilly and Müller 1986; Lun et al. 2015). The loose mesenchyme around most of the brain at five weeks of development (CS 15) forms the primary meninx. At six weeks (CS 17), the dural limiting layer is found basally and the skeletogenous layer of the head becomes visible. At seven weeks (CS 19), the cranial pachymeninx and leptomeninx are distinguishable. Hochstetter (1939) showed that, as the dural reflections develop, the posterior point of attachment between the tentorium cerebelli and the falx cerebri gradually moves to a more caudal position in the skull, thereby producing a continual reduction in the size of the posterior cranial fossa relative to the supratentorial fossae. Increases in supratentorial volume relative to infratentorial volume affect such an inferoposterior rotation of the human foetal tentorium cerebelli (Jeffery 2002). Klintworth (1967) found the tentorium cerebelli at CS 20 as a bilateral, three-layered structure. The two tentorial precursors were visible macroscopically by CS 23. They fuse at 55-mm crown-rump length (CRL) to create the straight sinus (Streeter 1915). It is now clear that the meninges of the forebrain and hindbrain serve as signalling centres coordinating developmental events between the cortex and the skull by releasing a variety of secreted factors (Siegenthaler and Pleasure 2011). Recently, Matsunari et al. (2023) studied the formation of the tentorium cerebelli during embryonic and foetal development. During the embryonic period, the lateral folds of the tentorium elongated to traverse the middle part of the midbrain, the tentorium and the falx cerebri appeared separated and no invagination at the parieto-occipital region was observed. In the early foetal period, the cerebrum covered about half of the midbrain, and the separation of

the dural limiting layer at the parieto-occipital region widened from the posterior cerebrum to the rostral cerebellum. The lateral tentorial folds were spread between its tip, continuous with the falx cerebri, and its base plase, located between the midbrain and the rostral hindbrain.

The development of the **spinal meninges** has been studied by Hochstetter (1934) and Sensenig (1951). The future pia mater appears as neural crest cells by CS 11, and at five weeks (CS 15) the primary meninx is represented by a loose zone between the developing vertebrae and the neural tube. After six weeks (CS 18), the mesenchyme adjacent to the vertebrae becomes condensed to form the dural lamella. At the end of the embryonic period (CS 23), the dura completely lines the wall of the vertebral canal. The spinal arachnoid, however, does not appear until either the third trimester or postnatally (O'Rahilly and Müller 1999).

A **choroid plexus** first appears in the roof of the fourth ventricle at CS 18, in the lateral ventricles at CS 19, and in the third ventricle at CS 21 (Ariëns Kappers 1958; Bartelmez and Dekaban 1962; Shiraishi et al. 2013; Lun et al. 2015). Shiraishi et al. (2013) studied the morphogenesis of the choroid plexus of the lateral ventricle during the embryonic period (◘ Fig. 1.38). The primordia appear as simple or club-shaped folds protruding into the ventricles. During CS 21, the choroid plexuses become vascularized. The early choroid plexus of the lateral ventricle is lobulated with vessels running in the mesenchymal stroma and forming capillary nets under the single-layered ependyma. The embryonic choroid plexus is converted into the foetal type during the ninth week of development as the embryonic capillary net is replaced by elongated loops of wavy capillaries that lie under regular longitudinal epithelial folds (Kraus and Jirásek 2002). The stroma of the plexus originates from extensions of the arachnoid into the interior of the brain that form the **vela interposita**. This may explain the origin of the sporadically occurring intraventricular meningiomas, most commonly found in the trigone of the third ventricle (Nakamura et al. 2003). For recent studies on the development of the choroid plexus and the blood–cerebrospinal fluid (CSF) barrier, see Johansson (2014), Liddelow (2015) and Moretti et al. (2015).

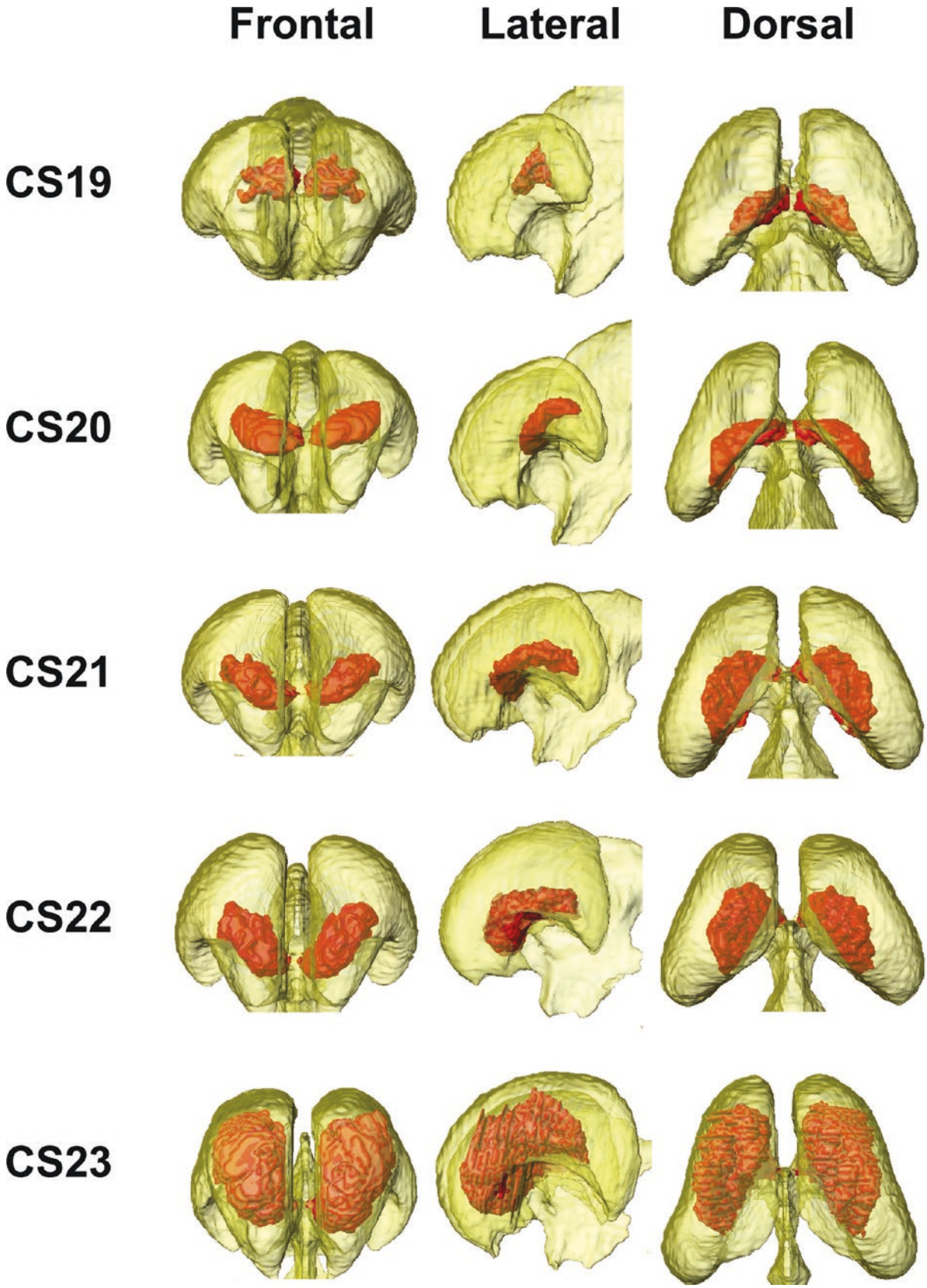

Fig. 1.38 Frontal, lateral and dorsal 3D images of the choroid plexus (in *red*) within the lateral ventricle (in *yellow*). (Modified from Shiraishi et al. 2013, with permission; courtesy Tetsuya Takakuwa, Kyoto)

1

1.10 Development of the Blood Supply of the Brain

The brain is supplied by two pairs of internal carotid and vertebral arteries, connected by the circle of Willis. During the closure of the neural tube, primordial endothelial blood-containing channels are established. From these all other vessels, arteries, veins and capillaries are derived. At CS 12, capital venous plexuses, the capital vein and three aortic arches are present (Streeter 1918; Congdon 1922; Padget 1948, 1957; Raybaud 2010b; ◘ Fig. 1.39). The internal carotids develop early (CS 11–13), followed by the posterior communicating artery, the caudal branch of the internal carotid at CS 14, the basilar and vertebral arteries (CS 16), the main cerebral arteries (CS 17) and finally the anterior communicating

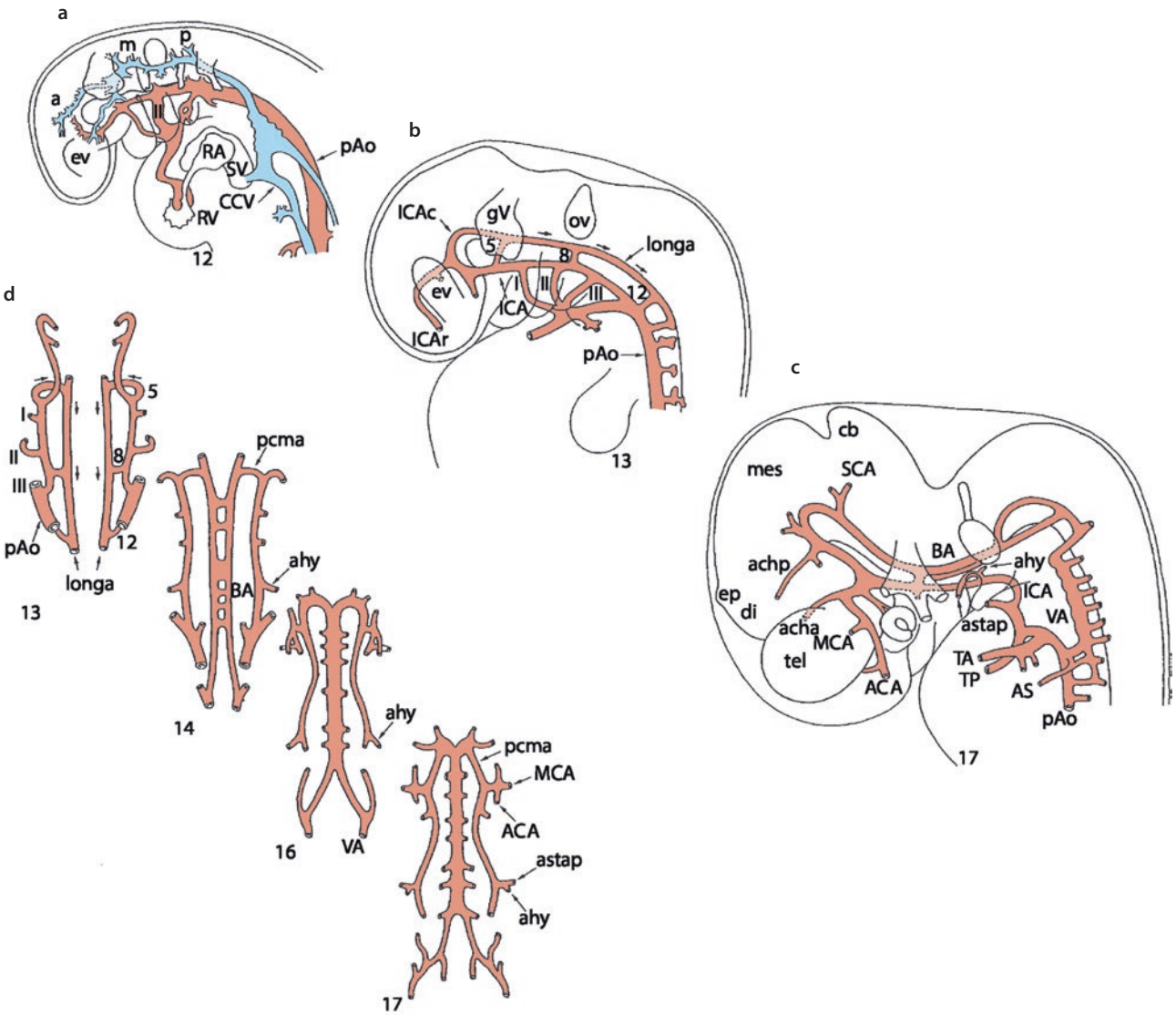

◘ **Fig. 1.39** Overview of the development of the blood supply of the human brain in CS 12 **a**, CS 13 **b**, CS 17 **c** and CS 21 **e**, in the first foetal week **f**, and in the neonate **g**. In **d**, the fusion of the longitudinal arteries to the basilar artery is shown in CS 13, 14, 16 and 17. Arteries are in *red*, veins in *blue*. *a* anterior capital plexus, *AA* aortic arch, *ACA* anterior cerebral artery, *acha, achp* anterior and posterior choroidal arteries, *AICA* anterior inferior cerebellar artery, *ahy* hyoid artery, *AS* subclavian artery, *astap* stapedial artery, *BA* basilar artery, *cb* cerebellum, *cc* corpus callosum, *CCV* common cardinal vein, *DA* ductus arteriosus, *di* diencephalon, *ECA* external carotid artery, *ep* epiphysis, *ev* eye vesicle, *gV* trigeminal ganglion, *ICA* internal carotid artery, *ICAc*, *ICAr* caudal and rostral branches of ICA, *longa* longitudinal artery, *m* middle capital plexus, *MCA* middle cerebral artery, *mes* mesencephalon, *OA* ophthalmic artery, *ov* otic vesicle, *p* posterior capital plexus, *pAo* posterior aorta, *PCA* posterior cerebral artery, *pcma* posterior communicating artery, *PICA* posterior inferior cerebellar artery, *plch* plexus choroideus, *RA* right atrium, *RV* right ventricle, *SCA* superior cerebellar artery, *SV* sinus venosus, *TA* truncus arteriosus, *tel* telencephalon, *TP* truncus pulmonalis, *VA* vertebral artery, *I–III* aortic branches, *5*, *8*, *12* temporary trigeminal, otic and hypoglossal arteries. (After Padget 1948; O'Rahilly and Müller 1999)

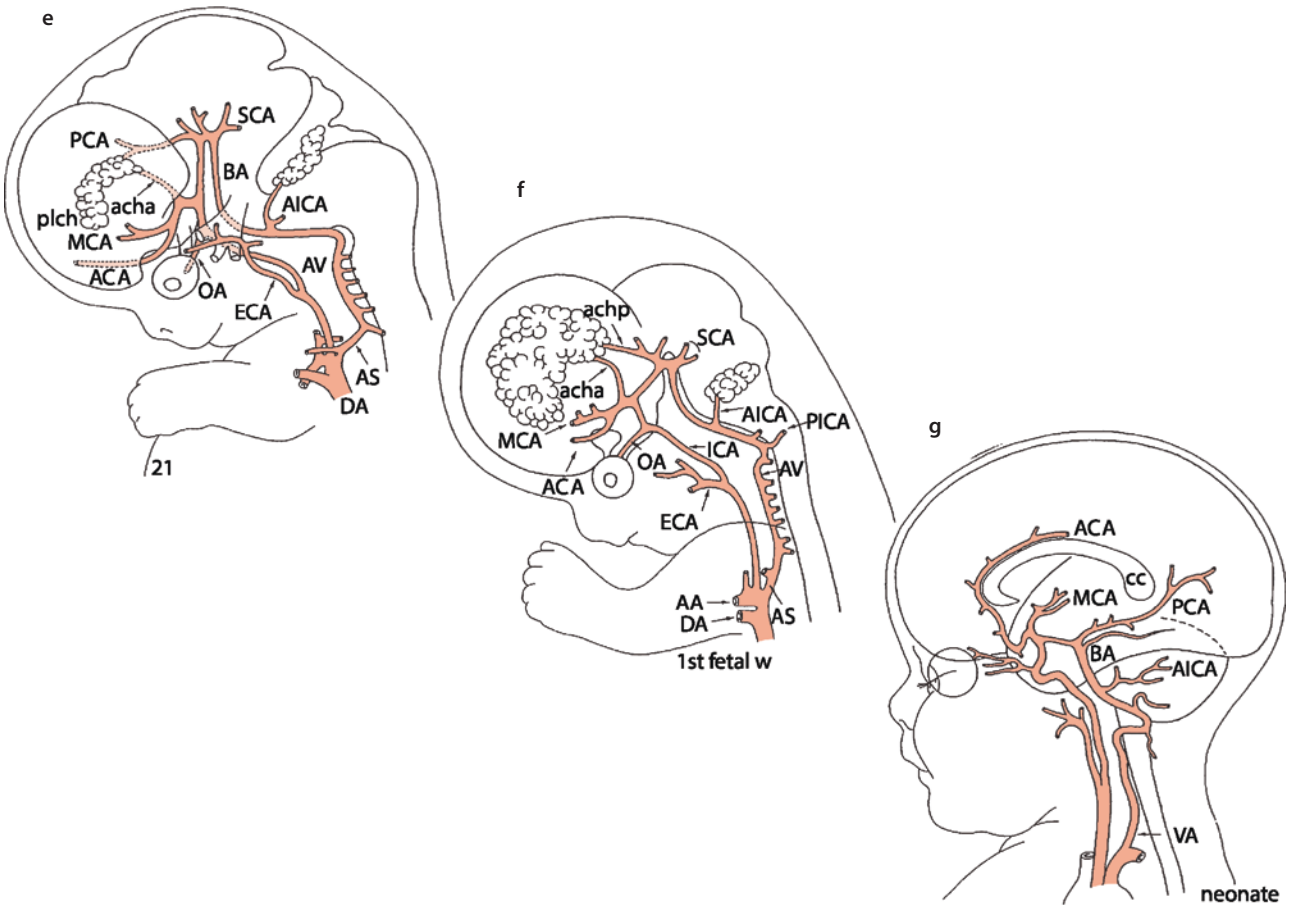

Fig. 1.39 (continued)

artery, thereby completing the circle of Willis (Evans 1911, 1912; Padget 1948; Gillilan 1972). Bilaterally, longitudinal arteries are established at CS 13 and are connected with the internal carotids by temporary trigeminal, otic and hypoglossal arteries. At first, the posterior communicating artery provides the major blood supply to the brain stem. Anastomotic channels unite the two longitudinal arteries, thereby initiating the formation of the basilar artery. The temporary arteries are gradually eliminated, but each of them may persist. The primitive trigeminal artery is the most common of the carotid–basilar anastomoses that persist into adulthood, with an incidence of 0.1–1.0% (Wollschlaeger and Wollschlaeger 1964; Lie 1968; Salas et al. 1998; Suttner et al. 2000; Fig. 1.40). Persistence of a primitive otic artery is shown in Fig. 1.41. The development of the large vessels can be studied with 3D-ultrasound (Pooh 2009; Pooh et al. 2011). For variations of the circle of Willis at the end of the embryonic period, see Furuichi et al. (2018).

Capillaries at the level of the cerebral hemispheres begin to appear at five weeks, and probably earlier in the brain stem (Padget 1948; O'Rahilly and Müller 1999). By five weeks (CS 16), many of the definitive arteries are present and are being transformed into the definitive pattern. At the end of the embryonic period, an anular network of **leptomeningeal arteries** arises from each middle cerebral artery and extends over each developing hemisphere. Similar meningeal branches, originating from the vertebral and basilar arteries, embrace the brain stem and cerebellum. From these leptomeningeal arteries branches grow into the brain. Both supratentorially and infratentorially, **paramedian**, **short circumferential** and **long circumferential arteries** can be distinguished. The first vessels penetrate the telencephalon in the seventh week of gestation, forming a subventricular plexus at about GW 12 (Duckett 1971). The paramedian branches of the anterior cerebral artery have a short course before they penetrate the cerebral parenchyma, whereas the short circumferential arteries such as the striatal artery have a slightly longer course and the long circumferential arteries may reach the dorsal surface of the cerebral hemispheres. At GW 16, the anterior, middle and posterior cerebral arteries, contributing to the formation of the circle of Willis, are well established (Padget 1948). During the further foetal

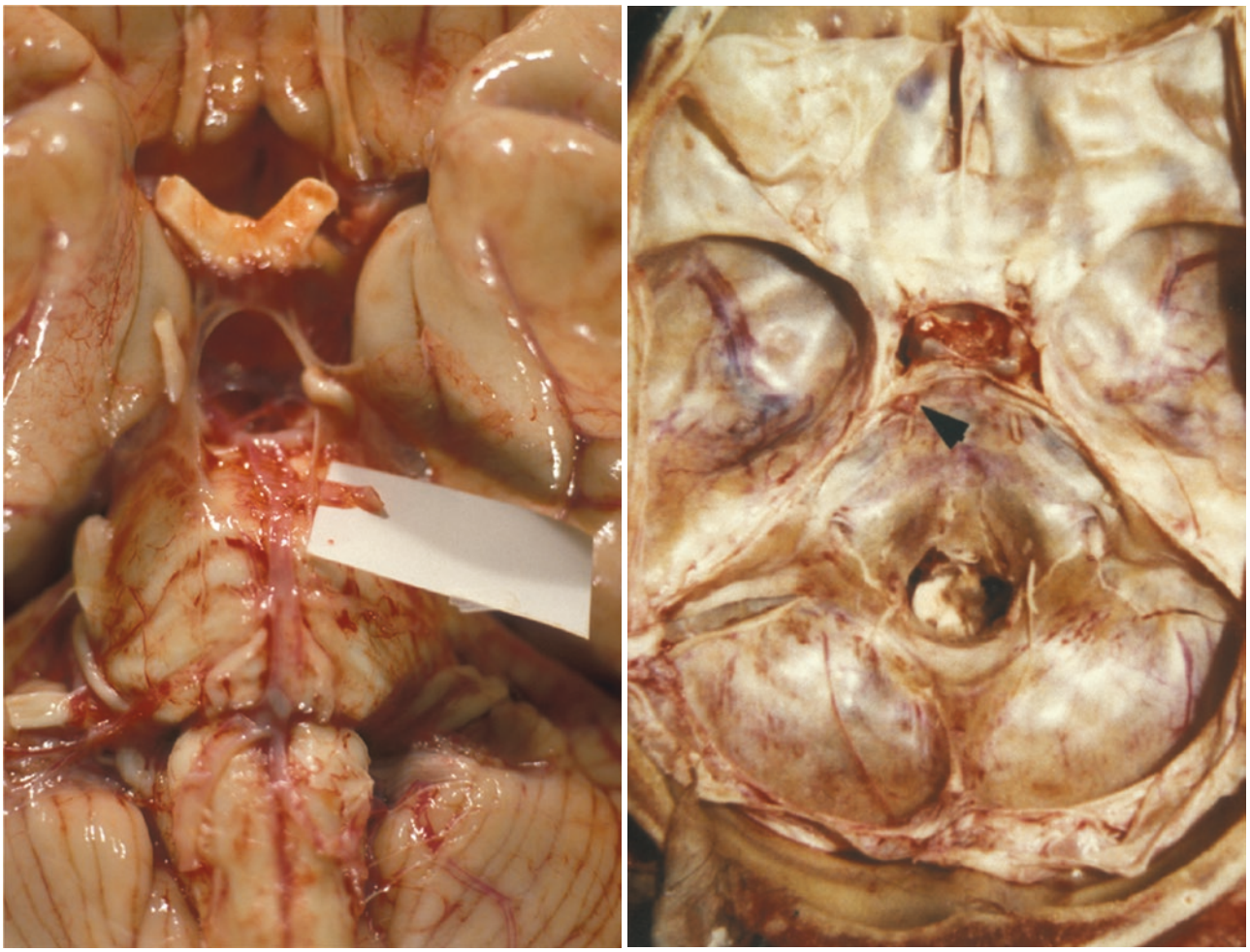

Fig. 1.40 Persistence of the primitive trigeminal artery. Occasional autopsy finding by Akira Hori in a 42-year-old woman

period the relatively simple leptomeningeal arteries increase in tortuosity, size and number of branches. Their branching pattern is completed by GW 28 (Takashima and Tanaka 1978).

Recently, Puelles et al. (2019) attempted a prosomeric analysis of the hypothesis that major vessels invade the brain wall in patterns that are congruent with its intrinsic natural developmental units, as postulated in the prosomeric model. They explored the possibility that brain vascularization in rodents and humans may relate systematically to the genoarchitectonic subdivision of the forebrain. A heterochronic pattern of vascular invasion was found that distinguished between adjacent brain areas with differential molecular profiles. A topological representation of known or newly postulated forebrain arteries, mapped upon the prosomeric model, is shown in Fig. 1.42.

The central parts of the cerebrum are supplied by deep penetrating branches (Kuban and Gilles 1985; Nelson et al. 1991; Rorke 1992; Gilles and Nelson 2012). Smooth muscle is present at the basal ends of striatal arteries by midgestation and extends well into the vessels in the caudate nucleus by the end of the second trimester (Kuban and Gilles 1985). The intracortical vessels also develop gradually (Allsop and Gamble 1979). From GW 13 to 15, radial arteries without side branches course through the cortex. By GW 20, horizontal side branches and recurrent collaterals appear, and from GW 27 to term, shorter radial arteries increase in number. Growth of the intracortical capillaries continues well after birth (Norman and O'Kusky 1986). In the foetal brain, the density of capillaries is much higher in the ventricular zone than in the cortical plate until GW 17 (Duckett 1971; Allsop and Gamble 1979; Norman and O'Kusky 1986). After GW 25, cortical vascularization increases.

At GW 24, a large part of the basal ganglia and internal capsule is supplied by a prominent **Heubner artery**, arising from the anterior cerebral artery (Hambleton and Wigglesworth 1976). The capillary bed in the ventricular zone is supplied mainly by the Heubner artery and terminal branches of the lateral striate arter-

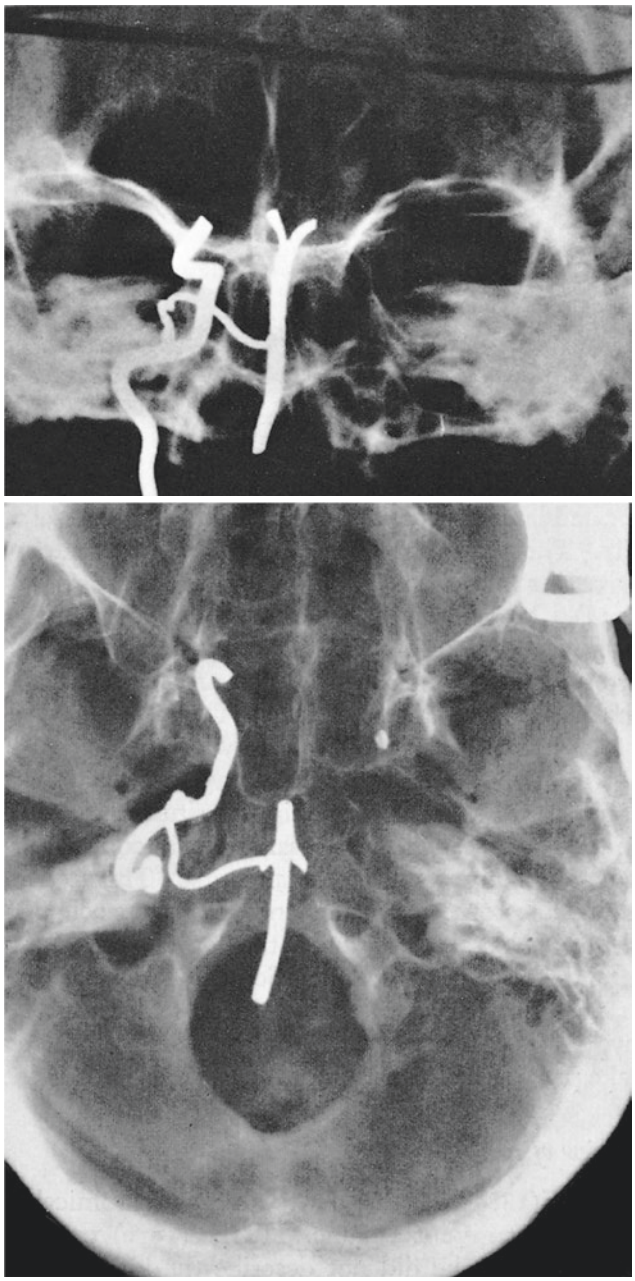

Fig. 1.41 Persistence of the primitive otic artery. (From Lie 1968)

ies from the middle cerebral artery (Wigglesworth and Pape 1980). The cortex and the underlying white matter are rather poorly vascularized at this stage of development. Gradually, the area supplied by the middle cerebral artery becomes predominant when compared to the territories supplied by the anterior and posterior cerebral arteries (Okudera et al. 1988). Early arterial anastomoses appear around GW 16. The sites of arterial anastomoses between the middle and the anterior cerebral arteries move from the convexity of the brain towards the superior sagittal sinus and those between the middle and posterior cerebral arteries move towards the basal aspect of the brain. By GW 32–34, the ventricular zone involutes and the cerebral cortex acquires its complex gyral pattern with an increased vascular supply. The ventricular zone capillaries blend with the capillaries of the caudate nucleus and the territory of the Heubner artery becomes reduced to only a small medial part of the caudate nucleus. In the cortex, there is progressive elaboration of the cortical blood vessels (Hambleton and Wigglesworth 1976; Weindling 2002). Towards the end of the third trimester, the balance of cerebral circulation shifts from a central, ventricular zone oriented circulation to a circulation predominant in the cerebral cortex and white matter. These changes are of major importance in the pathogenesis and distribution of hypoxic/ischaemic lesions in the developing human brain.

Cerebrovascular density correlates with regional metabolic demand (Pearce 2002). Correspondingly, cerebrovascular conductance in the vertebrobasilar and carotid systems increases more slowly than brain weight, particularly during the postnatal period of rapid cerebral growth, myelination and differentiation. As part of normal development, most immature human cerebral arteries appear to have regions of weakened media near vessel bifurcations. These weakened areas are reinforced during maturation via the deposition of additional smooth muscle, but can comprise areas of heightened vulnerability to rupture during early postnatal development (Pearce 2002).

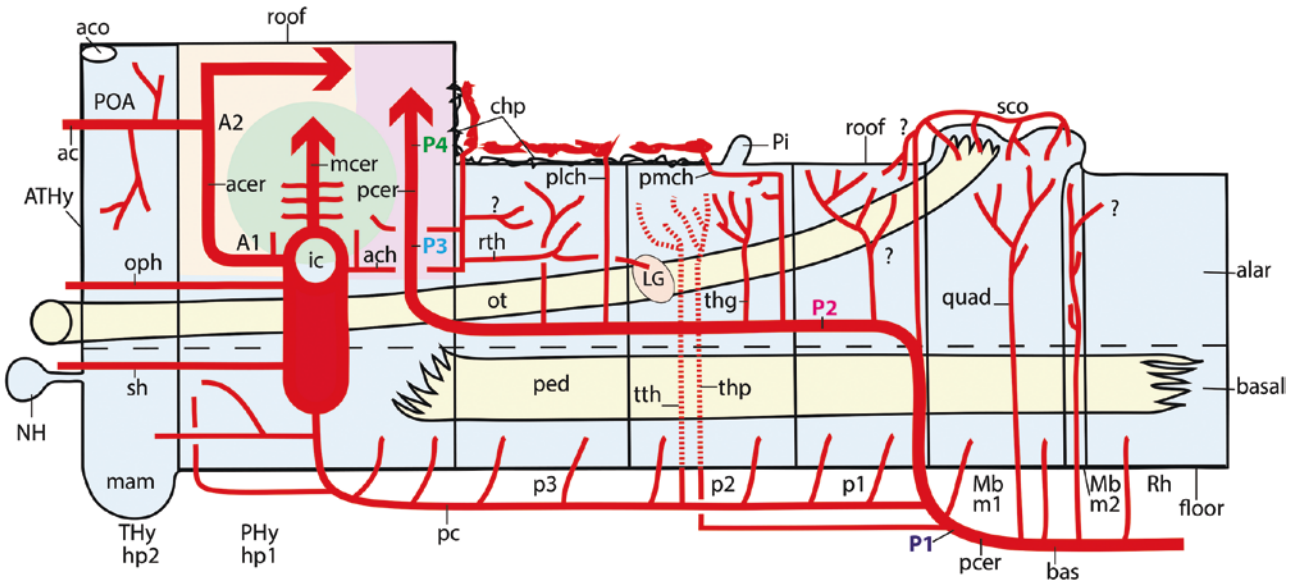

Fig. 1.42 Schematic topological representation of known or new postulated forebrain arteries mapped upon the prosomeric model. All neuromeres and their borders are orthogonally transversal to the axial dimension. The main brain arteries serving this territory derive from the internal carotid (*ic*), posterior communicating (*pc*), posterior cerebral (*pcer*) and basilar (*bas*) arteries. The internal carotid artery courses transversally to the peduncular hypothalamic sector (*PHy*). Its major terminal branches are the anterior cerebral (*acer*) and middle cerebral (*mcer*) arteries. Their territories are indicated in *yellow* and *light green*, respectively. The posterior telencephalic field is supplied by the posterior cerebral artery (*pcer*; in *light red*). The thick arrows in each case represent simplified pallial arborizations and the thin collaterals central branches to the subpallium. The anterior communicating artery (*ac*) supplies the preoptic (*POA*) and septal regions. The posterior communicating artery arises from the internal carotid and bends caudalwards until it meets the posterior cerebral artery near its origin from the basilar artery. A multiplicity of basal arteries enters the basal tegmentum at all neuromeric levels. Only the thalamic perforant arteries (*tth* and *thp*) further extend into the alar domain, whereas a separate set of arteries address the hindbrain, midbrain and diencephalic alar plates. Other abbreviations: *ach* anterior choroidal artery, *aco* anterior commissure, *ATHy* acroterminal preopticohypothalamic domain, *chp* choroid plexus, *hp1*, *hp2* hypothalamic prosomeres, *LG* lateral geniculate body, *mam* mammillary body, *Mb* midbrain, *m1*, *m2* mesomeres, *NH* neurohypophysis, *oph* ophthalmic artery, *ot* optic tract, *P1–P4* segments of posterior cerebral artery, *p1–p3* diencephalic prosomeres, *ped* cerebral peduncle, *plch*, *pmch* posterior lateral and medial choroidal branches, *quad* quadrigeminal artery, *Rh* rhombencephalon, *sco* superior colliculus, *sh* superior hypophysial artery, *Thy* terminal hypothalamic sector. (From Puelles L et al. 2019 *Patterned vascularization of embryonic mouse forebrain, and neuromeric topology of major human subarachnoidal arterial branches: A prosomeric mapping.* Front Neuroanat 13:59; with permission; kindly provided by José Luis Ferran, Murcia)

In younger premature infants (22–30 weeks old), the blood vessels of the germinal, periventricular zone and the perforating ventriculopetal vessels are particularly vulnerable to ***perinatal asphyxia*** (Marín-Padilla 1996; Volpe 1998; Weindling 2002). Damage to these vessels often causes focal haemorrhagic lesions. In **older premature infants** (30–34 weeks), the foetal white matter seems to be particularly vulnerable to hypoxic–ischaemic injury, leading to ***periventricular leukomalacia*** or *PVL* (▶ Chap. 3), and often resulting in infarction (necrosis) and cavitation (Banker and Larroche 1962; Marín-Padilla 1997, 1999; Volpe 2001, 2009, 2019; Squier 2002; Weindling 2002; Rutherford et al. 2010). PVL refers to necrosis of white matter in a characteristic distribution, i.e. in the white matter dorsal and lateral to the external angles of the lateral ventricles. The corticospinal tracts run through the periventricular region. Therefore, ***impaired motor function*** is the most common neurologic sequela of periventricular white matter injury (Banker and Larroche 1962; Aida et al. 1998; Staudt et al. 2000). Periventricular white matter lesions account for the pathogenesis of a large number of children with spastic hemiparesis (Niemann et al. 1994). In **younger premature infants** with very low birth weight (less than 1500 g), however, ***cognitive deficits*** without major motor deficits are by far the dominant neurodevelopmental sequelae in infants (Woodward et al. 2006; Volpe 2009). In PVL, the primary event is most likely to be a destructive process and the subsequent developmental disturbances are secondary. The necrosis involves all cellular elements, and, therefore, focal loss of premyelinating oligodendrocytes, axons and perhaps late-migrating interneurons (Fig. 1.43). ***Cystic PVL*** probably accounts for the small group of infants who show spastic diplegia, whereas ***non-cystic PVL*** cor-

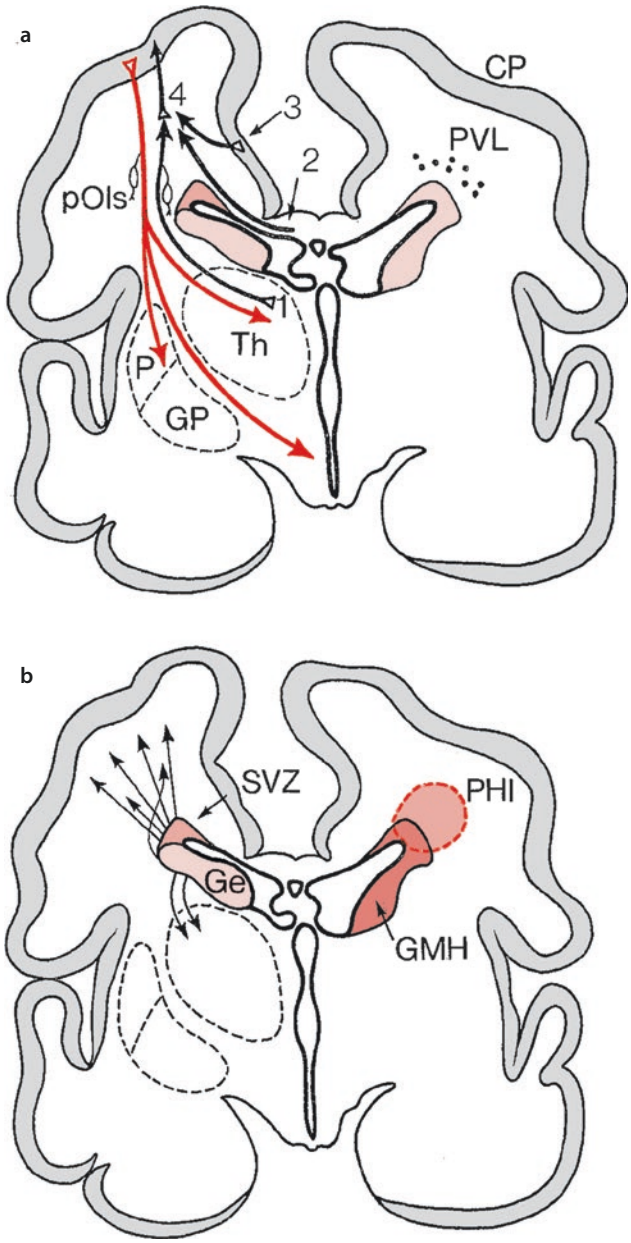

Fig. 1.43 Anatomical relationships between the major developmental events and the topography of periventricular leukomalacia (*PVL*) (**a**) and germinal matrix haemorrhage (*GMH*) and periventricular haemorrhagic infarction (*PHI*) (**b**). The fibre connections that may become involved arise from *1*, the thalamus (*Th*); *2*, the contralateral hemisphere via the corpus callosum; *3*, the ipsilateral hemisphere; and synapse initially on subplate neurons (*4*). Corticofugal projections are shown in *red*. Premyelinating oligodendrocytes (*pOls*) ensheathe axons before full differentiation to mature myelin-producing oligodendrocytes. *GE* ganglionic eminence, *GP* globus pallidus, *P* putamen, *SVZ* subventricular zone. (After Volpe 2009)

relates with the cognitive deficits observed later, usually in the absence of major motor deficits. The consequences will be lesser than the wider cellular effects of diffuse PVL (Volpe 2009, 2019; ▶ Chap. 3).

Dural plexuses associated with the precardinal veins become modified to form the various dural sinuses around the brain (Streeter 1915, 1918; Lindenberg 1956; Padget 1957). Definitive venous channels emerge from the primitive vascular net later than the arteries do. Moreover, the complicated venous anastomoses are essential to facilitate a greater adjustment to the changing needs of their environment over a considerably longer period (Padget 1957). The development of the human **cranial venous system** is summarized in ◘ Fig. 1.44. During Padget's venous stage 1 (CS 12), **capital venous plexuses** and the **capital vein** are forming (◘ Fig. 1.44a). By venous stage 2 (CS 14), three relatively constant **dural stems**, anterior, middle and posterior, are present draining into a **primary head sinus** (capital or 'head' vein) that is continuous with the anterior cardinal vein. During venous stages 3 and 4 (CS 16 and 17), the dural venous channels come to lie more laterally as the cerebral hemispheres and the cerebellar anlage expand and the otic vesicles enlarge (◘ Fig. 1.44c). The head sinus and the primitive internal jugular vein also migrate laterally. By venous stage 5 (CS 19), the head sinus is replaced by a secondary anastomosis, the **sigmoid sinus**. Moreover, more cranially the **primitive transverse sinus** is formed. During venous stage 6 (CS 21), the external jugular system arises (◘ Fig. 1.44d). Most parts of the brain, except for the medulla, drain into the junction of the sigmoid sinus with the primitive transverse sinus. Meanwhile, the Galenic system of intracerebral drainage emerges as the result of accelerated growth of the ganglionic eminences. Subsequent venous changes depend largely upon the expansion of the cerebral and cerebellar hemispheres and the relatively late ossification of the skull (◘ Fig. 1.44e, f). One of the most common malformations of the cerebral venous system is the ***vein of Galen malformation*** (▶ Chap. 3). This malformation can be defined by direct arteriovenous fistulas between choroidal and/or quadrigeminal arteries and an overlying single median venous sac (Raybaud et al. 1989; Raybaud 2010b; Pooh et al. 2003, 2011; Rama Murthy 2019). This median venous sac may be due to persistence of the embryonic **median prosencephalic** *vein* of Markowski (1921, 1931).

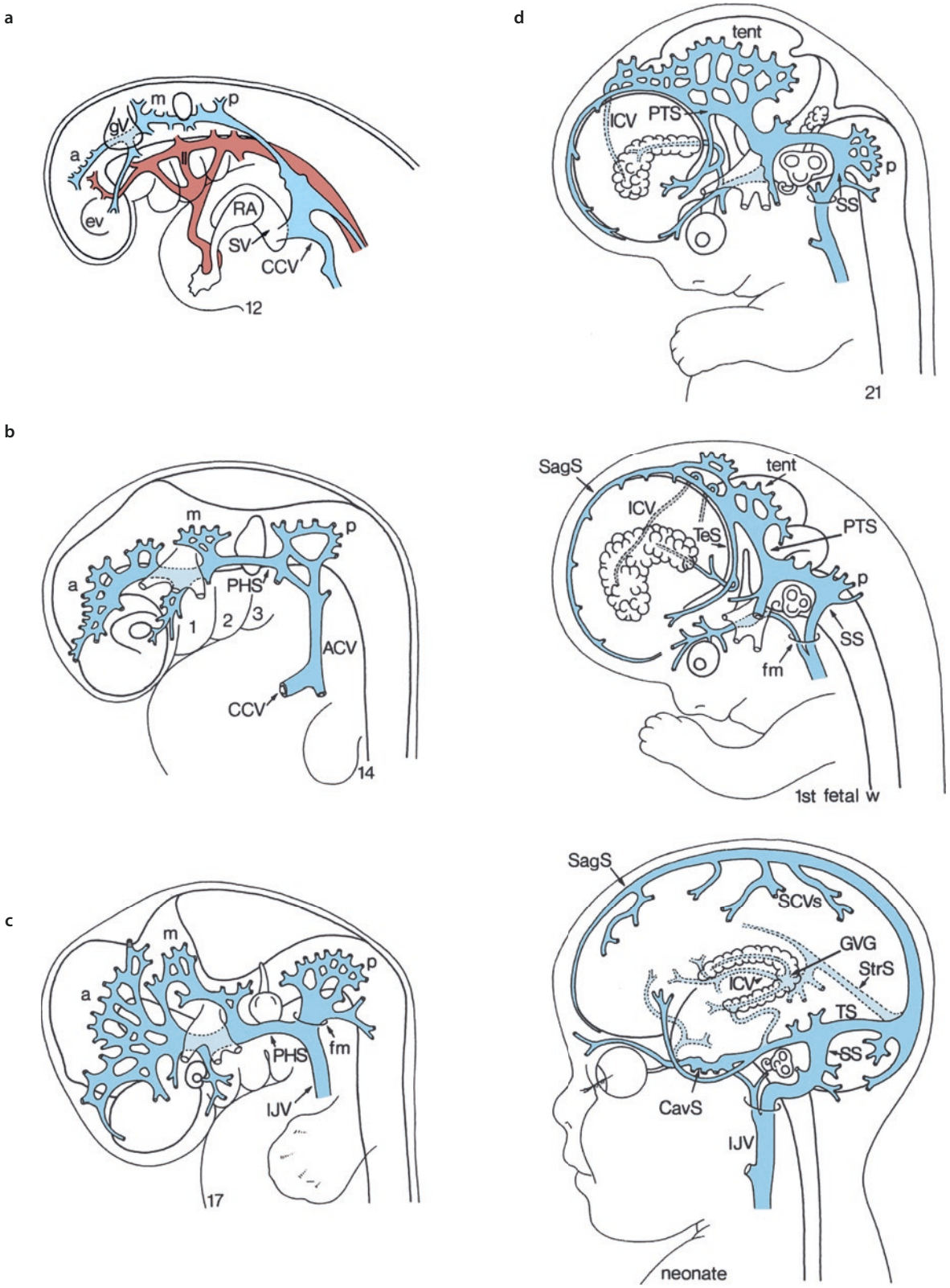
a
m
p
gV
a
ev
RA
SV
CCV
12
b
m
p
a
PHS
1
2
3
ACV
CCV
14
c
m
p
a
PHS
fm
IJV
17
d
tent
ICV
PTS
p
SS
21
SagS
tent
ICV
TeS
PTS
p
SS
fm
1st fetal w
SagS
SCVs
GVG
StrS
ICV
TS
SS
CavS
IJV
neonate

1.11 Development of Fibre Tracts and Their Myelination

1.11.1 Development of Fibre Tracts

Early generated, 'pioneer' neurons lay down an axonal scaffold, containing guidance cues that are available to later outgrowing axons (► Chap. 2). The first descending brain stem projections to the spinal cord can be viewed as pioneer fibres. They arise in the interstitial nucleus of the medial longitudinal fasciculus (MLF) and in the reticular formation (Müller and O'Rahilly 1988a, b). At early developmental stages (from CS 11/12 onwards), in the brain stem a ventral longitudinal tract can be distinguished, followed by lateral and medial longitudinal fasciculi at CS 13. Descending fibres from the medullary reticular formation reach the spinal cord in embryos of 10–12 mm CRL (Windle and Fitzgerald 1937). Interstitiospinal fibres from the interstitial nucleus of the MLF start to descend at CS 13, i.e. at 28 days. In 12-mm-CRL embryos (about CS 17/18), vestibulospinal projections were found (Windle 1970). At the end of the embryonic period, the MLF is well developed, and receives ascending and descending (the medial vestibulospinal tract) components from the vestibular nuclear complex (Müller and O'Rahilly 1990c). The lateral vestibulospinal tract arises from the lateral vestibular nucleus. Windle and Fitzgerald (1937) also followed the ingrowth of dorsal root projections and the development of commissural, ascending and descending spinal pathways (► Chap. 6). Ascending fibres in the dorsal funiculus have reached the brain stem at CS 16 (Müller and O'Rahilly 1989). Decussating fibres, forming the medial lemniscus, were first noted at CS 20 (Müller and O'Rahilly 1990a, b; ► Chap. 7).

The **corticospinal tract** is one of the latest developing descending pathways (ten Donkelaar 2000). At CS 21, the cortical plate starts to develop, whereas a definite internal capsule is present by CS 22 (Müller and O'Rahilly 1990b). Hewitt (1961) found the earliest sign of the internal capsule (probably the thalamocortical component; Yamadori 1965) in CS 18 (13–17 mm CRL). Humphrey (1960) studied the ingrowth of the corticospinal tract into the brain stem and spinal cord with a silver technique (◘ Fig. 1.45). The pyramidal tract reaches the level of the pyramidal decussation at the end of the embryonic period, i.e. at eight weeks of development (Müller and O'Rahilly 1990c). Pyramidal decussation is complete by GW 17, and the rest of the spinal cord is invaded by GW 19 (lower thoracic cord) and GW 29 (lumbosacral cord; Humphrey 1960). Owing to this protracted development, ***developmental disorders of the pyramidal tract*** may occur over almost the entire prenatal period, and may include aplasia, hypoplasia, hyperplasia, secondary malformations due to destructive lesions, anomalies of crossing and disorders of myelination (ten Donkelaar et al. 2004). Aplasia of the pyramidal tracts is characterized by the absence of the pyramids (see ► Chap. 6).

With **diffusion tensor imaging (DTI)**, a novel branch of MRI, anatomical components can be delineated with high contrast and revealed at almost microscopical level (Mori et al. 2005; Kasprian et al. 2008; Catani and Thiebaut de Schotten 2012). Huang et al. (2006, 2009) analysed DTI data of fixed second-trimester human foetal brains. DTI tractography revealed that important white matter tracts, such as the corpus callosum, the uncinate fasciculus and the inferior longitudinal fasciculus, become apparent during this period. Three-dimensional reconstruction of white matter tracts of postmortem foetal brains of 13, 15 and 19 weeks are shown in ◘ Fig. 1.46. Vasung et al. (2010) further analysed the development of axonal pathways in the human foetal frontolimbic brain, combining histochemical data and DTI (◘ Fig. 1.47; ► Chap. 10). For an extensive analysis of the ingrowth of thalamocortical fibres in human foetuses, Krsnik et al. (2017) again combined histochemical and DTI data (see ► Chap. 10). Tractography pathways at later foetal stages are shown in ◘ Fig. 1.48 (Takahashi et al. 2012; Huang and Vasung 2014). Tractography at GW 19 shows dominant radial pathways with immature forms of projection, as well as limbic and few emerged association pathways. At GW 22, apart from dominant radial pathways, emerging long-range connectivity patterns are found. At GW 26, radial pathways are less prominent in dorsal frontal, parietal and inferior frontal parts of the brain, and emergent short-range cortical and long-range association pathways become evident. At GW 33, radial pathways are also less dominant in the temporal and occipital lobes, and emergent short-range corticocortical and long-range association pathways become evident ventrally. At GW 42, radial

◘ **Fig. 1.44** Development of the venous system of the human brain from CS 12 (**a**) until the neonatal period (**f**) . Veins are in *blue*, early arteries in *red*. *a* anterior capital plexus, *ACV* anterior cardinal vein, *CavS* cavernous sinus, *CCV* common cardinal vein, *ev* eye vesicle, *fm* foramen magnum, *GVG* great vein of Galen, *ICV* internal cerebral vein, *IJV* internal jugular vein, *m* middle capital plexus, *p* posterior capital plexus, *PHS* primary head sinus, *PTS* primitive transverse sinus, *RA* right atrium, *SagS* sagittal sinus, *SCVs* superior cerebral veins, *SS* sigmoid sinus, *StrS* straight sinus, *SV* sinus venosus, *tent* tentorial plexus, *TeS* tentorial sinus, *TS* transverse sinus, *II* second aortic branch, *1*, *2*, *3* pharyngeal arches. (After Streeter 1918; Padget 1957)

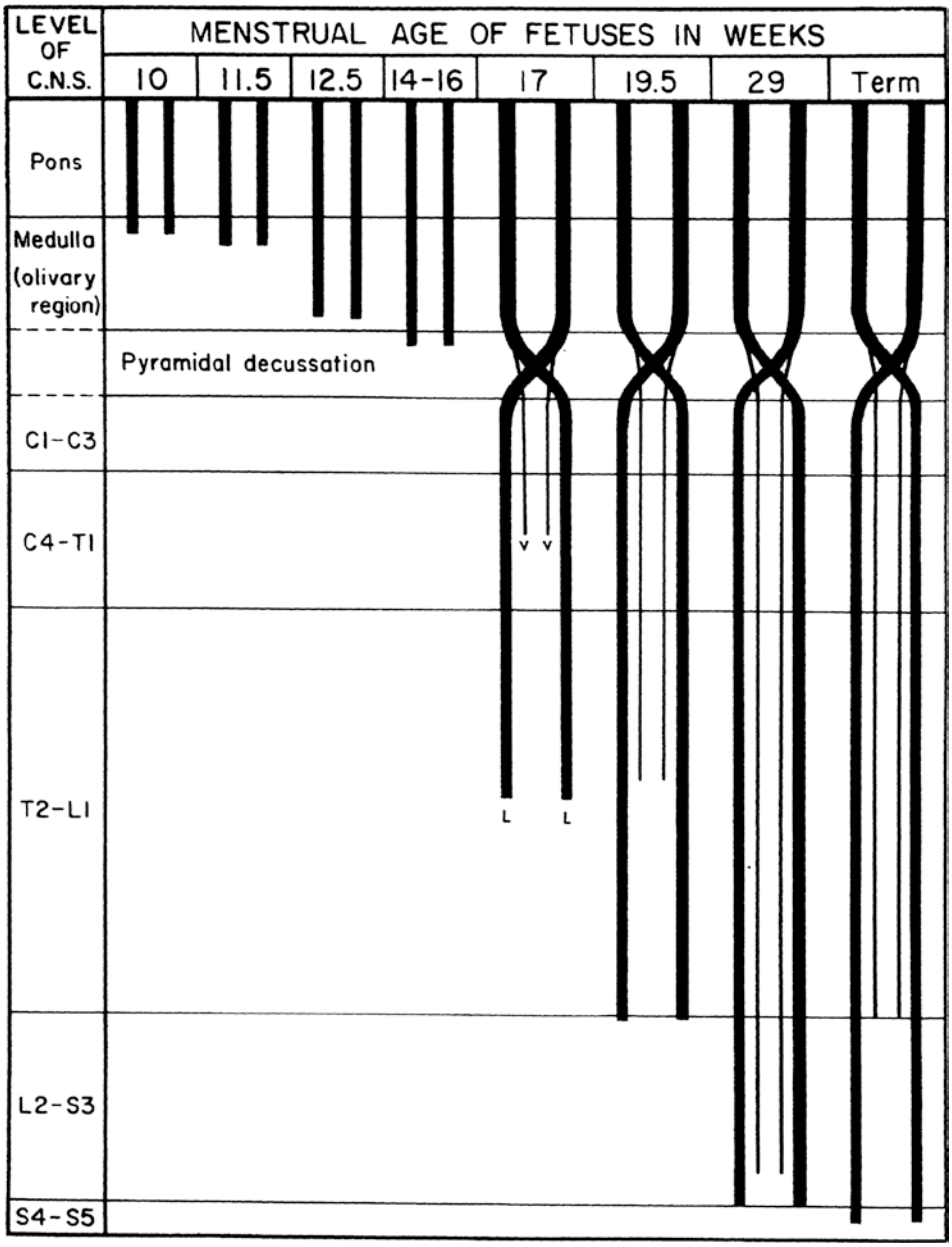

Fig. 1.45 The outgrowth of the human corticospinal tracts. (After Humphrey 1960)

pathways are not evident anymore, and abundant complex, crossing short- and long-range association pathways are present. In Fig. 1.49, diffusion MRI tractography of the white matter tracts in developing foetal and infant brains is shown for 16 postmenstrual weeks until 2 years of age (Ouyang et al. 2019). For a review on methodological challenges and neuroscientific advances in MRI of the neonatal brain, see Dubois et al. (2021). The DTI technique can also be applied to congenital brain malformations (Kasprian et al. 2008; Wahl and Mukherjee 2009; Mitter et al. 2015; Vasung et al. 2017, 2019).

Fig. 1.46 3D depiction of the development of white matter tracts in 13-, 15- and 19-week-old brains. **a** Lateral views of limbic tracts with the fornix and stria terminalis in *pink* and the cingulum bundle in *purple*; **b** oblique views of commissural fibres with the corpus callosum in *pink* and the middle cerebellar peduncle in *green*; **c** lateral views of projection fibres with the cerebral peduncle in *red* and the inferior cerebellar peduncle in *purple*; **d** lateral views of association tracts with the extreme capsule in *blue*, the inferior longitudinal fasciculus/inferior fronto-occipital peduncle in *green* and the uncinate fasciculus in *red*. (From Huang et al. 2009 J Neurosci 29:4263–4273; kindly provided by Hao Huang, Philadelphia; reproduced with permission from the Society for Neuroscience)

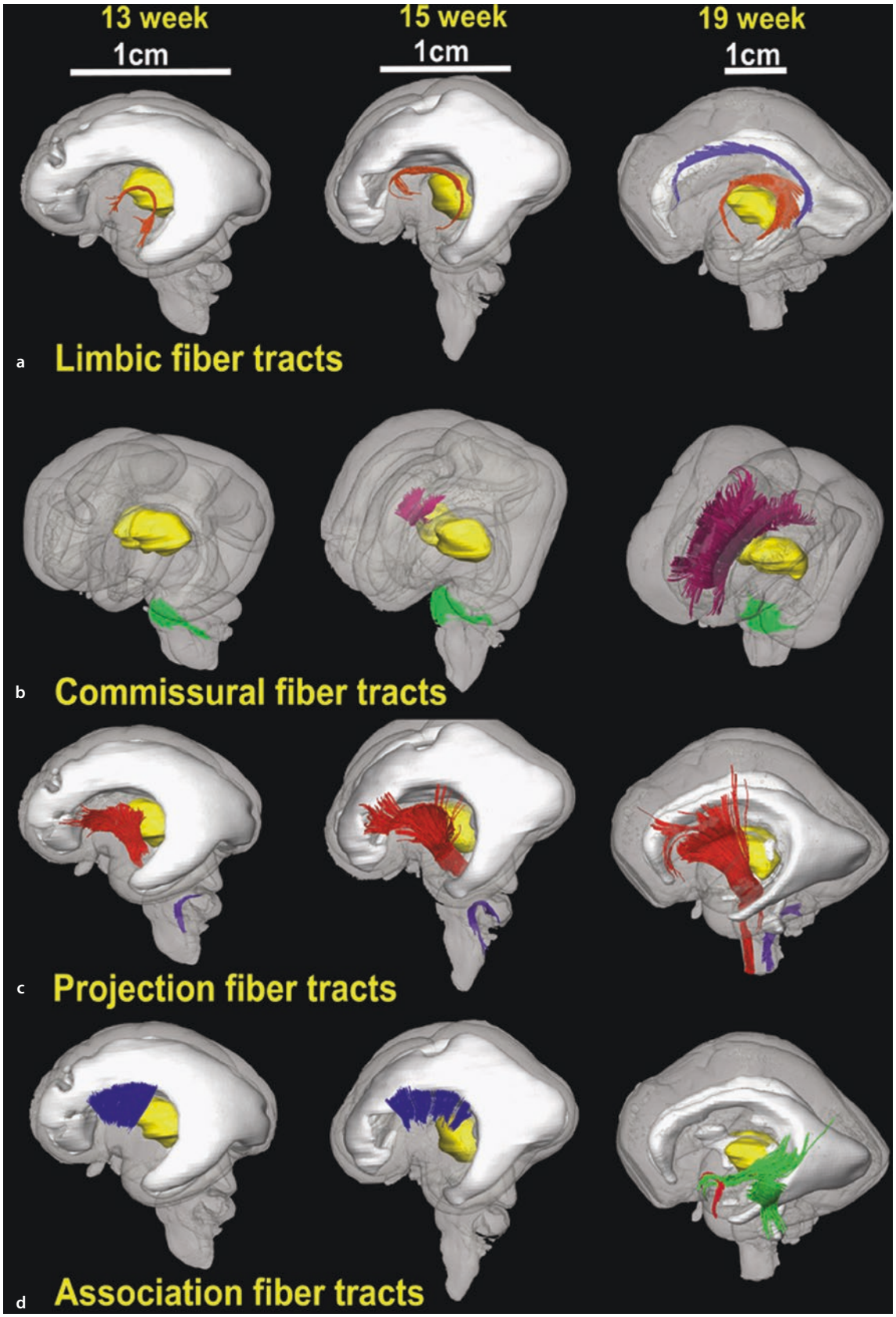
13 week
1cm
15 week
1cm
19 week
1cm
a Limbic fiber tracts
b Commissural fiber tracts
c Projection fiber tracts
d Association fiber tracts

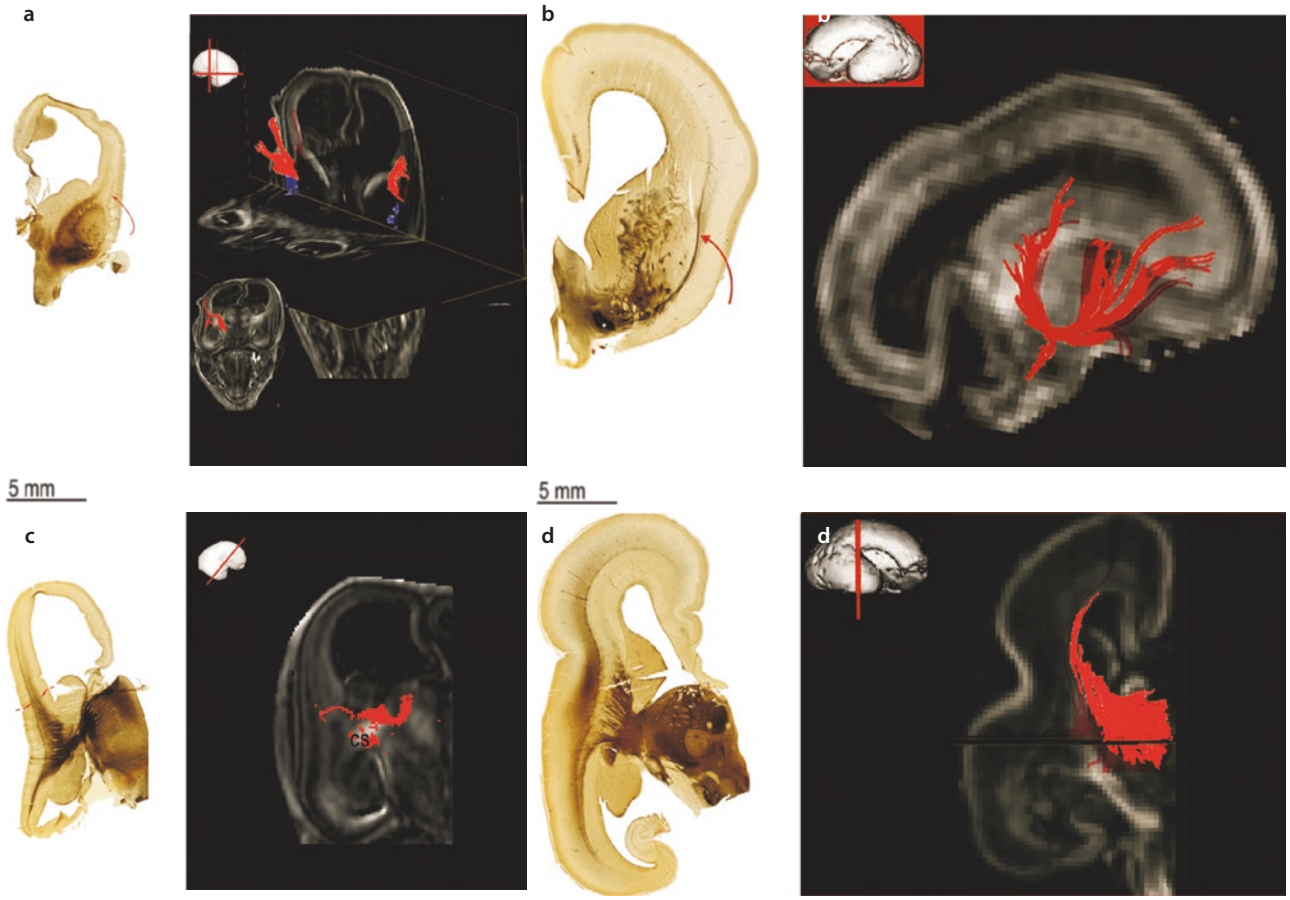

Fig. 1.47 Development of cortical afferent fibres at 11 **A, a, C, c**, 15 **B, b, D** and 17 **d** postconceptual weeks (PCW) revealed by acetylcholinesterase (AChE) histochemical staining **A–D** and DTI **a–d**. The upper row of figures **A, B** shows the external capsule (*curved red arrow*) in AChE-stained sections at PCW 11 and 15, respectively. The DTI tractography reconstructions show the bifurcating appearance of the external capsule at PCW 11 **a** into the external sagittal stratum at PCW 15 **b**. The diencephalotelencephalic junction can be seen at PCW 11 on AChE-stained sections (**C**, *red arrows*). At PCW 11, DTI reveals thalamocortical fibres originating from the mediodorsal thalamus and passing through the cerebral stalk (*cs* in **c**). At PCW 15, thalamocortical fibres running through the internal sagittal stratum can be shown by AChE-staining **D**, whereas they are revealed by DTI tractography at PCW 17 **d**. (The figures were modified from Vasung et al. 2010, with permission)

1.11.2 Development of Myelination

Fibre tracts that appear early in development generally undergo myelination before later-appearing tracts (Flechsig 1920; Yakovlev and Lecours 1967; Gilles et al. 1983; Brody et al. 1987; Kinney et al. 1988; Gilles and Nelson 2012; Fig. 1.50). **Myelination** in the CNS is undertaken by oligodendrocytes, and is a very slow process. The presence of myelin has been noted in the spinal cord at the end of the first trimester and proceeds caudorostrally. The motor roots precede the dorsal roots slightly. In the CNS, the afferent tracts become myelinated earlier than the motor pathways. In the brain stem, myelination starts in the MLF at eight postovulatory weeks. The vestibulospinal tracts become myelinated at the end of the second trimester, whereas the pyramidal tracts begin very late (at the end of the third trimester), and myelination is not completed in them until about two years (Fig. 1.51). In Fig. 1.52, anatomical images of the developing brain for a preterm newborn at GW 31, term-born infants at 6, 19 and 34 weeks of postnatal age, and a young adult are shown (Dubois et al. 2014). The myelin water fraction shows its increase with age, and the decrease in T1 and T2 within the white matter. Cortical association fibres are the last to become myelinated. The appearance of myelin in MRI lags about one month behind the histological time tables (van der Knaap and Valk 1995; Ruggieri 1997). As judged from relative signal intensities, myelin is present at 30–34 weeks of development in the following structures (Sie et al. 1997; van Wezel-Meijler et al. 1998): the medial lemniscus, the superior and inferior colliculi, the decussation of the superior cerebellar

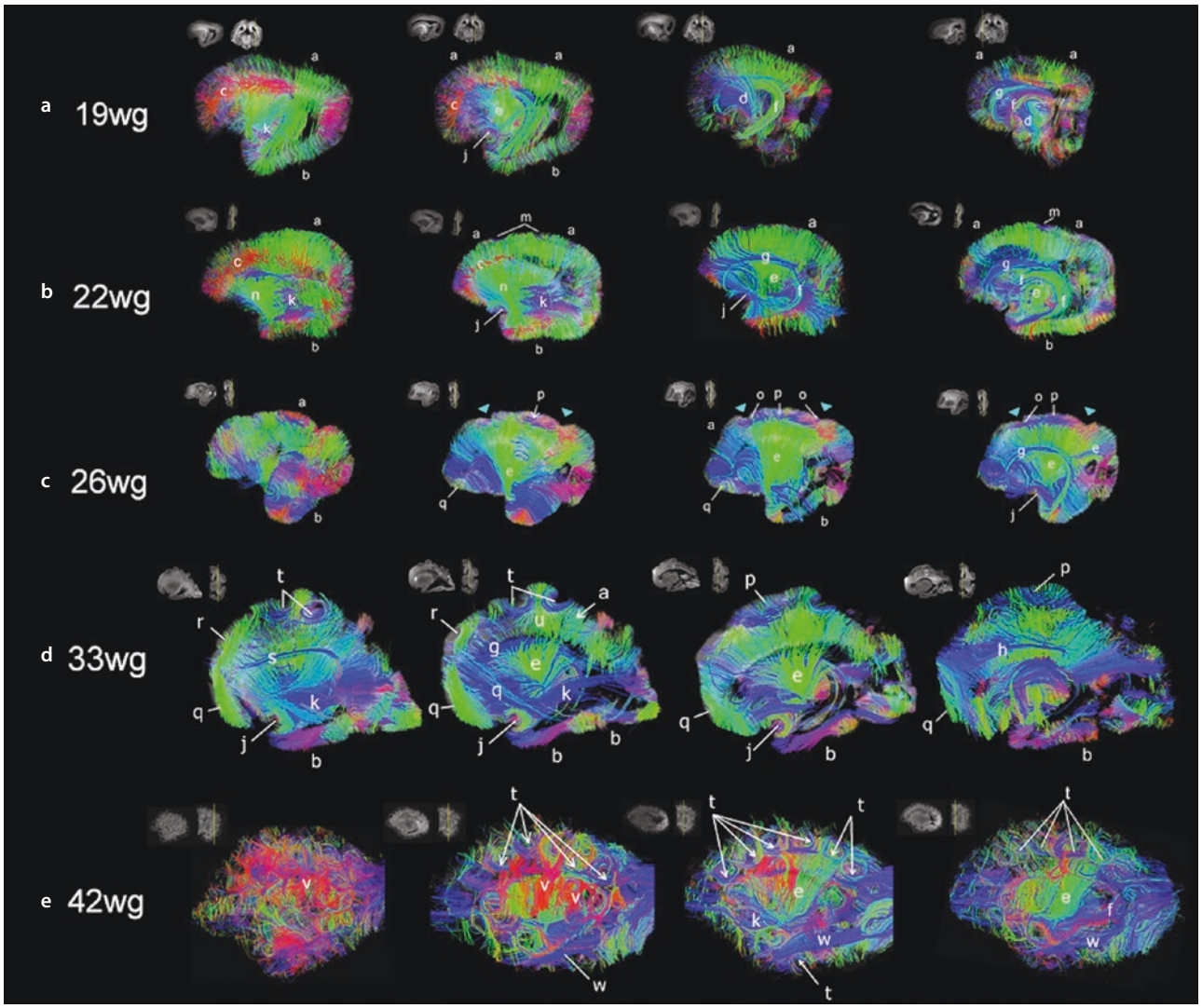

Fig. 1.48 Tractography pathways at GW 19 **a**, 22 **b**, 26 **c**, 33 **d** and 42 **e**. At GW 19, dominant radial pathways (**a** in dorsal areas, **b** in ventral areas, **c** in mediolateral direction) are present with immature forms of projection, limbic and few emergent association pathways (**d** corticospinal tract, **e** corticothalamic/thalamocortical tract, **f** fornix, **g** ganglionic eminence, **j** uncinate fasciculus, **k** inferior fronto-occipital fasciculus); at GW 22, dominant radial pathways (**a** in dorsal areas, **b** in ventral areas) and emerging long-range connectivity patterns are found (**e** corticothalamic/thalamocortical tract, **f** fornix, **g** ganglionic eminence, **j** uncinate fasciculus, **k** inferior fronto-occipital fasciculus, **m** superficial horizontal pathways, **n** frontotemporal pathways); at GW 26, radial pathways (**a** in dorsal areas, **b** in ventral areas) are less predominant in dorsal and inferior parts of the frontal lobe as well as in the parietal lobe, and emergent short-range corticocortical and long-range association pathways are present (**e** corticothalamic/thalamocortical tract, **f** fornix, **g** ganglionic eminence, **j** uncinate fasciculus, **o**, **p**, **q** corticocortical pathways); at GW 33, less dominant radial pathways are also found in the temporal and occipital lobes (**a** in dorsal areas, **b** in ventral areas), and emergent short-range corticocortical and long-range association pathways are present ventrally (**e** corticothalamic/thalamocortical tract, **f** fornix, **g** ganglionic eminence, **h** cingulum, **j** uncinate fasciculus, **k** inferior fronto-occipital fasciculus, **p**, **q**, **r**, **s** corticocortical pathways); at GW 42, no evident radial pathways are present anymore, but abundant complex, crossing short- and long-range corticocortical pathways are found (**e** corticothalamic/thalamocortical tract, **f** fornix, **k** inferior fronto-occipital fasciculus, **t** cortical u-fibres, **v** corticocortical fibres, **w** inferior longitudinal fasciculus). In all panels, tractography pathways passing through a sagittal slice in upper left corner is shown. In a coronal slice next to the upper left corner sagittal slice, the location of the sagittal slice is shown as a yellow line. Colours indicate the orientation of the pathways: red, left-right; blue, anterior-posterior; green, dorsal-ventral. (Modified from Takahashi et al. 2012; and from Huang and Vasung 2014, with permission)

peduncles, the cerebral peduncle, the ventrolateral thalamus, the lateral globus pallidus and dorsolateral putamen, the dentate nucleus, the middle and superior cerebellar peduncles, the vermis, the cortex around the central sulcus and the hippocampus. Between 34 and 46 weeks, myelin appears in the lateral part of the posterior limb of the internal capsule and the central part of the corona radiata; therefore, at birth the human brain is rather immature in regard to the extent of its myelination. The rate of deposition of myelin is great-

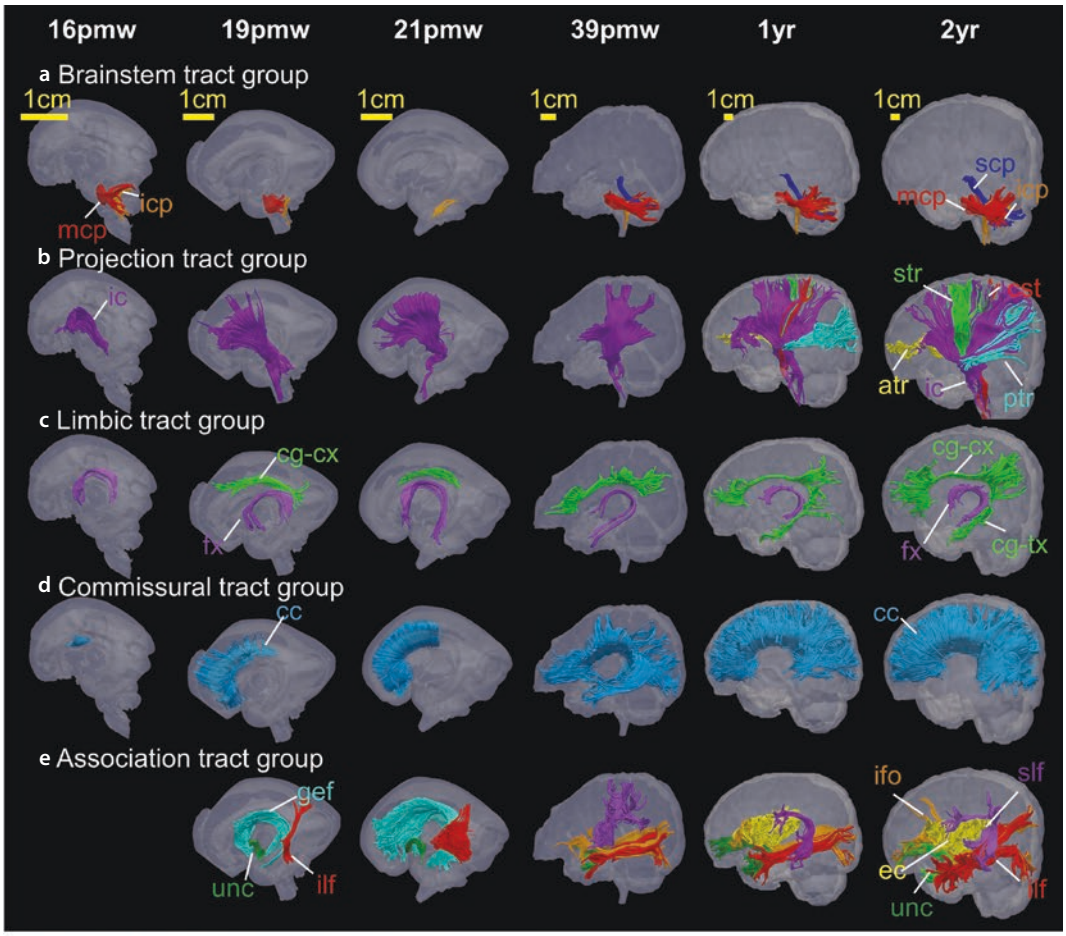
16pmw
19pmw
21pmw
39pmw
1yr
2yr
a Brainstem tract group
1cm
icp
mcp
scp
b Projection tract group
ic
str
cst
atr
ptr
c Limbic tract group
cg-cx
fx
d Commissural tract group
cc
e Association tract group
gef
unc
ilf
ifo
slf
ec

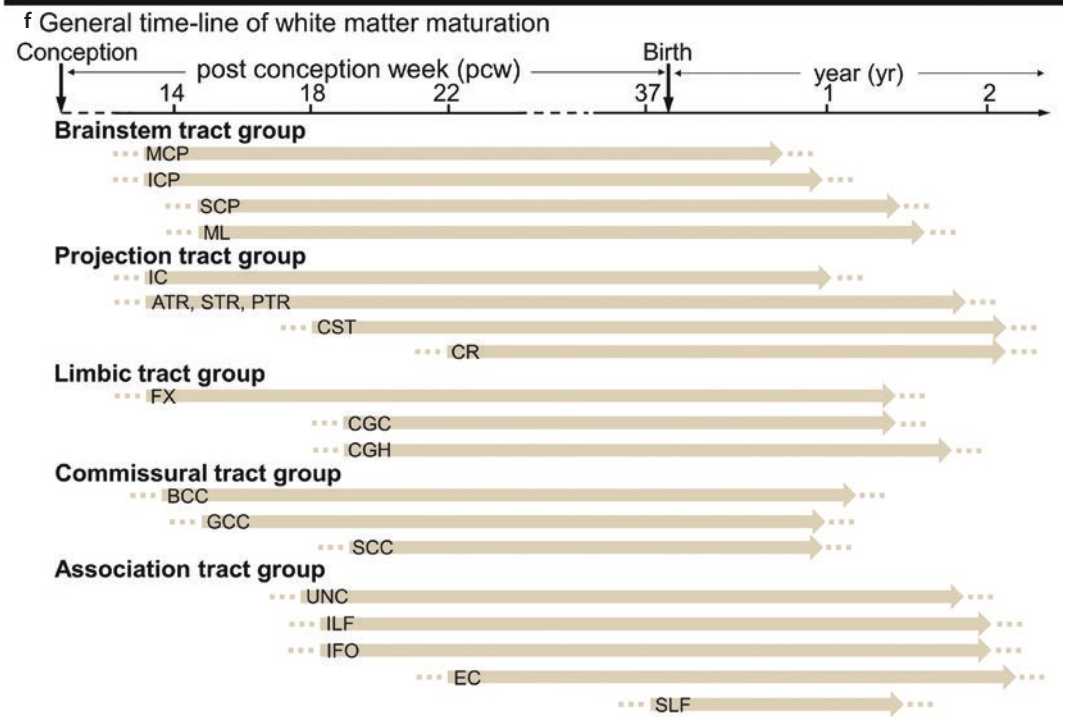
f General time-line of white matter maturation
Conception
post conception week (pcw)
Birth
year (yr)
14
18
22
37
1
2
Brainstem tract group
MCP
ICP
SCP
ML
Projection tract group
IC
ATR, STR, PTR
CST
CR
Limbic tract group
FX
CGC
CGH
Commissural tract group
BCC
GCC
SCC
Association tract group
UNC
ILF
IFO
EC
SLF

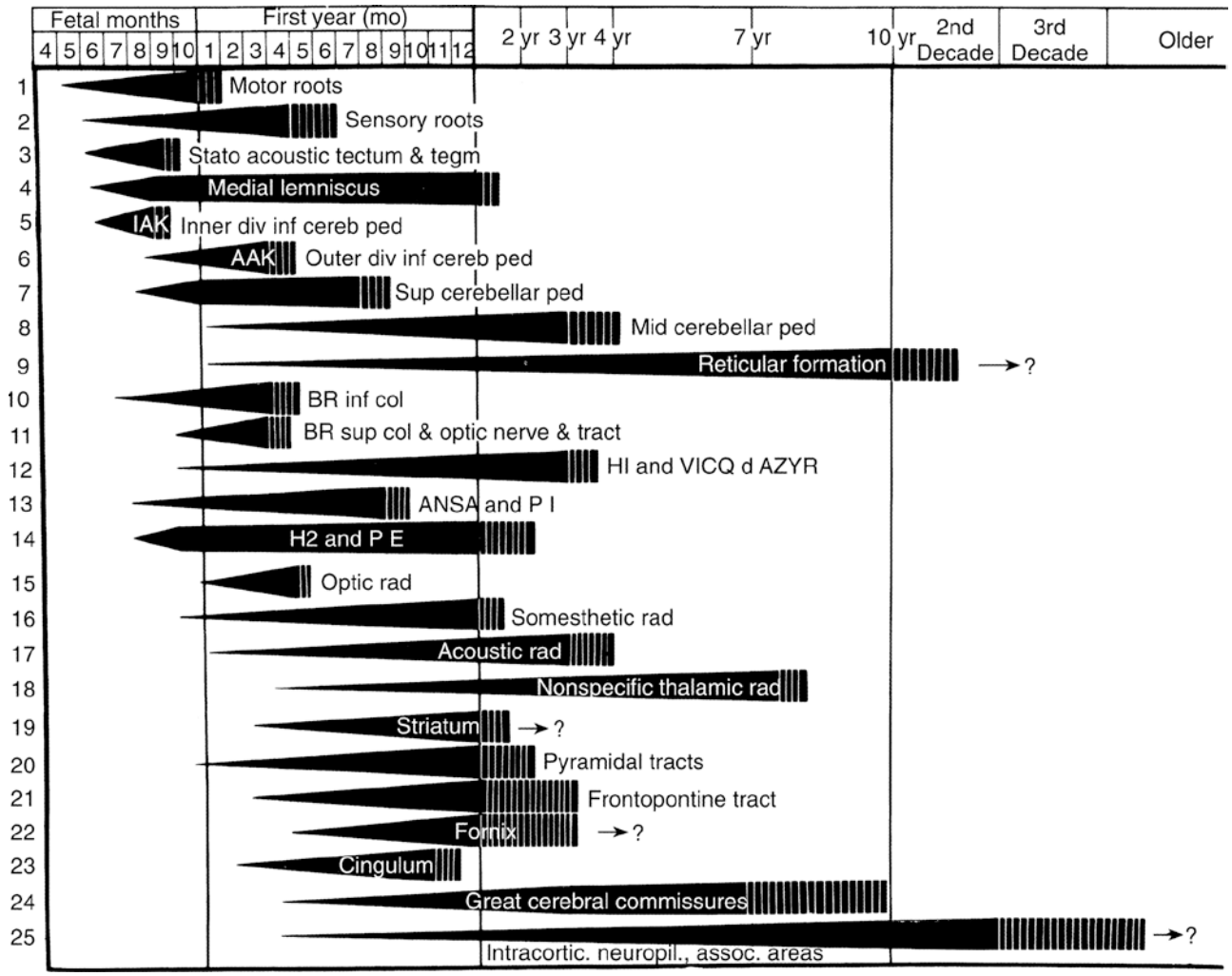

Fig. 1.50 Development of myelination of the main fibre tracts in the human CNS. (From Yakovlev and Lecours 1967)

est during the first two postnatal years (van der Knaap and Valk 1990, 1995). On MR images, a significant decrease in water content leads to a decrease in longitudinal relaxation times (T1) and transverse relaxation times (T2). Consequently, 'adult-like' appearance of T1-weighted and T2-weighted images becomes evident towards the end of the first year of life. Age-related changes in white matter myelination continue during childhood and adolescence (Paus et al. 2001).

1.11.3 Prenatal Motor Behaviour

Prenatal motor behaviour has been analysed in ultrasound studies. The first, just discernible movements emerge at six to seven weeks of postmenstrual age (Ianniruberto and Tajani 1981; de Vries et al. 1982; de Vries and Fong 2006, 2007). About two weeks later, movements involving all parts of the body appear. Two major forms of such movements can be distinguished,

Fig. 1.49 Diffusion MRI tractography of the white matter tracts in developing foetal and infant brain from 16 postmenstrual weeks (pmw) to 2 years. **a** Brain stem tracts, including the inferior, middle and superior cerebellar peduncles (ICP, MCP, SCP) and the medial lemniscus (ML); **b** projection tracts, including the internal capsule (IC), the corona radiata (CR), the corticospinal tract (CST), and anterior, superior and posterior thalamic radiations (ATR, STR and PTR); **c** limbic tracts, including the cingulum in the cingulate cortex (CGC) and the temporal cortex (CGH) and the fornix (FX); **d** commissural tracts, including body, genu and splenium of the corpus callosum (BCC, GCC and SCC); **e** association tracts, including fibres in the external capsule (EC), the inferior longitudinal fasciculus (ILF), the inferior occipito-frontal fasciculus (IFO), the superior longitudinal fasciculus (SLF) and the uncinate fascicules (UF); **f** germline timeline of white matter maturation across different tracts and tract groups. *Dotted lines* indicate that white matter tracts emerge at these ages, though to a relatively minor degree, and arrows indicate that overall white matter tracts are formed with continuous maturational processes such as myelination. (Based on data from the Huang lab; from Ouyang et al. 2019, with permission; kindly provided by Hao Huang, Philadelphia)

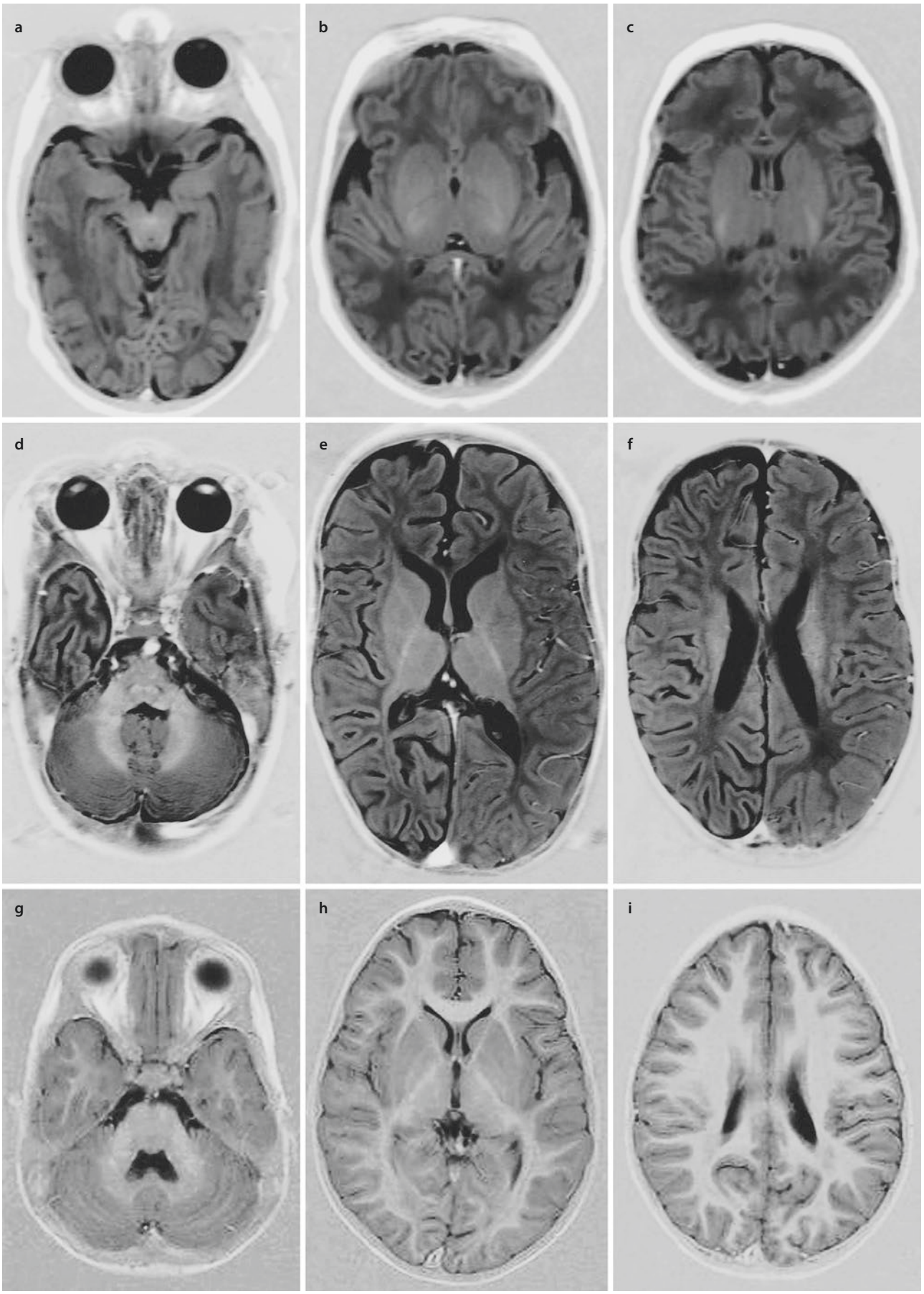
a
b
c
d
e
f
g
h
i

the startle and the general movement (Hadders-Algra and Forssberg 2002; Hadders-Algra 2018). The first movements appear prior to the formation of the spinal reflex arc, which is completed at eight weeks of postmenstrual age (Okado and Kojima 1984). This means that the first human movements, just like those of chick embryos (Hamburger et al. 1966), are generated in the absence of afferent information. During the following weeks, new movements are added to the foetal repertoire such as isolated arm and leg movements, various movements of the head, stretches, periodic breathing movements and sucking and swallowing movements (de Vries et al. 1982; de Vries and Fong 2006, 2007). Arm and leg movements, just like the palmar and plantar grasp reflexes, develop at 9–12 weeks, suggesting that foetal motility develops without a clear craniocaudal sequence. The age at which the various movements develop shows considerable interindividual variation, but at about 16 weeks' postmenstrual age all foetuses exhibit the entire foetal repertoire. This repertoire continues to be present throughout gestation (Hadders-Algra and Forssberg 2002; Kurjak et al. 2009; Salihagic-Kadic et al. 2009; Hadders-Algra 2018). If these movements are diminished or even absent due to cerebral, spinal, nervous or muscular defects, the ***foetal akinesia deformation sequence*** occurs (Moessinger 1983), the phenotype of which was first described as Pena-Shokeir phenotype. This phenotype is characterized by multiple joint contractures, limb pterygia, lung hypoplasia, short umbilical cord, craniofacial deformities, growth retardation, hydrops and polyhydramnios (Hall 1986). The foetal akinesia sequence has been detected by ultrasound as early as GW 13 owing to cerebral deformities leading to hydranencephaly (Witters et al. 2002) and at GW 16 in a case of muscular origin (Lammens et al. 1997; see also ▶ Chap. 6). One of the most promising advances in the field of ultrasonography has been the invention of the 4D-ultrasound technology (Lee 2001), giving visualization of the intrauterine neurological condition in almost real time (Kurjak et al. 2009).

1.12 The Foetal Connectome

Investigating the entire connectivity network of the human brain remains among the most challenging tasks in neuroscience. Developing and applying novel techniques to visualize large brain networks is essential to achieve a complete reconstruction of the human brain connectome (Sporns 2011, 2012). The term **connectome** was first used to define 'the comprehensive structural description of the network of elements and connections forming the human brain' (Sporns et al. 2005). Connectome has since come to reflect a more global systematic account of connections, from local circuits to networks forming entire nervous systems (Bota et al. 2015). Connectomes are connection matrices that can be directed or undirected, binary or weighted. Connectomes may be viewed as simply compilations of neuroanatomical data, but they have added a new dimension to neuroanatomy; in particular in combination with tools from network science, they provide insights into the topological organization of the network as a whole. Perturbations of the normal human connectome have been named ***connectopathies*** (Lichtman and Sanes 2008).

The brain's anatomical and functional organization can be approached mathematically in terms of graphs or networks comprising **nodes** (neurons and/or brain regions) and **edges** (synaptic connections or interregional pathways) as shown in ◘ Fig. 1.53. The connectome represents a structural basis for dynamic interactions (Sporns et al. 2005; Sporns 2011, 2012; van den Heuvel and Sporns 2013). A principal aim of connectome studies is to unravel the architecture of brain networks and to explain how the topology of structural networks shape and modulate brain function. Network science of 'graph theory' can be used to elucidate key organizational features of the brain's connectome architecture and to make predictions about the role of network elements and contributions in brain function. Brain networks can be mathematically described as graphs comprising sets of nodes (neuronal elements) and edges (their interconnections) whose pairwise couplings are summarized in the network topology (◘ Fig. 1.53). Network analyses of several species, including humans, have suggested connectomes to display several features of efficient communication networks (van den Heuvel et al. 2016), including a cost-efficient wiring, pronounced structural and functional modular organization and the formation of densely connected hub nodes. To ensure efficient global organization, some regions are densely connected to many other regions in the network. These network nodes, positioned to make strong contributions to global network function, are generally referred to as network hubs. **Hubs** can be detected using numerous different graph measures, most of which express aspects of node centrality. For a study of the role of hubs in the foetal brain, see van den Heuvel et al. (2018).

Patterns of brain connectivity can be recorded using anatomical or physiological methods that yield structural and functional brain networks, respectively. These

◘ **Fig. 1.51** Myelination in T1-weighted horizontal (or axial) images of a newborn **a**–**c**, a child of 1.5 years of age **d**–**f** and a young adult **g**–**i**. In **a** myelination is visible in the decussation of the brachia conjunctiva, and in **b** and **c** in the posterior limb of the internal capsule. Myelination is far more advanced in the pictures of the infant in **d**–**f**

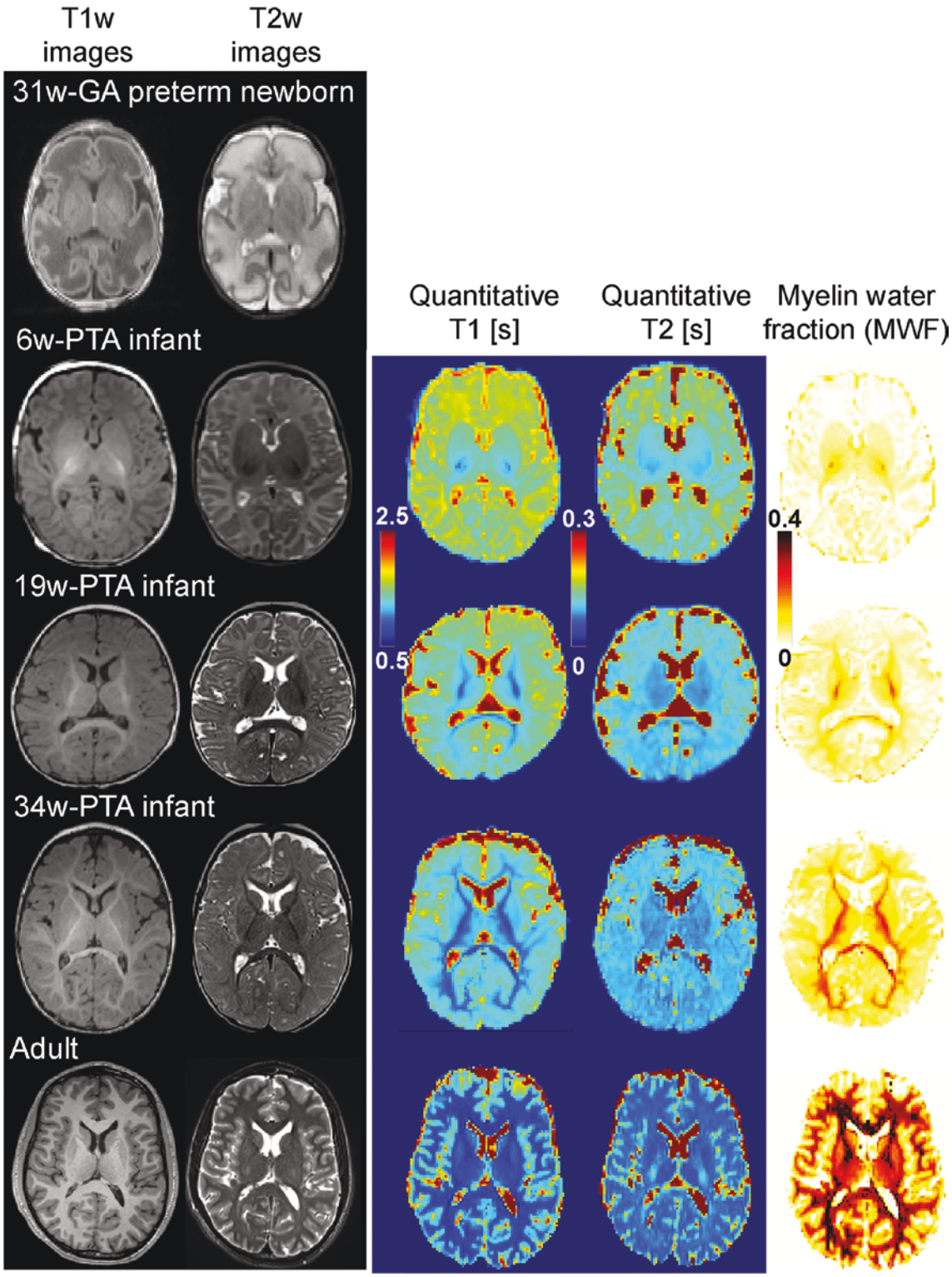

Fig. 1.52 Anatomical images of the developing brain. T1-weighted and T2-weighted images are shown for subjects of 31 weeks of gestational age (GA), term-born infants at a post-term age (PTA) of 6, 19 and 34 weeks, and a young adult. Note the contrast inversion between grey and white matter during the first postnatal year. For the infants and the adult, quantitative maps of T1 and T2 relaxation times (in seconds), and of myelin water fraction (MWF) are also shown. Within the white matter, T1 and T2 decrease with age, whereas MWF increases. (From Dubois et al. 2014, with permission; kindly provided by Jessica Dubois, Gif-sur-Yvette)

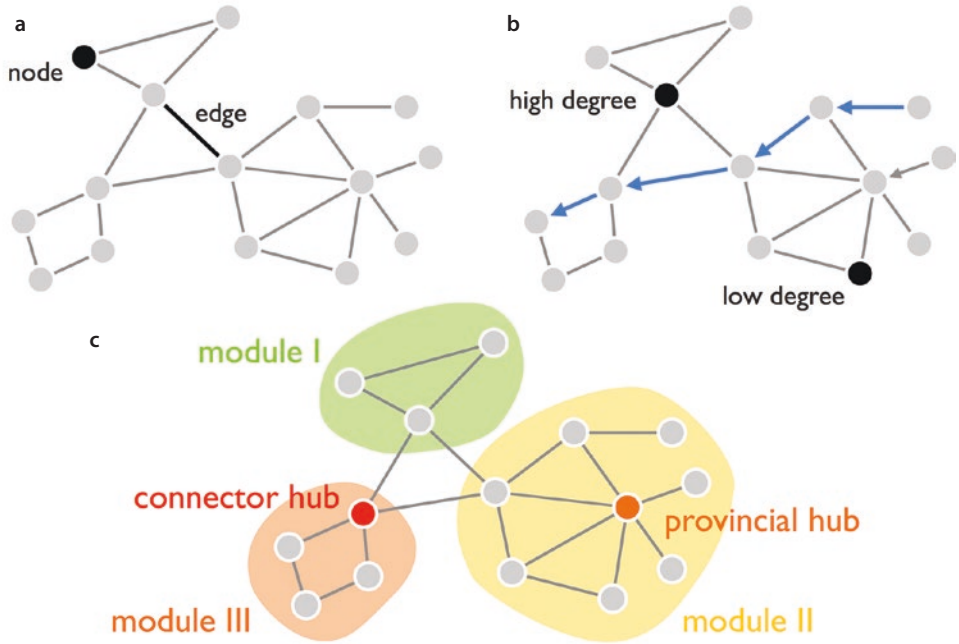

Fig. 1.53 Basic network attributes. **a** Brain networks can be described as graphs comprising a collection of nodes (describing neurons/brain regions) and a collection of edges (describing structural connections or functional relationships). The arrangement of nodes and edges defines the topological organization of the network. **b** A path corresponds to a sequence of unique edges that are crossed when travelling between two nodes in the network. Low-degree nodes are nodes that have a relatively low number of edges; high-degree nodes (often referred to as hubs) are nodes that have a relatively high number of edges. **c** A module includes a subset of nodes of the network that show a relatively high level of within-module connectivity and a relatively low level of intermodule connectivity. 'Provincial hubs' are high-degree nodes that primarily connect to nodes in the same module. 'Connector hubs' are high-degree nodes that show a diverse connectivity profile by connecting to several different modules within the network. (From van den Heuvel and Sporns 2013; with permission; courtesy Martijn van den Heuvel, Amsterdam)

two domains of brain networks differ in the way they are constructed and they express different aspects of the underlying neurobiological reality (van den Heuvel and Sporns 2013). **Structural networks** describe anatomical connectivity. Edges in structural networks correspond to (reconstructions of) axonal links that form the biological infrastructure for neuronal signalling and communication. Three hierarchical levels of analysis are considered (Swanson and Bota 2010; Bota et al. 2015; Swanson et al. 2017): (1) a **macroconnection** between two grey matter regions, the highest, most coarse-grained level with the nodes as grey matter regions, the edges formed by (long) fibre connections; (2) a **mesoconnection** between two neuron types within or between regions, nested within a macroconnection; and (3) a **microconnection** between two individual neurons, anywhere in the nervous system, nested within a mesoconnection.

Developmental connectomics is increasingly used from the second and third trimester of pregnancy, and from infancy through early childhood (Cao et al. 2016, 2017a, b; Song et al. 2017; Gilmore et al. 2018; Wilson et al. 2021). High-resolution diffusion MRI (dMRI) and resting-state functional MRI (magnetic resonance imaging) (fMRI) have been used in early-born neonates (van den Heuvel et al. 2015; Yu et al. 2016; Song et al. 2017), in foetuses between 20 and 40 weeks (van den Heuvel and Thomason 2016; Turk et al. 2019; Wilson et al. 2021) and through infancy and childhood (Huang et al. 2015; Cao et al. 2016, 2017a, b). During GW 20–40, human foetal brains develop into a much stronger and more efficient structural network and the network strength and efficiency increased faster in GW 20–35 than in GW 35–40, possibly due to the growth of long-range association fibres. A flow chart demonstrating the structural network construction is shown in Fig. 1.54. Some examples on neurobehavioural disorders will be discussed in ▶ Chap. 10.

Structural outgrowth of fibre connections is supported by spontaneous firing of neurons that reinforce the appropriate connections and trigger activity-dependent signalling processes (Thomason 2018), giving rise to structural and functional cortical connectivity (Kostović and Jovanov-Milošević 2006; Vasung et al. 2017, 2019; Kostović et al. 2019a, 2021). MRI studies demonstrated a small-world type of network organization with functional and structural rich-club hubs, increasing global efficiency, as well as structural and functional coupling in the preterm brain (van den Heuvel et al. 2015; Scheinost et al. 2016; Cao

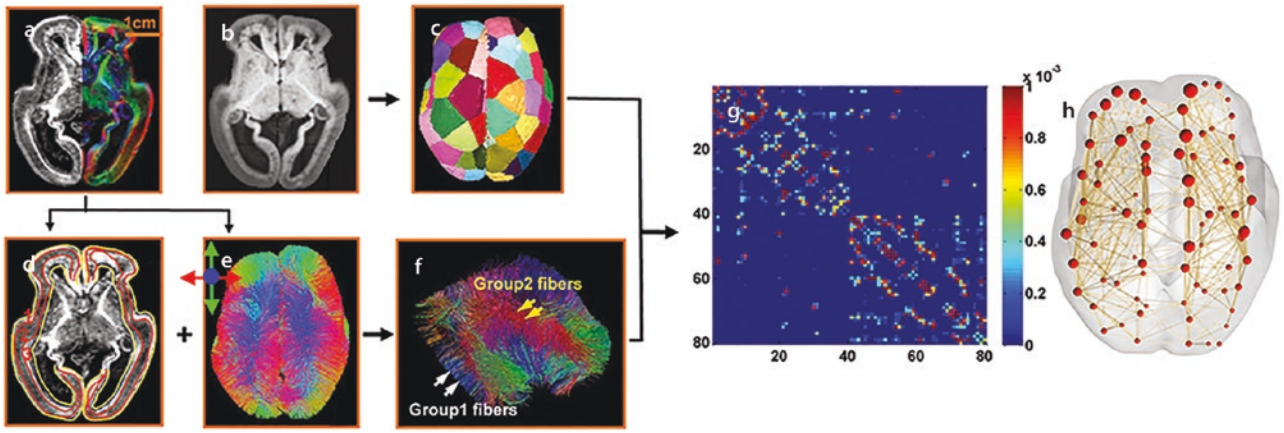

Fig. 1.54 Flow chart demonstrating the data analysis process to quantify the structural connectome of the human foetal brain with DTI data from a typical GW 20 foetal brain. **a** The high-resolution fractional anisotrophy (FA) map of the left and DTI direction-encoded colour map on the right; **b** averaged diffusion weighted imaging (DWI) image; **c** parcellation of the foetal brain into evenly distributed regions; **d** segmentation of the cerebral wall into three layers based on the contrasts of the FA map; **e** superior view of whole brain fibres based on DTI tractography; **f** categorization of group 1 and group 2 fibres based on the fibre terminal locations in the cerebral wall; **g** the connectivity matrix of the structural network in this GW 20 foetal brain; **h** the 3D reconstructed structural network based on the connectivity matrix. (From Song L et al. 2017 *Human fetal brain connectome: Structural network development from middle fetal stages to birth.* Front Neurosci 11:561; with permission; courtesy Hao Huang, Philadelphia)

et al. 2017a, b). Major white matter pathways associated with the development of the structural rich club in preterm neonates are established before the third trimester of pregnancy (Ball et al. 2014; van den Heuvel et al. 2015). Turk et al. (2019) showed that the most densely functionally connected areas in the foetal cortex, which they termed 'functional hubs', are predominantly confined to temporal and midline cortical regions of the insular and frontal lobes as well as the primary somatosensory regions. This is in line with fMRI and electrencephalography (EEG) studies in the neonatal brain (Arichi et al. 2017; van den Heuvel et al. 2018). A high overlap was found of foetal and adult resting-state networks for coordinating motor, visual, auditory and some cognitive functions. The frontomedial network associated with higher cognitive functions shows a less strong association. The frontoparietal network is still fragmentary around birth and during the first year of life.

References

Acampora D, Gulisano M, Broccoli V, Simeone A (2001) *Otx* genes in brain morphogenesis. Prog Neurobiol 64:69–95

Aicardi J (1992) Diseases of the nervous system in childhood. Clinics in developmental medicine. Nr 115/118. Mac Keith, London

Aida N, Nishimura G, Hachiya Y, Matsui K, Takeuchi M, Itani Y (1998) MR imaging of perinatal brain damage: comparison of clinical outcome with initial and follow-up MR findings. AJNR Am J Neuroradiol 19:1909–1921

Allendoerfer KL, Shatz CJ (1994) The subplate, a transient neocortical structure: its role in the development of connections between thalamus and cortex. Annu Rev Neurosci 17:185–218

Allsop G, Gamble HJ (1979) Light and electron microscopic observations on the development of the blood vascular system of the human brain. J Anat (Lond) 128:461–477

Alonso A, Merchán P, Sandoval JE, Sánchez-Arrones L, Garcia-Cazorla A, Artuch R et al (2013) Development of the serotoninergic cells in murine raphe nuclei and their relations with rhombomeric domains. Brain Struct Funct 218:1229–1277

Altman J, Bayer SA (1997) Development of the cerebellar system: in relation to its evolution, structure and functions. CRC, Boca Raton, FL

Alzu'bi A, Clowry GJ (2019) Expression of ventral telencephalon transcription factors ASCL1 and DLX2 in the early fetal human cerebral cortex. J Anat (Lond) 235:555–568

Alzu'bi A, Lindsay SJ, Harkin LF, McIntyre J, Lisgo SN, Clowry GJ (2017a) The transcription factors COUP-TFI and COUP-TFII have distinct roles in arealisation and GABAergic interneuron specification in the early human fetal telencephalon. Cereb Cortex 27:4677–4690

Alzu'bi A, Lindsay SJ, Kerwin J, Looi SJ, Khalil F, Clowry GJ (2017b) Distinct cortical and subcortical neurogenic domains for GABAergic interneuron precursor transcription factors NKX2.1, OLIG2 and COUP-TFII in early fetal human telencephalon. Brain Struct Funct 222:2309–2328

Anderson SA, Mione M, Yun K, Rubenstein JLR (1999) Differential origins of neocortical projection and local circuit neurons: Role of Dlx genes in neocortical interneuronogenesis. Cereb Cortex 9:646–654

Anderson SA, Marín O, Horn C, Jennings K, Rubenstein JLR (2001) Distinct cortical migrations from the medial and lateral ganglionic eminences. Development 128:353–363

Arichi T, Whitehead K, Barone G, Pressler R, Padormo F, Edwards AD, Fabrini L (2017) Localization of spontaneous bursting neuronal activity in the preterm brain with simultaneous EEG-fMRI. eLife 6:e27814

Ariëns Kappers JA (1958) Structural and functional changes in the telencephalic choroid plexus during brain ontogenesis. In: Wolstenholme GEW, O'Connor CM (eds) The cerebrospinal fluid. Little, Brown, Boston, MA, pp 3–25

Arnold SE, Trojanowski JQ (1996) Human fetal hippocampal development: I. Cytoarchitecture, myeloarchitecture, and neuronal morphologic features. J Comp Neurol 367:274–292

Ball G, Aljabar N, Zebari S, Tusor N, Arichi T, Merchant N et al (2014) Rich-club organization of the newborn human brain. Proc Natl Acad Sci U S A 111:7456–7461

Banker BQ, Larroche JC (1962) Periventricular leukomalacia of infancy. Arch Neurol 7:386–410

Barkovich AJ, Raybaud C (2018) Pediatric neuroimaging, 6th edn. Lippincott/Wolters Kluwer, Philadelphia, PA

Barkovich AJ, Kuzniecky RI, Jackson GD, Guerrini R, Dobyns WB (2001) Classification system for malformations of cortical development. Update 2001. Neurology 57:2168–2178

Barkovich AJ, Millen KJ, Dobyns WB (2009) A developmental and genetic classification for midbrain-hindbrain malformations. Brain 132:3199–3230

Barkovich AJ, Guerrini R, Kuzniecky RI, Jackson GD, Dobyns WB (2012) A developmental and genetic classification for malformations of cortical development: update 2012. Brain 135:1348–1369

Bartelmez GW (1923) The subdivisions of the neural folds in man. J Comp Neurol 35:231–295

Bartelmez GW, Dekaban AS (1962) The early development of the human brain. Contrib Embryol Carnegie Instn 37:13–32

Barth PG (1993) Pontocerebellar hypoplasias. An overview of a group of inherited neurodegenerative disorders with fetal onset. Brain Dev 15:411–422

Bassuk AG, Kibar Z (2009) Genetic basis of neural tube defects. Semin Pediatr Neurol 16:101–110

Bayer SA, Altman J (1991) Neocortical development. Raven, New York

Bayer SA, Altman J (2002) Atlas of human central nervous system development. In: Vol 1: The spinal cord from gestational week 4 to the 4th postnatal month. CRC, Boca Raton, FL

Bayer SA, Altman J (2003) Atlas of human central nervous system development. In: Vol 2: The The human brain during the third trimester. CRC, Boca Raton, FL

Bayer SA, Altman J (2005) Atlas of human central nervous system development. In: Vol 3: The human brain during the second trimester. CRC, Boca Raton, FL

Bayer SA, Altman J (2006) Atlas of human central nervous system development. In: Vol 4: The human brain during the late first trimester. CRC, Boca Raton, FL

Bayer SA, Altman J (2007) Atlas of human central nervous system development. In: Vol 5: The human brain during the early first trimester. CRC, Boca Raton, FL

Bayer SA, Altman J, Russo RJ, Zhang X (1995) Embryology. In: Duckett S (ed) Pediatric neuropathology. Williams & Wilkins, Baltimore, MD, pp 54–107

Ben-Arie N, Bellen HJ, Armstrong DL, McCall AE, Gordadze PR, Guo Q et al (1997) *Math1* is essential for genesis of cerebellar granule neurons. Nature 390:169–172

Bergquist H (1952) The formation of neuromeres in homo. Acta Soc Med Ups 57:23–32

Bergquist H, Källén B (1954) Notes on the early histogenesis and morphogenesis of the central nervous system in vertebrates. J Comp Neurol 100:627–659

Blaas H-GK (1999) The embryonic examination. Ultrasound studies on the development of the human embryo. Thesis, Norwegian University of Science and Technology, Trondheim. TAPIR, Trondheim, Norway

Blaas H-GK, Eik-Nes SH (1996) Ultrasound assessment of early brain development. In: Jurkovic D, Jauniaux E (eds) Ultrasound and early pregnancy. Parthenon, New York, pp 3–18

Blaas H-G, Eik-Nes SH (2002) The description of the early development of the human central nervous system using two-dimensional and three-dimensional ultrasound. In: Lagercrantz H, Hanson M, Evrard P, Rodeck CH (eds) The newborn brain—neuroscience and clinical applications. Cambridge University Press, Cambridge, pp 278–288

Blaas H-G, Eik-Nes SH (2009) Sonoembryology and early prenatal diagnosis of neural anomalies. Prenat Diagn 29:312–325

Blaas H-G, Eik-Nes SH, Kiserud T, Hellevik LR (1994) Early development of the forebrain and midbrain: a longitudinal ultrasound study from 7 to 12 weeks of gestation. Ultrasound Obstet Gynecol 4:183–192

Blaas H-G, Eik-Nes SH, Kiserud T, Berg S, Angelsen B, Olstad B (1995a) Three-dimensional imaging of the brain cavities in human embryos. Ultrasound Obstet Gynecol 5:228–232

Blaas H-G, Eik-Nes SH, Kiserud T, Hellevik LR (1995b) Early development of the hindbrain: a longitudinal ultrasound study from 7 to 12 weeks of gestation. Ultrasound Obstet Gynecol 5:151–160

Boltshauser E, Schmahmann J (eds) (2012) Cerebellar disorders in children. Mac Keith, London

Bota M, Sporns O, Swanson LW (2015) Architecture of the cerebral cortical association connectome underlying cognition. Proc Natl Acad Sci U S A:E2093–E2101

Boulder Committee (1970) Embryonic vertebrate central nervous system: revised terminology. Anat Rec 166:257–262

Brazel CY, Romanko MJ, Rothstein RP, Levison SW (2003) Roles of the mammalian subventricular zone in brain development. Prog Neurobiol 69:49–69

Brody BA, Kinney HC, Kloman AS, Gilles FH (1987) Sequence of central nervous system myelination in human infancy. I. An autopsy study of myelination. J Neuropathol Exp Neurol 46:283–301

Brun A (1965) The subpial granular layer of the foetal cerebral cortex in man. Its ontogeny and significance in congenital cortical malformations. Acta Pathol Microbiol Scand 179(Suppl):1–98

Bulfone A, Puelles L, Porteus MH, Frohman MA, Martin GR, Rubenstein JLR (1993) Spatially restricted expression of *Dlx-1, Dlx-2, (Tes-1), Gbx-2,* and *Wnt-3* in the embryonic day 12.5 mouse forebrain defines potential transverse and longitudinal boundaries. J Neurosci 13:3155–3172

Bystron I, Rakic P, Molnár Z, Blakemore C (2006) The first neurons of the human cerebral cortex. Nat Neurosci 9:880–886

Bystron I, Blakemore C, Rakic P (2008) Development of the human cerebral cortex: Boulder Committee revisited. Nat Rev Neurosci 9:110–112

Cao M, Huang H, Peng Y, Dong Q, He Y (2016) Toward developmental connectomics of the human brain. Front Neuroanat 10:25

Cao M, He Y, Dai Z, Liao X, Jeon T, Ouyang M et al (2017a) Early development of functional network segregation revealed by connectmics analysis of the preterm human brain. Cereb Cortex 27:1949–1963

Cao M, Huang H, He Y (2017b) Developmental connectomics from infancy through early childhood. Trends Neurosci 40:494–505

Carlson BM (1999) Human embryology & development, 2nd edn. Mosby, St. Louis, MI

Carney RS, Bystron I, Lopez-Bendito G, Molnár Z (2007) Comparative analysis of extra-ventricular mitoses at early stages of cortical development in rat and human. Brain Struct Funct 212:37–54

Catani M, Thiebaut de Schotten M (2012) Atlas of human brain connections. Oxford University Press, Oxford

Clowry GJ (2015) An enhanced role and expanded developmental origins for gamma-aminobutyric acidergic interneurons in the human. J Anat (Lond) 227:384–393
Clowry GJ, Alzu'bi A, Harkin LF, Sarma S, Kerwin J, Lindsay SJ (2018) Charting the protomap of the human telencephalon. Semin Cell Dev Biol 76:3–14
Collins P, Billett FS (1995) The terminology of early development. Clin Anat 8:418–425
Congdon ED (1922) Transformation of the aortic-arch system during the development of the human embryo. Contrib Embryol Carnegie Instn 14:47–110
Corner GW (1929) A well-preserved human embryo of 10 somites. Contrib Embryol Carnegie Instn 20:81–102
Crelin EA (1973) Functional anatomy of the newborn. Yale University Press, London
de Bakker BS, de Jong KH, Hagoort J, Oostra R-J, Moorman AFM (2012) Towards a 3-dimensional atlas of the developing human embryo: the Amsterdam experience. Reprod Toxicol 34:225–236
de Bakker BS, de Jong KH, Hagoort J, de Bree K, Besselink CT, de Kanter FEC et al (2016) An interactive three-dimensional digital atlas and quantitative database of human development. Science 354:6315
de Bakker BS, Driessen S, Boukens BJD, van den Hoff MJB, Oostra R-J (2017) Single-site neural tube closure in human embryos revisited. Clin Anat 30:988–999
de Carlos JA, Lopez-Mascaraque L, Valverde F (1996) Dynamics of cell migration from the lateral ganglionic eminence in the rat. J Neurosci 16:6146–6156
de Souza FSJ, Niehrs C (2000) Anterior endoderm and head induction in early vertebrate embryos. Cell Tissue Res 300:207–217
de Vries JI, Fong BF (2006) Normal fetal motility: an overview. Ultrasound Obstet Gynecol 27:701–711
de Vries JI, Fong BF (2007) Changes in fetal motility as a result of congenital disorders: an overview. Ultrasound Obstet Gynecol 29:590–599
de Vries JIP, Visser GHA, Prechtl HFR (1982) The emergence of fetal behaviour. I. Qualitative aspects. Early Hum Dev 7:301–322
Desikan RS, Barkovich AJ (2016) Malformations of cortical development. Ann Neurol 80:797–810
Doetsch F, García-Verdugo JM, Alvarez-Buylla A (1997) Cellular composition and three-dimensional organization of the subventricular germinal zone in the adult mammalian brain. J Neurosci 17:5046–5061
Drooglever Fortuyn AB (1912) Die Ontogenie der Kernes des Zwischenhirns mein Kaninchen. Arch Anat Physiol, Anat Abt 36:303–352
Dubois J, Benders M, Borradori-Tolsa C, Cachia A, Lazeyras F, Ha-Vinh Leuchter R et al (2008a) Primary folding of the human newborn: an early marker of later functional development. Brain 131:2028–2041
Dubois J, Benders M, Cachia A, Lazeyras F, Ha-Vinh Leuchter R, Sizonenko SV et al (2008b) Mapping the early cortical folding process in the preterm newborn brain. Cereb Cortex 18:1444–1454
Dubois J, Benders M, Lazeyras F, Borradori-Tolsa C, Ha-Vinh Leuchter R, Magin JF, Hüppi PS (2010) Structural asymmetries of perisylvian regions in the preterm newborn. Neuroimage 52:32–42
Dubois J, Dehaene-Lambertz G, Kulikova S, Poupon C, Hüppi PS, Hertz-Pannier L (2014) The early development of brain white matter: a review of imaging studies in fetuses, newborns and infants. Neuroscience 286:48–71
Dubois J, Alison M, Counsell SJ, Hertz-Pannier L, Hüppi PS, Benders MJNL (2021) MRI of the neonatal brain: a review of methodological challenges and neuroscientific advances. J Magn Reson Imaging 53:1318–1343
Duckett S (1971) The establishment of internal vascularization in the human telencephalon. Acta Anat (Basel) 80:107–113
Duvernoy HM (1998) The Human Hippocampus. Functional anatomy, vascularization and serial sections with MRI, 2nd edn. Springer, Berlin, Heidelberg, New York
Edwards TJ, Sherr EH, Barkovich AJ, Richards LJ (2014) Clinical, genetic and imaging findings identify new causes for corpus callosum development syndromes. Brain 137:1579–1613
Essick CR (1912) The development of the nuclei pontis and the nucleus arcuatus in man. Am J Anat 13:25–54
Evans HM (1911) Die Entwicklung des Blutgefäßsystems. In: Keibel F, Mall FP (Hrsg) Handbuch der Entwicklungsgeschichte des Menschen, Zweiter Band. Hirzel, Leipzig, pp 551–688
Evans HM (1912) The development of the vascular system. In: Keibel F, Mall FP (eds) Manual of human embryology, Lippincott, vol 2. Philadelphia, PA, pp 570–709
Favier B, Dollé P (1997) Developmental functions of mammalian *Hox* genes. Mol Hum Reprod 3:115–131
Feess-Higgins A, Larroche J-C (1987) Le développement du cerveau foetal humain. Atlas anatomique. Masson, Paris
Fertuzinhos S, Krsnik Z, Kawasawa YI, Rašin M-R, Kwan KY, Chen J-G et al (2009) Selective depletion of molecularly defined cortical interneurons in human prosencephaly with severe striatal hypoplasia. Cereb Cortex 19:2196–2207
Fietz SA, Kelava I, Vogt J, Wilsch-Brauninger M, Stenzel D, Fish JL et al (2010) OSVZ progenitors of human and ferret neocortex are epithelial-like and expand by integrin. Nat Neurosci 13:690–699
Flechsig PE (1920) Anatomie des menschlichen Gehirns und Rückenmarks auf myelogenetischer Grundlage. Thieme, Leipzig
Flores-Sarnat L, Sarnat HB (2008) Axes and gradients of the neural tube and gradients for a morphological molecular genetic classification of nervous system malformations. Hb Clin Neurol 87:3–11
Francis-West PH, Robson L, Evans DJR (2003) Craniofacial development: the tissue and molecular interactions that control development of the head. Adv Anat Embryol Cell Biol 169:1–144
Furuichi K, Ishikawa A, Uwabe C, Makishima H, Yamada S, Takakuwa T (2018) Variations in the circle of Willis at the end of the human embryonic period. Anat Rec 301:1312–1319
Gadisseux J-F, Goffinet AM, Lyon G, Evrard P (1992) The human transient subpial granular layer: an optical, immunohistochemical, and ultrastructural analysis. J Comp Neurol 324:94–114
Gardner RJM, Coleman LT, Mitchell LA, Smith LJ, Harvey AS, Scheffer IE et al (2001) Near-total absence of the cerebellum. Neuropediatrics 32:62–68
Garel C (2004) MRI of the fetal brain. In: Normal development and cerebral pathologies. Springer, Berlin, Heidelberg, New York
Gilles FH, Nelson MD (2012) The developing human brain: growth and adversities. Mac Keith, London
Gilles FH, Shankle W, Dooling EC (1983) Myelinated tracts. In: Gilles FH, Leviton A, Dooling EC (eds) The developing human brain. Wright, Bristol, pp 117–183
Gillilan LA (1972) Anatomy and embryology of the arterial system of the brain stem and cerebellum. Handb Clin Neurol 11:24–44
Gilmore JH, Knickmeyer RC, Gao W (2018) Imaging structural and functional brain development in early childhood. Nat Rev Neurosci 19:123–137
Gleeson JG, Walsh CA (2000) Neuronal migration disorders: from genetic diseases to developmental mechanisms. Trends Neurosci 23:352–359
Golden JA (1998) Holoprosencephaly: a defect in brain patterning. J Neuropathol Exp Neurol 57:991–999
Gribnau AAM, Geijsberts LGM (1985) Morphogenesis of the brain in staged rhesus monkey embryos. Adv Anat Embryol Cell Biol 91:1–69

Guimarães Gonçalves F, Hwang M (2021) Superficial anatomy of the neonatal cerebrum. Pediatr Radiol 51:353–370
Habas PA, Scott JA, Roosta A, Rajagopalan V, Kim K, Rousseau F et al (2012) Early folding patterns and asymmetries of the normal human brain detected from in utero MRI. Cereb Cortex 22:13–25
Hadders-Algra M (2018) Early human motor development: from variation to the ability to vary and adapt. Neurosci Biobehav Rev 90:411–427
Hadders-Algra M, Forssberg H (2002) Development of motor functions in health and disease. In: Lagercrantz H, Hanson M, Evrard P, Rodeck CH (eds) The newborn brain—neuroscience and clinical applications. Cambridge University Press, Cambridge, pp 479–507
Hall JG (1986) Analysis of Pena Shokeir phenotype. Am J Med Genet 25:99–117
Hambleton G, Wigglesworth JS (1976) Origin of intraventricular haemorrhage in the preterm infant. Arch Child Dis 51:651–659
Hamburger V, Wenger E, Oppenheim RW (1966) Motility in the chick embryo in the absence of sensory input. J Exp Zool 162:133–160
Hamilton WJ, Mossman HW (1972) Hamilton, Boyd and Mossman's human embryology. Prenatal development of form and function, 4th edn. Heffer, Cambridge
Hansen DV, Lui JH, Parker PR, Kriegstein AR (2010) Neurogenic radial glia in the outer subventricular zone of human neocortex. Nature 464:554–561
Hansen DV, Lui JH, Flandin P, Yoshikawa K, Rubenstein JL, Alvarez-Byulla A, Kriegstein AR (2013) Non-epithelial stem cells and cortical interneuron production in the human ganglionic eminences. Nat Neurosci 16:1576–1587
Hatten ME (1999) Central nervous system neuronal migration. Annu Rev Neurosci 22:511–539
Hatten ME, Alder J, Zimmerman K, Heintz N (1997) Genes involved in cerebellar cell specification and differentiation. Curr Opin Neurobiol 7:40–47
Herrick CJ (1910) The morphology of the forebrain in Amphibia and Reptilia. J Comp Neurol 20:413–545
Heuser CH, Corner GW (1957) Developmental horizons in human embryos. Description of age group X, 4 to 12 somites. Contrib Embryol Carnegie Instn 36:29–39
Hevner RF, Kinney HC (1996) Reciprocal entorhinal-hippocampal connections established by human fetal midgestation. J Comp Neurol 372:384–394
Hewitt W (1961) The development of the human internal capsule and lentiform nucleus. J Anat (Lond) 95:191–199
His W (1880) Anatomie menschlicher Embryonen. I. Embryonen des ersten Monats. Vogel, Leipzig
His W (1889) Die Formentwickelung des menschlichen Vorderhirns vom Ende des ersten bis zum Beginn des dritten Monats. Abh Kön Sächs Ges Wiss Math Phys Kl 15:675–735
His W (1890) Die Entwickelung des menschlichen Rautenhirns vom Ende des ersten bis zum Beginn des dritten Monats. I. Verlängertes Mark. Abh Kön Sächs Ges Wiss Math Phys Kl 29:1–74
His W (1893) Vorschläge zur Eintheilung des Gehirns. Arch Anat EntwGesch 3(4):173–179
His W (1895) Die Anatomische Nomenklatur. Nomina Anatomica: Verzeichniss der von der Anatomischen Gesellschaft auf ihrer IX. In: Versammlng in Basel angenommenen Namen. Veit, Leipzig
His W (1904) Die Entwickelung des menschlichen Gehirns während der ersten Monate. Hirzel, Leipzig
Hochstetter F (1919) Beiträge zur Entwicklungsgeschichte des menschlichen Gehirns, I. Teil. Deuticke, Vienna
Hochstetter F (1929) Beiträge zur Entwicklungsgeschichte des menschlichen Gehirns, II. Teil, 3. Lieferung. Die Entwicklung des Mittel- und Rautenhirns. Deuticke, Vienna
Hochstetter F (1934) Über die Entwicklung und Differenzierung der Hüllen des Rückenmarkes beim Menschen. Morphol Jahrb 74:1–104
Hochstetter F (1939) Über die Entwicklung und Differenzierung der Hüllen des menschlichen Gehirns. Morphol Jahrb 83:359–494
Hori A, Friede RL, Fischer G (1983) Ventricular diverticles with localized dysgenesis of the temporal lobe in a cloverleaf skull anomaly. Acta Neuropathol (Berl) 60:132–136
Hori A, Eubel R, Ulbrich R (1984a) Congenital ventricular diverticulum in the brainstem. Report of four cases. Acta Neuropathol (Berl) 63:330–333
Hori A, Bardosi A, Tsuboi K, Maki Y (1984b) Accessory cerebral ventricle of the occipital lobe. Morphogenesis and clinical and pathological appearance. J Neurosurg 61:767–771
Hoshino M (2012) Neuronal subtypes specification in the cerebellum and dorsal hindbrain. Dev Growth Diff 54:317–326
Huang H, Vasung L (2014) Gaining insight of fetal brain development with diffusion MRI and histology. Int J Devl Neurosci 32:11–22
Huang H, Zhang J, Wakana S, Zhang W, Ren T, Richards LJ et al (2006) White and gray matter development in human fetal, newborn and pediatric brains. Neuroimage 33:27–38
Huang H, Xue R, Zhang J, Ren T, Richards LJ, Yarowsky P et al (2009) Anatomical characterization of human fetal brain development with diffusion tensor magnetic resonance imaging. J Neurosci 29:4263–4273
Huang H, Shu N, Mishra V, Jeon T, Chalak L, Wang ZJ et al (2015) Development of human brain structural networks through infancy and childhood. Cereb Cortex 25:1389–1404
Humphrey T (1960) The development of the pyramidal tracts in human fetuses, correlated with cortical differentiation. In: Tower DB, Schadé JP (eds) Structure and function of the cerebral cortex. Elsevier, Amsterdam, pp 93–103
Humphrey T (1966) The development of the human hippocampal formation correlated with some aspects of its phylogenetic history. In: Hassler R, Stephan H (eds) Evolution of the forebrain. Thieme, Stuttgart, pp 104–116
Hunter AGW, Stevenson RE (2008) Gastroschisis: clinical presentation and associations. Am J Med Genet Part C 148C:219–230
Ianniruberto A, Tajani E (1981) Ultrasonographic study of fetal movements. Sem Perinatol 5:175–181
Inoue T, Nakamura S, Osumi N (2000) Fate mapping of the mouse prosencephalic neural plate. Dev Biol 219:373–383
Insausti R, Cebada-Sánchez S, Marcos P (2010) Postnatal development of the human hippocampus. Adv Anat Embryol Cell Biol 206:1–89
Jakob A (1928) Das Kleinhirn. In: von Möllendorf W (ed) Handbuch der mikroskopischen Anatomie des Menschen, Teil 1, vol 4. Springer, Berlin, Heidelberg, New York, pp 674–916
Jeffery N (2002) Differential regional brain growth and rotation of the prenatal human tentorium cerebelli. J Anat (Lond) 200:135–144
Jirásek JE (1983) Atlas of human prenatal morphogenesis. Nijhoff, Baltimore, MD
Jirásek JE (2001) An Atlas of the human embryo and fetus. Parthenon, New York
Jirásek JE (2004) An Atlas of human prenatal developmental mechanisms. Anatomy and staging. Taylor & Francis, London, New York
Johanson PA (2014) The choroid plexuses and their impact on developmental neurogenesis. Front Neuroanat 8:340
Judaš M, Sedmak G, Pletikos M, Jovanov-Milošević N (2010) Populations of subplate and interstitial neurons in fetal and adult human telencephalon. J Anat (Lond) 217:381–399
Judaš M, Šimić G, Petanjek M, Jovanov-Milošević N, Pletikos M, Vasung L et al (2011) The Zagreb collection of human brains: a

unique, versatile, but underexploited resource for the neuroscience community. Ann NY Acad Sci 1225(Suppl. 1):105–130
Kahle W (1969) Die Entwicklung der menschlichen Grosshirnhemisphäre. Schriftenr Neurol 1:1–116
Kanold PO, Luhmann HJ (2010) The subplate and early cortical circuits. Annu Rev Neurosci 33:23–48
Kasprian G, Brugger PC, Weber M, Krssak M, Krampl E, Herold C et al (2008) *In utero* tractography of fetal white matter development. Neuroimage 43:213–224
Keibel F, Elze C (1908) Normentafeln zur Entwicklungsgeschichte des Menschen. Hirzel, Leipzig
Kerwin J, Yang Y, Merchan P, Sarma S, Thompson J, Wang X et al (2010) The HUDSEN atlas: a three-dimensional (3D) spatial framework for studying gene expression in the developing human brain. J Anat (Lond) 217:289–299
Keyser AJM (1972) The development of the diencephalon of the Chinese hamster. Acta Anat (Basel) 83(Suppl. 59):1–178
Kiecker C, Lumsden A (2012) The role of organizers in patterning the nervous system. Annu Rev Neurosci 35:347–367
Kinney HC, Brody BA, Kloman AS, Gilles FH (1988) Sequence of central nervous system myelination in human infancy. II. Patterns of myelination in autopsied infants. J Neuropathol Exp Neurol 47:217–234
Klintworth GK (1967) The ontogeny and growth of the human tentorium cerebelli. Anat Rec 158:433–442
Kollias SS, Ball WS (1997) Congenital malformations of the brain. In: Ball WS (ed) Pediatric neuroradiology. Lippincott, Philadelphia, PA, pp 91–174
Konstantinidou AD, Silos-Santiago I, Flaris N, Snider WD (1995) Development of the primary afferent projection in human spinal cord. J Comp Neurol 354:1–12
Kornack DR, Rakic P (2001) The generation, migration, and differentiation of olfactory neurons in the adult primate brain. Proc Natl Acad Sci U S A 98:4752–4757
Kostović I, Jovanov-Milošević N (2006) The development of cerebral connections during the first 20–45 weeks' gestation. Semin Fetal Neonatal Med 11:415–422
Kostović I, Judaš M (2007) Transient patterns of cortical lamination during prenatal life: do they have implications for treatment? Neurosci Biobehav Rev 31:1157–1168
Kostović I, Judaš M (2010) The development of the subplate and thalamocortical connections in the human foetal brain. Acta Paediatr 99:1119–1127
Kostović I, Rakic P (1990) Developmental history of the transient subplate zone in the visual and somatosensory cortex of the macaque monkey and human brain. J Comp Neurol 297:441–470
Kostović I, Vasung L (2009) Insights from *in vitro* fetal magnetic resonance imaging of cerebral development. Semin Perinatol 33:220–233
Kostović I, Sedmak G, Judaš M (2019a) Neural histology and neurogenesis of the human fetal and infant brain. Neuroimage 188:743–773
Kostović I, Žunić Išasegi I, Krsnik Ž (2019b) Sublaminar organization of the human subplate: developmental changes in the distribution of neurons, glia, growing axons and extracellular matrix. J Anat (Lond) 235:481–508
Kostović I, Radoš M, Kostović-Srzentić M, Krsnik Ž (2021) Fundamentals of the development of connectivity in the human fetal brain in late gestation: from 24 weeks gestational age to term. J Neuropathol Exp Neurol 80:393–414
Kraus I, Jirásek JE (2002) Some observations of the structure of the choroid plexus and its cysts. Prenat Diagn 22:1223–1228
Kriegstein AR, Alvarez-Buylla A (2009) The glial nature of embryonic and adult neural stem cells. Annu Rev Neurosci 32:149–118
Krsnik Ž, Majić V, Vasung L, Huang H, Kostović I (2017) Growth of thalamocortical fibers to the somatosensory cortex in the human fetal brain. Front Neuroanat 11:233
Kuban KCK, Gilles FH (1985) Human telencephalic angiogenesis. Ann Neurol 17:539–548
Kurjak A, Pooh RK, Tikvica A, Stanojevic M, Miskovic B, Ahmed B, Azumendi G (2009) Assessment of fetal neurobehavior by 3D/4D ultrasound. In: Pooh RK, Kurjak A (eds) Fetal neurology. Jaypee, St. Louis, MI, pp 221–285
Lammens M, Moerman P, Fryns JP, Lemmens F, van de Kamp GM, Goemans N, Dom R (1997) Fetal akinesia sequence caused by nemaline myopathy. Neuropediatrics 28:116–119
Langman J (1963) Medical embryology. Williams & Wilkins, Baltimore, MD
Lavdas AA, Grigoriou M, Pachnis V, Parnavelas JG (1999) The medial ganglionic eminence gives rise to a population of early neurons in the developing cerebral cortex. J Neurosci 19:7881–7888
Le Douarin NM, Kalcheim C (1999) The neural crest, 2nd edn. Cambridge University Press, Cambridge
Lee A (2001) Four-dimensional ultrasound in prenatal diagnosis: leading edge in imaging technology. Ultrasound Rev Obstet Gynecol 1:194–198
Lemire RJ, Loeser JD, Leech RW, Alvord EC (1975) Normal and abnormal development of the human nervous system. Harper & Row, Hagerstown, MD
Letinić K, Kostović I (1997) Transient fetal structure, the gangliothalamic body, connects telencephalic germinal zone with all thalamic regions in the developing human brain. J Comp Neurol 384:373–395
Letinić K, Rakic P (2001) Telencephalic origin of human thalamic GABAergic neurons. Nat Neurosci 9:931–936
Letinić K, Zoncu R, Rakic P (2002) Origin of GABAergic neurons in the human neocortex. Nature 417:645–649
Leto K, Arancillo M, Becker EBE, Buffo A, Chiang C, Ding B et al (2016) Consensus paper: cerebellar development. Cerebellum 15:789–828
Lichtman JW, Sanes JR (2008) Ome sweet ome: What can the genome tell us about the connectome? Curr Opin Neurobiol 18:346–353
Liddelow SA (2015) Development of the choroid plexus and blood-CSF barrier. Front Neurosci 9:32
Lie KTA (1968) Congenital anomalies of the carotid arteries. Thesis, University of Amsterdam, Excerpta Medica Foundation, Amsterdam
Lindenberg R (1956) Die Gefässversorgung und ihre Bedeutung für Art und Ort von kreislaufgedingten Gewebsschäden und Gefässprozessen. In: Lubarsch-Henke-Rössle's Handbuch der speziellen pathologischen Anatomie und Histologie, Vol 13 (Scholz W, Hrsg), Teil 1B. Springer, Berlin, Heidelberg, New York, pp. 1071–1164
Lowenstein ED, Cui K, Hernandez-Miranda LR (2022) Regulation of early cerebellar development. FEBS J:16426
Luckett WP (1978) Origin and differentiation of the yolk sac and extraembryonic mesoderm in presomite human and rhesus monkey embryos. Am J Anat 152:59–97
Lui JH, Hansen DV, Kriegstein AR (2011) Development and evolution of the human neocortex. Cell 146:18–36
Lumsden A, Krumlauf AR (1996) Patterning the vertebrate neuraxis. Science 274:1109–1115
Lun MP, Monuki ES, Lehtinen MK (2015) Development and functions of the choroid plexus-cerebrospinal fluid system. Nat Rev Neurosci 16:445–457
Ma T, Wang C, Wang L, Zhou X, Tian M, Zhang Q et al (2013) Subcortical origins of human and monkey neocortical interneurons. Nat Neurosci 16:1588–1597
Macchi G (1951) The ontogenetic development of the olfactory telencephalon in man. J Comp Neurol 95:245–305
Marín O, Rubenstein JLR (2001) A long, remarkable journey: tangential migration in the telencephalon. Nat Rev Neurosci 2:780–790

Marín O, Rubenstein JLR (2002) Patterning, regionalization, and cell differentiation in the forebrain. In: Rossant J, Tam PPL (eds) Mouse development—patterning, morphogenesis, and organogenesis. Academic Press, San Diego, CA, pp 75–106
Marín O, Anderson SA, Rubenstein JLR (2000) Origin and molecular specification of striatal interneurons. J Neurosci 20:6063–6076
Marín O, Yaron A, Bagri A, Tessier-Lavigne M, Rubenstein JLR (2001) Sorting of striatal and cortical interneurons regulated by semaphorin-neuropilin interactions. Science 293:872–875
Marín F, Aroca P, Puelles L (2008) Hox gene colinear expression in the avian medulla oblongata is correlated with pseudorhombomeric domains. Dev Biol 323:230–247
Marín-Padilla M (1990) Origin, formation, and prenatal maturation of the human cerebral cortex: an overview. J Craniofac Genet Dev Biol 10:137–146
Marín-Padilla M (1996) Developmental neuropathology and impact of perinatal brain damage. I. Hemorrhagic lesions of neocortex. J Neuropathol Exp Neurol 55:758–773
Marín-Padilla M (1997) Developmental neuropathology and impact of perinatal brain damage. II. White matter lesions of the neocortex. J Neuropathol Exp Neurol 56:219–235
Marín-Padilla M (1998) Cajal-Retzius cells and the development of the neocortex. Trends Neurosci 21:64–71
Marín-Padilla M (1999) Developmental neuropathology and impact of perinatal brain damage. III. Gray matter lesions of the neocortex. J Neuropathol Exp Neurol 58:407–429
Markowski J (1921) Entwicklung der Sinus durae matris und der Hirnvenen des Menschen. Bull Int Acad Sci Lett, Classe des sciences mathematiques et naturelles. Serie B (Suppl. 1):1–269
Markowski J (1931) Über die Entwicklung der Falx cerebri und des Tentorium cerebelli des Menschen mit Berücksichtigung ihres venösen Sinus. Z Anat EntwGesch 94:395–439
Marti E, Bovolenta P (2002) Sonic hedgehog in CNS development: one signal, multiple outputs. Trends Neurosci 25:89–96
Martínez S, Puelles E, Puelles L, Echevarria D (2012) Molecular regionalization of the developing neural tube. In: Watson C, Paxinos G, Puelles L (eds) The mouse nervous system. Elsevier, Amsterdam, pp 2–18
Massarwa R, Niswander L (2013) In toto live imaging of mouse morphogenesis and new insights into neural tube closure. Development 140:226–236
Matsuda Y, Ono S, Otake Y, Handa S, Kose K, Haishi T et al (2007) Imaging of a large collection of human embryos using a superparallel MR microscope. Magn Reson Med Sci 6:139–146
Matsunari C, Kanahashi T, Otani H, Imai H, Yamada S, Okada T, Takakuwa T (2023) Tentorium cerebelli formation during human embryonic and early fetal development. Anat Rec. 306:515–526
Medina L, Abellán A (2012) Subpallial structures. In: Watson C, Paxinos G, Puelles L (eds) The mouse nervous system. Elsevier, Amsterdam, pp 173–220
Mehler MF, Mabie PC, Zhang D, Kessler JA (1997) Bone morphogenetic proteins in the nervous system. Trends Neurosci 20:309–317
Meng H, Zhang Z, Geng H, Lin X, Feng L, Feng G et al (2012) Development of the subcortical brain structures in the second trimester: assessment with 7.0-T MRI. Neuroradiology 54:1153–1159
Meyer G (2007) Genetic control of neuronal migrations in human cortical development. Adv Anat Embryol Cell Biol 189:1–111
Meyer G (2010) Building a human cortex: The evolutionary differentiation of Cajal-Retzius cells and the cortical hem. J Anat (Lond) 217:334–343
Meyer G, Goffinet AM (1998) Prenatal development of reelin-immunoreactive neurons in the human neocortex. J Comp Neurol 397:29–40
Meyer G, González-Gómez M (2018) The subpial granular layer and transient versus persisting Cajal-Retzius neurons of the fetal human cortex. Cereb Cortex 28:2043–2058
Meyer G, Wahle P (1999) The paleocortical ventricle is the origin of reelin-expressing neurons in the marginal zone of the foetal human neocortex. Eur J Neurosci 11:3937–3944
Meyer G, Goffinet AM, Fairén A (1999) What is a Cajal-Retzius cell? A reassessment of a classical cell type based on recent observations in the developing neocortex. Cereb Cortex 9:765–775
Meyer G, Schaaps JP, Moreau L, Goffinet AM (2000) Embryonic and early fetal development of the human neocortex. J Neurosci 20:1858–1868
Meyer G, González-Arnay E, Moll U, Nemajerova A, Tissir F, González-Gómez M (2019) Cajal-Retzius neurons are required for the development of the human hippocampal fissure. J Anat (Lond) 235:569–589
Millen KJ, Millonig JH, Wingate RJT, Alder J, Hatten ME (1999) Neurogenetics of the cerebellar system. J Child Neurol 14:574–582
Millen KJ, Steshina EY, Iskusnykh IY, Chizhikov VV (2014) Transformation of the cerebellum into more ventral brainstem fates causes cerebellar agenesis in the absence of Ptf1a function. Proc Nat Acad Sci U S A 111:E1777–E1786
Mitter C, Jakab A, Brugger PC, Ricken G, Gruber GM, Bettelheim D et al (2015) Validation of *in utero* tractography of human fetal commissural and internal capsule fibers with histological structure tensor analysis. Front Neuroanat 9:164
Moessinger AC (1983) Fetal akinesia deformation sequence: an animal model. Pediatrics 72:857–863
Molnár Z, Clowry GJ, Šestan N, Alzu'bi A, Bakken T, Hevner RF et al (2019) New insights into the development of the human cerebral cortex. J Anat (Lond) 235:432–451
Monteagudo A, Timor-Tritsch IE (2009) Normal sonographic development of the central nervous system from the second trimester onwards using 2D, 3D and transvaginal tomography. Prenat Diagn 29:326–329
Monuki ES, Golden JA (2018) Midline field defects. In: Adle-Biassette H, Harding BN, Golden JA (eds) Developmental neuropathology, 2nd edn. Wiley, Hoboken, NJ, pp 29–40
Monuki ES, Walsh CA (2001) Mechanisms of cerebral cortical patterning in mice and human. Nat Neurosci 4:1199–1206
Moore KL, Persaud TVN, Shiota K (2000) Color Atlas of clinical embryology, 2nd edn. Saunders, Philadelphia, PA
Moretti R, Pansiot J, Bettati D, Strazielle N, Ghersi-Egea J-F, Damante G et al (2015) Blood-brain barrier dysfunction in disorders of the developing brain. Front Neurosci 9:40
Mori S, Wakana S, Nagao-Poetscher LM, van Zijl PCM (2005) MRI Atlas of human white matter. Elsevier, Amsterdam
Morriss-Kay GM, Wilkie AOM (2005) Growth of the normal skull vault and its alteration in craniosynostosis: Insights from human genetics and experimental studies. J Anat (Lond) 207:637–653
Muenke M, Beachy PA (2000) Genetics of ventral forebrain development and holoprosencephaly. Curr Opin Genet Dev 10:262–269
Müller F, O'Rahilly R (1983) The first appearance of the major divisions of the human brain at stage 9. Anat Embryol (Berl) 168:419–432
Müller F, O'Rahilly R (1985) The first appearance of the neural tube and optic primordium in the human embryo at stage 10. Anat Embryol (Berl) 172:157–169
Müller F, O'Rahilly R (1988a) The development of the human brain from a closed neural tube at stage 13. Anat Embryol (Berl) 177:203–224
Müller F, O'Rahilly R (1988b) The first appearance of the future cerebral hemispheres in the human embryo at stage 14. Anat Embryol (Berl) 177:495–511

Müller F, O'Rahilly R (1989) The human brain at stage 16, including the initial evagination of the neurohypophysis. Anat Embryol (Berl) 179:551–569
Müller F, O'Rahilly R (1990a) The human brain at stages 18-20, including the choroid plexuses and the amygdaloid and septal nuclei. Anat Embryol (Berl) 182:285–306
Müller F, O'Rahilly R (1990b) The human brain at stages 21–23, with particular reference to the cerebral cortical plate and to the development of the cerebellum. Anat Embryol (Berl) 182: 375–400
Müller F, O'Rahilly R (1990c) The human rhombencephalon at the end of the embryonic period proper. Am J Anat 189:127–145
Müller F, O'Rahilly R (1997) The timing and sequence of appearance of neuromeres and their derivatives in staged human embryos. Acta Anat (Basel) 158:83–99
Nakamura M, Roser F, Rundschuh O, Vorkapic P, Samii M (2003) Intraventricular meningiomas: a review of 16 cases with reference to the literature. Surg Neurol 59:491–503
Nakashima I, Hirose A, Yamada S, Uwabe C, Kose K, Takakuwa T (2011) Morphometric analysis of the brain vesicles during the human embryonic period by magnetic resonance microscopic imaging. Cong Anom 52:55–58
Nakatsu T, Uwabe C, Shiota K (2000) Neural tube closure in humans initiates at multiple sites: Evidence from human embryos and implications for the pathogenesis of neural tube defects. Anat Embryol (Berl) 201:455–466
Nelson MD, Gonzalez-Gomez I, Gilles FH (1991) The search for human telencephalic ventriculofugal arteries. Am J Neuroradiol 12:215–222
Niemann G, Wakat JP, Krägeloh-Mann I, Grodd W, Michaelis R (1994) Congenital hemiparesis and periventricular leukomalacia: Pathogenetic aspects on magnetic resonance imaging. Dev Med Child Neurol 36:943–950
Nieuwenhuys R (1998) Morphogenesis and general structure. In: Nieuwenhuys R, ten Donkelaar HJ, Nicholson C (eds) The central nervous system of vertebrates. Springer, Berlin, Heidelberg, New York, pp 159–228
Nieuwkoop PD, Albers B (1990) The role of competence in the craniocaudal segregation of the central nervous system. Dev Growth Diff 32:23–31
Nishimura H, Semba R, Tanimura T, Tanaka O (1977) Prenatal development of the human with special reference to craniofacial structures. An atlas. Department of Health, Education & Welfare, National Institute of Health, Bethesda, MD
Noden DM (1991) Cell movements and control of patterned tissue assembly during craniofacial development. J Craniofac Genet Dev Biol 11:192–213
Noden DM, Trainor PA (2005) Relations and interactios between cranial mesoderm and neural crest populations. J Anat (Lond) 207:575–601
Norman MG, O'Kusky JR (1986) The growth and development of microvasculature in human cerebral cortex. J Neuropathol Exp Neurol 45:222–232
Norman MG, McGillivray BC, Kalousek DK, Hill A, Poskitt KJ (1995) Congenital malformations of the brain. Pathological, embryological, clinical, radiological and genetic aspects. Oxford University Press, New York
O'Rahilly R (1973) Developmental stages in human embryos. Part A: Embryos of the first three weeks (stages 1–9). Carnegie Institution of Washington Publication 631, Washington, DC
O'Rahilly R (1975) A color atlas of human embryology. A slide presentation. Saunders, Philadelphia, PA
O'Rahilly R, Gardner E (1979) The initial development of the human brain. Acta Anat (Basel) 104:123–133
O'Rahilly R, Müller F (1981) The first appearance of the human nervous system at stage 8. Anat Embryol (Berl) 163:1–13
O'Rahilly R, Müller F (1986) The meninges in human development. J Neuropathol Exp Neurol 45:588–608
O'Rahilly R, Müller F (1987) Developmental stages in human embryos. Carnegie Institution of Washington Publication 637, Washington, DC
O'Rahilly R, Müller F (1999) The embryonic human brain. An atlas of developmental stages, 2nd edn. Wiley-Liss, New York
O'Rahilly R, Müller F (2001) Human embryology & teratology, 3rd edn. Wiley-Liss, New York
O'Rahilly R, Müller F (2008) Significant features in the early prenatal development of the human brain. Ann Anat 190:105–118
Okado N (1981) Onset of synapse formation in the human spinal cord. J Comp Neurol 201:211–219
Okado N, Kojima T (1984) Ontogeny of the central nervous system: neurogenesis, fibre connections, synaptogenesis and myelination in the spinal cord. In: Prechtl HFR (ed) Continuity of neural functions from prenatal to postnatal life. Blackwell, Oxford, pp 31–45
Okado N, Kahimi S, Kojima T (1979) Synaptogenesis in the cervical cord of the human embryo: sequence of synapse formation in a spinal reflex pathway. J Comp Neurol 184:491–517
Okudera T, Ohta T, Huang YP, Yokota A (1988) Development and radiological anatomy of the superficial cerebral convexity vessels in the human fetus. J Neuroradiol 15:205–224
Olson EC, Walsh CA (2002) Smooth, rough and upside-down neocortical development. Curr Opin Genet Dev 12:320–327
Opitz JM (1993) Blastogenesis and the "primary field" in human development. Birth Defects 29:3–37
Opitz JM, Wilson GN, Gilbert-Barness E (1997) Abnormalities of blastogenesis, organogenesis, and phenogenesis. In: Gilbert-Barness E (ed) Potter's pathology of the fetus and infant. Mosby, St. Louis, MI, pp 65–105
Ouyang M, Dubois J, Yu Q, Mukherjee P, Huang H (2019) Delineation of early brain development from fetuses to infants with diffusion MRI and beyond. Neuroimage 185:836–850
Padget DH (1948) The development of the cranial arteries in the human embryo. Contrib Embryol Carnegie Instn 32:205–261
Padget DH (1957) The development of the cranial venous system in man, from the viewpoint of comparative anatomy. Contrib Embryol Carnegie Instn 36:79–140
Parnavelas JG (2000) The origin and migration of cortical neurones: new vistas. Trends Neurosci 23:126–131
Paul LK, Brown WS, Adolphs R, Tyszka JM, Richards LJ, Mukherjee P, Sherr EH (2007) Agenesis of the corpus callosum: genetic, developmental and functional aspects of connectivity. Nat Rev Neurosci 8:287–299
Paus T, Collins DL, Evans AC, Leonard G, Pike B, Zijdenbos A (2001) Maturation of white matter in the human brain: a review of magnetic resonance studies. Brain Res Bull 54:255–266
Pearce WJ (2002) Cerebrovascular regulation in the neonate. In: Lagercrantz H, Hanson M, Evrard P, Rodeck CH (eds) The newborn brain—neuroscience and clinical applications. Cambridge University Press, Cambridge, pp 252–277
Pearlman AL, Faust PL, Hatten ME, Brunstrom JE (1998) New directions for neuronal migration. Curr Opin Neurobiol 8:45–54
Pearson AA (1941) The development of the olfactory nerve in man. J Comp Neurol 75:199–217
Pilz D, Stoodley N, Golden JA (2002) Neuronal migration, cerebral cortical development, and cerebral cortical anomalies. J Neuropathol Exp Neurol 61:1–11
Pooh RK (2009) Neuroanatomy visualized by 2D and 3D. In: Pooh RK, Kurjak A (eds) Fetal neurology. Jaypee, St. Louis, MI, pp 16–38

Pooh RK, Kurjak A (eds) (2009) Fetal neurology. Jaypee, St. Louis, MI
Pooh RK, Maeda K, Pooh K (2003) An atlas of fetal central nervous system diseases. Diagnosis and treatment. Parthenon, Boca Raton, FL
Pooh RK, Shiota K, Kurjak A (2011) Imaging of the human embryo with magnetic resonance imaging microscopy and high-resolution transvaginal 3-dimensional sonography: human embryology in the 21st century. Am J Obstet Gynecol 204:77.e1–77.16
Prayer D (2011) Fetal MRI. Springer, Heidelberg, New York
Prayer D, Kasprian G, Krampl E, Ulm B, Witzani L, Prayer L, Brugger PC (2006) MRI of normal fetal brain development. Eur J Radiol 57:199–216
Pringsheim M, Mitter D, Schröder S, Warthemann R, Plümacher K, Kluger G et al (2019) Structural brain anomalies in patients with FOXG1 syndrome and in Foxg+/– mice. Ann Clin Translat Neurol. https://doi.org/10.1002/acn3.735
Puelles L (1995) A segmental morphological paradigm for understanding vertebrate forebrains. Bran Behav Evol 46:319–337
Puelles L (2013) Plan of the developing vertebrate nervous system. Relating embryology to the adult nervous system (prosomere model, overview of brain organization). In: Rakic P, Rubenstein JLR (eds) Comprehensive developmental neuroscience, vol 1. Elsevier, New York, pp 187–209
Puelles L (2019) Survey of midbrain, diencephalon, and hypothalamus neuroanatomic terms whose prosomeric definition conflicts with columnar tradition. Front Neuroanat 13:20
Puelles L (2021) Recollections on the origins and development of the prosomeric model. Front Neuroanat 15:787913
Puelles L, Rubenstein JLR (1993) Expression patterns of homeobox and other putative regulatory genes in the embryonic forebrain suggest a neuromeric organization. Trends Neurosci 16:472–479
Puelles L, Rubenstein JLR (2003) Forebrain gene expression domains and the evolving prosomeric model. Trends Neurosci 26:469–476
Puelles L, Verney C (1998) Early neuromeric distribution of tyrosine-hydroxylase-immunoreactive neurons in human embryos. J Comp Neurol 394:283–308
Puelles L, Kuwana E, Puelles E, Bulfone A, Shimamura K, Keleher J et al (2000) Pallial and subpallial derivatives in the embryonic chick and mouse telencephalon, traced by the expression of the genes Dlx-2, Emx-1, Nkx-2.1, Pax-6, and Tbr-1. J Comp Neurol 424:409–438
Puelles L, Martínez S, Martínez de la Torre M (2008) Neuroanatomía. Médica Panamericana, Buenos Aires, Madrid. (in Spanish)
Puelles L, Martínez-de-la-Torre M, Bardet S, Rubenstein JLR (2012) Hypothalamus. In: Watson C, Paxinos G, Puelles L (eds) The mouse nervous system. Elsevier, Amsterdam, pp 221–312
Puelles L, Harrison M, Paxinos G, Watson C (2013) A developmental ontology for the mammalian brain based on the prosomeric model. Trends Neurosci 36:570–578
Puelles L, Martínez-Marín R, Melgarejo-Otalara P, Ayad A, Valavanis A, Ferran JL (2019) Patterned vascularization of embryonic mouse forebrain, and neuromeric topology of major human subarachnoidal arterial branches: a prosomeric mapping. Front Neuroanat 13:39
Pyrgaki C, Trainor P, Hadjantonakis A-K, Niswander L (2010) Dynamic imaging of mammalian neural tube closure. Dev Biol 344:941–947
Radoš M, Judaš M, Kostović I (2006) In vitro MRI of brain development. Eur J Radiol 57:187–198
Rakic P (1972) Mode of cell migration to the superficial layers of fetal monkey neocortex. J Comp Neurol 145:61–84
Rakic P (2009) Evolution of the neocortex: a perspective from developmental biology. Nat Rev Neurosci 10:724–735
Rakić P, Sidman RL (1969) Telencephalic origin of pulvinar neurons in the fetal human brain. Z Anat Entw Gesch 129:53–82
Rakic P, Sidman RL (1970) Histogenesis of cortical layers in human cerebellum, particularly the lamina dissecans. J Comp Neurol 139:473–500
Rakic P, Yakovlev PI (1968) Development of the corpus callosum and cavum septi in man. J Comp Neurol 132:45–72
Rama Murthy BS (2019) Imaging of fetal brain and spine. Springer, Singapore
Ramaekers VT, Heimann G, Reul J, Thron A, Jaeken J (1997) Genetic disorders and cerebellar structural abnormalities in childhood. Brain 120:1739–1751
Ranke G (1910) Beiträge zur Kenntnis der normalen und pathologischen Hirnrindenbildung. Ziegl Beitr Path Anat 47:51–125
Raybaud C (2010a) The corpus callosum, the other great forebrain commissures, and the septum pellucidum: anatomy, development, and malformations. Neuroradiology 52:447–477
Raybaud C (2010b) Normal and abnormal embryology and development of the intracranial vascular system. Neurosurg Clin N Am 21:399–426
Raybaud C, Strother CM, Hald JK (1989) Aneurysms of the vein of Galen: embryonic considerations and anatomical features relating to the pathogenesis of the malformation. Neuroradiology 31:109–128
Rendahl H (1924) Embryologische und morphologische Studien über das Zwischenhirn beim Huhn. Acta Zool (Stockh) 5:241–344
Rhinn M, Brand M (2001) The midbrain-hindbrain boundary organizer. Curr Opin Neurobiol 11:34–42
Rifat Y, Parekh V, Wilanowski T, Hislop NR, Auden A, Ting SB et al (2010) Regional neural tube closure defined by the Grainy head-like transcription factors. Dev Biol 345:237–245
Rijli FM, Gavalas A, Chambon P (1998) Segmentation and specification in the branchial region of the head: the role of the *Hox* selector genes. Int J Dev Biol 42:393–401
Rorke LB (1992) Anatomical features of the developing brain implicated in pathogenesis of hypoxic-ischemic injury. Brain Pathol 2:211–221
Rubenstein JLR, Beachy PA (1998) Patterning of the embryonic forebrain. Curr Opin Neurobiol 8:18–26
Rubenstein JLR, Shimamura K, Martinez S, Puelles L (1998) Regionalization of the prosencephalic neural plate. Annu Rev Neurosci 21:445–477
Ruggieri PM (1997) Metabolic and neurodegenerative disorders and disorders with abnormal myelination. In: Ball WS (ed) Pediatric neuroradiology. Lippincott, Philadelphia, PA, pp 175–237
Rutherford MA, Supramaniam V, Ederies A, Chew A, Bassi L, Groppo M et al (2010) Magnetic resonance imaging of white matter disease of prematurity. Neuroradiology 52:505–521
Sadler TW, Feldkamp ML (2008) The embryology of body wall closure: relevance to gastroschisis and other ventral body wall defects. Am J Med Genet Part C 148C:180–185
Salas E, Ziyal IM, Sekhar LN, Wright DC (1998) Persistent trigeminal artery: an anatomic study. Neurosurgery 43:557–562
Salihagic-Kadic A, Predojevic M, Kurjak A (2009) Advances in fetal neurophysiology. In: Pooh RK, Kurjak A (eds) Fetal neurology. Jaypee, St. Louis, MI, pp 161–219
Sarnat HB, Flores-Sarnat L (2001) Neuropathologic research strategies in holoprosencephaly. J Child Neurol 16:918–931
Scheinost D, Kwon SH, Shen X, Lacadia C, Schneider KC, Dai F et al (2016) Preterm birth alters neonatal, functional rich club organization. Brain Struct Funct 221:3211–3222

Schuurmans C, Guillemot F (2002) Molecular mechanisms underlying cell fate specification in the developing telencephalon. Curr Opin Neurobiol 12:26–34

Sensenig EC (1951) The early development of the meninges of the spinal cord in human embryos. Contrib Embryol Carnegie Instn 34:145–157

Seress L, Ábrahám H, Tornóczky T, Kosztolányi G (2001) Cell formation in the human hippocampal formation from mid-gestation to the late postnatal period. Neuroscience 105:831–843

Shimamura K, Hartigan DJ, Martinez S, Puelles L, Rubenstein JLR (1995) Longitudinal organization of the anterior neural plate and neural tube. Development 121:3923–3933

Shiota K (2018) Study of normal and abnormal prenatal development using the Kyoto collection of human embryos. Anat Rec 301:955–959

Shiota K, Yamada S, Nakatsu-Komatsu T, Uwabe C, Kose K, Matsuda Y et al (2007) Visualization of human prenatal development by magnetic resonance imaging (MRI). Am J Med Genet Part A 143A:3121–3126

Shiraishi N, Nakashima T, Yamada S, Uwabe C, Kose K, Takaluwa T (2013) Morphogenesis of lateral choroid plexus during human embryonic period. Anat Rec 296:692–700

Shiraishi N, Katayama A, Nakashima T, Yamada S, Uwabe C, Kose K, Takakuwa T (2015) Morphology and morphometry of the human embryonic brain: a three-dimensional analysis. Neuroimage 115:96–103

Sidman RL, Rakic P (1982) Development of the human central nervous system. In: Haymaker W, Adams RD (eds) Histology and histopathology of the nervous system. Thomas, Springfield, IL, pp 3–145

Sie LTL, van der Knaap MS, van Wezel-Meijler G, Valk J (1997) MRI assessment of myelination of motor and sensory pathways in the brain of preterm and term-born infants. Neuropediatrics 28:97–105

Siegenthaler JA, Pleasure SJ (2011) We have got you 'covered': how the meninges control brain development. Curr Opin Genet Dev 21:249–254

Smart IHM, Dehay C, Giroud P, Berland M, Kennedy H (2002) Unique morphological features of the proliferative zones and postmitotic compartments of the neural epithelium giving rise to striate and extrastriate cortex in the monkey. Cereb Cortex 12:37–53

Song L, Mishra V, Ouyang M, Peng Q, Slinger M, Liu S, Huang H (2017) Human fetal brain connectome: structural network development from middle fetal stage to birth. Front Neurosci 11:561

Sporns O (2011) The human connectome: a complex network. Ann NY Acad Sci 1224:109–125

Sporns O (2012) Discovering the human connectome. MIT Press, Cambridge, MA

Sporns O, Tononi G, Kötter R (2005) The human connectome: a structural description of the human brain. PLoS Comp Biol 1:e42

Spreafico R, Arcelli P, Frassoni C, Canetti P, Giaccone G, Rizzutti T et al (1999) Development of layer I of the human cerebral cortex after midgestation: Architectonic findings, immunocytochemical identification of neurons and glia, and in situ labeling of apoptotic cells. J Comp Neurol 410:126–142

Squier W (2002) Pathology of fetal and neonatal brain development: identifying the timing. In: Squier W (ed) Acquired damage to the developing brain: timing and causation. Arnold, London, pp 110–127

Staudt M, Niemann G, Grodd W, Krägeloh-Mann I (2000) The pyramidal tract in congenital hemiparesis: Relationship between morphology and function in periventricular lesions. Neuropediatrics 31:257–264

Stephan H (1975) Allocortex. In: Handbuch der mikroskopischen Anatomie des Menschen, Band 4, Teil 9. Springer, Berlin, Heidelberg, New York

Streeter GL (1911) Die Entwicklung des Nervensystems. In: Keibel F, Mall FP (Hrsg) Handbuch der Entwicklungsgeschichte des Menschen, Zweiter Band. Hirzel, Leipzig, pp. 1–156

Streeter GL (1912) The development of the nervous system. In: Keibel F, Mall FP (eds) Manual of human embryology, Lippincott, vol 2. Philadelphia, PA, pp 1–156

Streeter GL (1915) The development of the venous sinuses in the dura mater in the human embryo. Am J Anat 18:145–178

Streeter GL (1918) The developmental alterations in the vascular system of the brain of the human embryo. Contrib Embryol Carnegie Instn 8:5–38

Streeter GL (1951) Developmental horizons in human embryos. Age groups XI to XXIII. Carnegie Institution of Washington, Washington, DC

Supèr H, Soriano E, Uylings HBM (1998) The functions of the preplate in development and evolution of the neocortex and hippocampus. Brain Res Rev 27:40–64

Suttner N, Mura J, Tedeschi H, Ferreira MAT, Wen HT, de Oliveira E, Rhoton AL Jr (2000) Persistent trigeminal artery: a unique anatomic specimen—analysis and therapeutic implications. Neurosurgery 47:428–434

Swanson LW, Bota M (2010) Foundational model of structural connectivity in the nervous system with a schema for wiring diagrams, connectome, and basic plan architecture. Proc Natl Acad Sci U S A 107:20610–20617

Swanson LW, Hahn JD, Sporns O (2017) Organizing principles for the cerebral cortex network of commissural and association connections. Proc Natl Acad Sci U S A:E9692–E9701

Takahashi E, Folkerth RD, Galaburda AM, Grant PE (2012) Emerging cerebral connectivity in the human fetal brain: an MR tractographic study. Cereb Cortex 22:455–464

Takakuwa T (2018) 3D analysis of human embryos and fetuses using digitized datasets from the Kyoto collection. Anat Rec 301:960–969

Takakuwa T, Shiraishi N, Terashima M, Yamanaka M, Okamoto I, Imai H et al (2021) Morphology and morphometry of the human early foetal brain: a three-dimensional analysis. J Anat (Lond) 239:498–516

Takashima S, Tanaka K (1978) Development of cerebrovascular architecture and its relationship to periventricular leukomalacia. Arch Neurol 35:11–16

TE2 (2017) Terminologia embryologica, 2nd ed. FIPAT.library.dal.ca. Federative Programme for Anatomical Terminology

ten Donkelaar HJ (2000) Development and regenerative capacity of descending supraspinal pathways in tetrapods: a comparative approach. Adv Anat Embryol Cell Biol 154:1–145

ten Donkelaar HJ (2020) Overview of the brain and spinal cord. In: ten Donkelaar HJ (ed) Clinical neuroanatomy: brain circuitry and its disorders, 2nd edn. Springer, Cham, pp 1–70

ten Donkelaar HJ, Lammens M (2009) Development of the human cerebellum and its disorders. Clin Perinatol 36:513–530

ten Donkelaar HJ, Lammens M, Wesseling P, Thijssen HOM, Renier WO (2003) Development and developmental disorders of the human cerebellum. J Neurol 250:1025–1036

ten Donkelaar HJ, Lammens M, Wesseling P, Hori A, Keyser A, Rotteveel J (2004) Development and malformations of the human pyramidal tract. J Neurol 251:1429–1442

ten Donkelaar HJ, Broman J, Neumann PE, Puelles L, Riva A, Tubbs RS, Kachlik D (2017) Towards a Terminologia Neuroanatomica. Clin Anat 30:145–155

ten Donkelaar HJ, Kachlik D, Tubbs RS (2018) An Illustrated Terminologia Neuroanatomica. Springer, Cham

Terashima M, Ishikawa A, Männer J, Yamada S, Takakuwa T (2021) Early development of the cortical layers in the human brain. J Anat (Lond) 239:1039–1049
Thomason ME (2018) Structured spontaneity: building circuits in the human prenatal brain. Trends Neurosci 41:1–3
TNA (2017) Terminologia neuroanatomica. FIPAT.library.dal.ca. Federative International Programme for Anatomical Terminology
Tomás-Roca L, Corral-San-Miguel R, Aroca P, Puelles L, Marín F (2016) Crypto-rhombomeres of the mouse medulla oblongata, defined by molecular and morphological features. Brain Struct Funct 221:815–838
Trainor P (ed) (2014) Neural crest cells. Evolution, development and disease. Academic Press/Elsevier, San Diego, CA
Tsuboi K, Maki Y, Hori A, Ebihara R (1984) Accessory ventricles of the posterior horn. Prog Comp Tomogr 6:529–534
Turk E, van den Heuvel MI, Benders MJ, de Heus R, Franx A, Manning JH et al (2019) Functional connectome of the fetal brain. J Neurosci 39:9716–9724
van den Heuvel MP, Sporns O (2013) Network hubs in the human brain. Trends Cogn Sci 17:683–696
van den Heuvel MI, Thomason ME (2016) Functional connectivity of the human brain in utero. Trends Cog Sci 20:931–939
van den Heuvel MP, Kersbergen KJ, de Reus MA, Keunen K, Kahn RS, Groenendaal F et al (2015) The neonatal connectome during preterm brain development. Cereb Cortex 25:3000–3013
van den Heuvel MP, Bullmore ET, Sporns O (2016) Comparative connectomics. Trends Cogn Sci 20:345–361
van den Heuvel MI, Turk E, Manning JH, Hect J, Hernandez-Andrade E, Hassan SS et al (2018) Hubs in the human fetal brain network. Dev Cogn Neurosci 30:108–115
van der Knaap MS, Valk J (1988) Classification of congenital abnormalities of the CNS. AJNR Am J Neuroradiol 9:315–326
van der Knaap MS, Valk J (1990) MR imaging of the various stages of normal myelination during the first year of life. Neuroradiology 31:459–470
van der Knaap MS, Valk J (1995) Magnetic resonance of myelin, myelination and myelin disorders, 2nd edn. Springer, Berlin, Heidelberg, New York
van Wezel-Meijler G, van der Knaap MS, Sie LTL, Oosting J, Taets van Amerongen AHM, Cranendonk A, Lafeber HN (1998) Magnetic resonance imaging of the brain in premature infants during the neonatal period. Normal phenomena and reflection of mild ultrasound abnormalities. Neuropediatrics 29:89–96
van Zalen-Sprock RM, van Vugt JMG, van Geijn HPM (1996) First-trimester sonographic detection of neurodevelopmental abnormalities in some single-gene defects. Prenat Diagn 16:199–202
Vasung L, Huang H, Jovanov-Milošević N, Pletikos M, Mori S, Kostović I (2010) Development of axonal pathways in the human fetal fronto-limbic brain: Histochemical characterization and diffusion tensor imaging. J Anat (Lond) 217:400–407
Vasung L, Lepage C, Radoš M, Goldman JS, Richiardi J, Raguž M et al (2016) Quantitative and qualitative analysis of transient fetal compartments during prenatal human brain development. Front Neuroanat 10:11
Vasung L, Raguž M, Kostović I, Takahashi E (2017) Spatiotemporal relationship of brain pathways during human fetal development using high-angular resolution diffusion MR imaging and histology. Front Neurosci 11:348
Vasung L, Abaci Turk E, Ferradal SL, Sutin J, Stout JN, Ahtam B et al (2019) Exploring early human brain development with structural and physiological neuroimaging. Neuroimage 187:226–254
Vieille-Grosjean I, Hunt P, Gulisano M, Boncinelli E, Thorogood P (1997) Branchial HOX gene expression and human craniofacial development. Dev Biol 183:49–60
Volpe JJ (1987) Neurology of the newborn, 2nd edn. Saunders, Philadelphia, PA
Volpe JJ (1998) Neurologic outcome of prematurity. Arch Neurol 55:297–300
Volpe JJ (2001) Neurobiology of periventricular leukomalacia in the premature infant. Pediatr Res 50:553–562
Volpe JJ (2009) Brain injury in premature infants: A complex amalgam of destructions and developmental disturbances. Lancet Neurol 8:110–124
Volpe JJ (2019) Dysmaturation of the premature brain: Importance, cellular mechanisms, and potential interventions. Pediatr Neurol 95:42–66
von Baer KE (1828) Über die Entwickelungsgeschichte der Thiere. Beobachtung und Reflexion, Bornträger, Königsberg
Wahl M, Mukherjee P (2009) Diffusion imaging of congenital brain malformations. Semin Ped Neurol 16:111–119
Wang VY, Zoghbi HY (2001) Genetic regulation of cerebellar development. Nat Rev Neurosci 2:484–491
Wang WZ, Hoerder-Suabedissen A, Oeschger FM, Bayatti N, Ip BK, Lindsay S et al (2010) Subplate in the developing cortex of mouse and human. J Anat (Lond) 217:368–386
Watson C (2012) Hindbrain. In: Watson C, Paxinos G, Puelles L (eds) The mouse nervous system. Elsevier, Amsterdam, pp 398–423
Watson C, Puelles L (2016) Developmental gene expression in the mouse clarified the organization of the claustrum and related endopiriform nuclei. J Comp Neurol 525:1499–1508
Watson C, Shimogori T, Puelles L (2017) Mouse Fgf8-Cre-LacZ lineage analysis defines the territory of the postnatal mammalian isthmus. J Comp Neurol 525:2782–2799
Watson C, Bartholomaeus C, Puelles L (2019) Time for radical changes in brain stem nomenclature—applying the lessons from developmental gene patterns. Front Neuroanat 13:10
Wechsler-Reya RJ, Scott MP (1999) Control of neuronal precursor proliferation in the cerebellum by sonic hedgehog. Neuron 22:103–114
Weindling M (2002) Clinical aspects of brain injury of the preterm brain. In: Lagercrantz H, Hanson M, Evrard P, Rodeck CH (eds) The newborn brain—neuroscience and clinical applications. Cambridge University Press, Cambridge, pp 443–478
Weninger WJ, Mohun T (2002) Phenotypic transgenic embryos: a rapid 3-D screening method based on episcopic fluorescence image capturing. Nat Genet 30:59–65
Wigglesworth JS, Pape KE (1980) Pathophysiology of intracranial haemorrhage in the newborn. J Perinat Med 8:119–133
Wilkie AOM, Morriss-Kay GM (2001) Genetics of craniofacial development and malformation. Nat Rev Genet 2:458–468
Wilson S, Pietsch M, Cordero-Grande L, Price AN, Hutter J, Xian J et al (2021) Development of human white matter pathways in utero over the second and third trimester. Proc Natl Acad Sci U S A 118:e2023598118
Windle WF (1970) Development of neural elements in human embryos of four to seven weeks gestation. Exp Neurol Suppl 5:44–83
Windle WF, Fitzgerald JE (1937) Development of the spinal reflex mechanism in human embryos. J Comp Neurol 67:493–509
Wingate RJT (2001) The rhombic lip and early cerebellar development. Curr Opin Neurobiol 11:82–88
Witters I, Moerman P, Devriendt K, Braet P, Van Schoubroeck D, Van Assche FA, Fryns JP (2002) Two siblings with early onset fetal akinesia deformation wequence and hydranencephaly: further evidence for autosomal recessive inheritance of hydranencephaly, Fowler type. Am J Med Genet 108:41–44
Wollschlaeger G, Wollschlaeger PB (1964) The primitive trigeminal artery as seen angiographically and at postmortem examination. AJR Am J Roentgenol 92:761–768

Woodward LJ, Anderson PJ, Austin NC, Howard K, Inder TE (2006) Neonatal MRI to predict neurodevelopmental outcomes in preterm infants. N Engl J Med 355:685–694

Wullimann MF (2017) Should we redefine the classic lateral pallium? J Comp Neurol 525:1509–1513

Wurst W, Bally-Cuif L (2001) Neural plate patterning: Upstream and downstream of the isthmic organizer. Nat Rev Neurosci 2:99–108

Yakovlev PI, Lecours AR (1967) The myelogenetic cycles of regional maturation of the brain. In: Minkowski A (ed) Regional development of the brain in early life. Blackwell, Oxford, pp 3–70

Yamada S, Uwabe C, Nakatsu-Komatsu T, Minekura Y, Iwakura M, Motoki T et al (2006) Graphic and movie illustrations of human prenatal development and their application to embryological education based on the human embryo specimens in the Kyoto collection. Dev Dyn 235:468–477

Yamada S, Samtani RR, Lee ES, Lockett E, Uwabe C, Shiota K et al (2010) Developmental atlas of the early first trimester human embryo. Dev Dyn 239:1585–1595

Yamadori T (1965) Die Entwicklung des Thalamuskerns mit ihren ersten Fasersystemen bei menschlichen Embryonen. J Hirnforsch 7:393–413

Yamaguchi Y, Yamada S (2018) The Kyoto collection of human embryos and fetuses: history and recent advancements in modern methods. Cells Tissues Organs 205:314–319

Yu Q, Ouyang A, Chalak L, Jeon T, Chia J, Mishra V et al (2016) Structural development of human fetal and preterm brain cortical plate based on population-averaged templates. Cereb Cortex 26:4381–4391

Zecevic N, Milosevic A, Rakic S, Marín-Padilla M (1999) Early development and composition of the human primordial plexiform layer: an immunohistochemical study. J Comp Neurol 412:241–254

Zecevic N, Chen Y, Filipovic R (2005) Contributions of cortical ventricular zone to the development of the human cerebral cortex. J Comp Neurol 491:109–122

Zecevic N, Hu F, Jakovcevski I (2011) Interneurons in the developing human neocortex. Dev Neurobiol 71:18–33